BAW-10147A, Rev. 1

Topical Report
May 1983

FUEL ROD BOWING IN BABCOCK & WILCOX FUEL DESIGNS

— Revision 1 —

Project Engineer:

J. C. Moxley

Principal Contributing Authors:

E. J. McGuinn
A. S. Heller
D. A. Farnsworth
J. C. Moxley

BABCOCK & WILCOX
Utility Power Generation Division
P. O. Box 1260
Lynchburg, Virginia 24505

Babcock & Wilcox
a McDermott company

UNITED STATES
NUCLEAR REGULATORY COMMISSION
WASHINGTON, D. C. 20555

FEB 15 1983

Mr. James H. Taylor, Manager
Licensing
Babcock & Wilcox Company
P. O. Box 1260
Lynchburg, Virginia 24505

Dear Mr. Taylor:

Subject: Acceptance for Referencing of Licensing Topical Report BAW-10147(P)

The Nuclear Regulatory Commission (NRC) has completed its review of the Babcock & Wilcox Company (B&W) licensing topical report BAW-10147(P) entitled "Fuel Rod Bowing in Babcock & Wilcox Fuel Designs" dated April 1981, and the response to NRC's requests numbers one and two for additional information submitted by Mr. J. H. Taylor (B&W) to Mr. J. R. Miller dated April 15, 1982. The report describes an evaluation of the extent and effects of fuel rod bowing in Babcock & Wilcox fuel assemblies during irradiation. The correlation of an extensive data base of rod bow measurements has resulted in a method of predicting the magnitude of rod bow as a function of burnup. The results of bowed rod critical heat flux tests along with the rod bow prediction equation, are incorporated into a correlation to be used for predicting departure from nucleate boiling ratio (DNBR) penalty as a function of burnup. The effects of rod bow on power peaking uncertainty and on the mechanical performance of the cladding are also addressed. The technical evaluation of the licensing topical report, prepared under contract by Dr. J. F. Carew of the Brookhaven National Laboratory and concurred in by the NRC staff, is enclosed.

Based on our review, we conclude that the proposed methodology provides an acceptable means for analyzing the effects of fuel rod bowing and determining the power peaking factor (F_Q) and departure from nucleate boiling ratio rod bow penalties. This acceptability is limited to the fuel designs, exposures and conditions stated in the licensing topical report and supporting documentation. It is based, in part, on the Babcock & Wilcox gap closure representation and the specific assumptions made in formulating this methodology.

As a result of our review, we find the Babcock & Wilcox licensing topical report BAW-10147(P), as augmented by the response to NRC's requests for additional information identified above is acceptable for referencing in license applications to the extent specified and under the limitations delineated in the licensing topical report and the enclosed technical evaluation. The acceptance is not applicable to fuel designs that exhibit a greater propensity for bowing than that of the data from that the models reviewed were developed. NRC would like to be notified when fuel rod bowing performance is perceived to be outside of that predicted. Should a licensee determine that a particular core loading might produce limiting fuel (with respect to a thermal-hydraulic penalty) at a burnup beyond that corresponding to the Babcock and Wilcox generic limit (24 GWd/MTU), then that licensee should analyze that particular core loading to determine whether any penalty to the fuel exceeding the generic burnup limit is warranted. As discussed in the technical evaluation, residual DNBR penalties due to fuel rod bowing remain as are described in the topical report. Traditionally, applicants have used generic and plant-specific margins to totally or partially offset such penalties. Offsetting margins that are so used must be documented in the bases to the technical specifications and any remanent penalties must be accommodated into the technical specifications. The quantification of margins that are employed will not debar licensees from conducting reloads under the provisions of 10 CFR 50.59 provided that the specified margins remain available. When this report is referenced, the reference must include both the proprietary and nonproprietary versions.

We do not intend to repeat the review of the safety features described in the licensing topical report, and found acceptable, when it appears as a reference in a license application except to assure that the material presented is applicable to the specific plant involved. Our acceptance applies only to the features described in the topical report as augmented by the response to the requests for additional information.

In accordance with established procedures (NUREG-0390), it is requested that Babcock & Wilcox Company publish an approved version of this report, proprietary and nonproprietary, within three months of receipt of this letter. The revisions are to incorporate this letter and the attached technical evaluation following the title page, and thus just in front of the abstract. The revised report must incorporate the supporting information identified in the above initial paragraph. The report identifications of the approved reports are to have a -A suffix.

Should Nuclear Regulatory Commission criteria or regulations change such that our conclusions as to the acceptability of the report are invalidated, Babcock & Wilcox Company and/or the applicants referencing the topical report will be expected to revise and resubmit their respective documentation or submit justification for the continued effective applicability of the topical report without revision of their respective documentation.

Sincerely,

Cecil O. Thomas

Cecil O. Thomas, Chief
Standardization & Special
Projects Branch
Division of Licensing

Enclosure: As Stated

TECHNICAL EVALUATION OF THE BABCOCK AND WILCOX FUEL ROD

BOWING TOPICAL REPORT BAW-10147P

Prepared By

J.F. Carew

Core Performance Group

Department of Nuclear Energy
Brookhaven National Laboratory
Upton, New York 11973

August 1982

REPORT TITLE:

REPORT DATE:

ORIGINATING ORGANIZATION: Babcock & Wilcox Company

1.0 Background

In 1973 Westinghouse reported fuel rod bowing observations in PWRs to the Atomic Energy Commission. This fuel rod bowing was a deviation in straightness of fuel rods believed to be caused by irradiation effects. The major concerns with this phenomenon were the potential effects on bundle power distribution and the margin of fuel rods to departure from nucleate boiling (DNB).

Later in 1973, Westinghouse presented to the AEC the results of experiments in which a 4x4 bundle of electrically heated rods was tested to determine the effect of fuel rod bowing to contact on thermal margin reduction (departure from nucleate boiling rato (DNBR)). The tests were performed at conditions representative of PWR coolant conditions. The results of these experiments showed that for the highest power density at the highest coolant pressure expected in a Westinghouse reactor, the DNBR reduction due to heated rods bowed-to-contact was approximtely 8%. These results were verified by computer calculations (COBRA IIIC, THINC IV).

In 1976, Westinghouse modified these experiments and replaced one of the center 4 fuel rods by an unheated tube of the same size as a Westinghouse thimble tube. This new test configuration was tested over the same range of power, flow and pressure as the earlier tests. These tests showed, however, that with the unheated larger diameter rod replacing the heated fuel rod, the reduction in DNBR was much larger than in the 1973 tests (reference 1).

Because of the 1973 results on fuel rod bowing reported by Westinghouse, Babcock & Wilcox (B&W) was requested in June 1974 by the AEC to evaluate fuel rod bowing for the B&W design. After reviewing the submitted B&W rod bowing evaluation, the AEC concluded that the DNBR rod-to-rod contact penalty was not conservatively predicted. During the following years, B&W performed critical heat flux (CHF) tests for a MK-C 17x17 fuel assembly and 125,000 measurements on fuel rod bowing.

In June 1978, the NRC requested from B&W the submittal of a topical report on fuel rod bowing which covers fuel rod bowing data as well as an assessment of the impact of fuel rod bowing on performance (reference 2). On December 13, 1978, B&W submitted an interim report on fuel rod bowing with preliminary CHF test data for a bundle containing a rod bowed to 55% closure (reference 3). Also included in this report was a determination of the fuel rod bow impact on DNBR using the statistical method proposed by the NRC. A final report on CHF test data was submitted to the NRC on March 27, 1979 (reference 4). In a letter to the NRC dated June 22, 1979 (reference 5), B&W described a statistical method for using experimental data from their C9 and C10 bundles (unbowed rod) to predict an upper limit on the DNBR penalty at 55% closure. These submittals received conditional NRC approval in a NRC letter to B&W dated October 18, 1979 (reference 6).

The final topical report on the fuel rod bowing evaluation (BAW-10147P) was submitted to the NRC for review in April, 1981. It describes the B&W experience with fuel rod bowing and its impact on performance.

2.0 Summary of Topical Report

The B&W report on the effects of fuel rod bowing is summarized in the following.

2.1. Rod Bowing Data

2.1.1 Data Base

A total of over 125,000 individual rod-to-rod measurements for fuel assemblies with burnups up to 40,000 MWd/MTU were carried out for 26 assemblies from 8 manufacturing batches. The water channel spacings were measured using a Sulo strain gauge probe. A linear correction was used to correct for the unavoidable spread of the rods when the probe is inserted. Measurements were carried out for both inner and peripheral rods. No distinction was made between data from 15x15 assemblies (MK-B) and 17x17 assemblies (MK-C).

The uncertainty in the gap size measurements is discussed.

2.1.2 Analysis

The normality of the gap spacing distributions was thoroughly tested. Babcock & Wilcox corrected the raw data for a bias introduced by the measurement technique.

No adjustments were made to account for the L/I (i.e., grid span length/ cladding axial moment of inertia) differences between the 15x15 and 17x17 assemblies. For later use, B&W extracted from their measurements the worst span data. The report does not show how gap closure data were translated into rod bow data for the neutronics analysis.

2.2 Methods and Basic Correlations

2.2.1 Gap Closure

The gap closure correlation was derived from a standard regression analysis of the worst span closure data. It yielded an essentially linear correlation between the standard deviation of the gap at the worst span and burnup:

$$S_{gap} = A + B\ (BU)^C,$$

where, the values of the A,B and C parameters are given in Section 5 of the report and BU is expressed as average fuel assembly burnup in GWd/MTU. The gap closure correlation was derived from MK-B assembly (15x15) data only. It is applied to both MK-B and MK-C assemblies. The recommended cold-to-hot correction factor of 1.2 has been included in S_{gap}. In converting the above rod bow correlation into a $S_{95/95}$ correlation B&W uses a burnup-dependent multiplier, which accounts for batch-to-batch variations in gap closure. For burnups in excess of 5,900 MWd/MTU, this results in a multiplier greater (i.e., more conservative) than the earlier NRC recommended 1.5 value.

2.2.2 Neutronics

The DOT code (reference 7) was used to calculate the power distribution for a 5x5 fuel rod array. The effect of rod bowing on the center-rod power distribution was calculated for different magnitudes and azimuthal directions of bow. The 5x5 array of fuel rods was surrounded by a homogenized fuel/moderator region. Reflective boundary conditions were employed. Macroscopic cross sections were calculated with the ANISN code (reference 8) using five thermal groups and one fast group. The cylindrical geometry of the fuel rods was approximated in rectangular coordinates.

2.2.3 DNBR

2.2.3.1 Experimental Data

Babcock & Wilcox has tested two 5x5 non-uniform guide tube bundles. These bundles (C9 and C10) were identical in design except that in the C10 bundle, one of the hot rods was bowed into the guide tube channel to achieve approximately 55% closure in the gap. Critical heat fluxes were measured for different pressures and flow rates. The relative heat fluxes for the eight rods surrounding the center guide tube were 1.117 for test C9 and 1.102 for test C10.

2.2.3.2 Analysis

For the subchannel analysis, the LYNX2 computer code was used in conjunction with the B&W MK-C CHF correlation (BWC). Critical heat flux (CHF) uncertainties were determined. The determination of the DNBR penalty was based on a combined deterministic-probabilistic approach thus not completely following the NRC recommendation for the calculation of the DNBR penalty (reference 2).

2.3 Summary of Results

2.3.1 Neutronics

The results of the neutronics analysis show that rod bow of 100 mils leads to a power change of less than 3% in the rod closest to the bowed rod. Only single rod bow has been analyzed in the 5x5 fuel rod array. The effect of the reflective boundary conditions on the prediction of power peaking is not discussed. The cross section sensitivity also is not addressed in the report.

2.3.2 Mechanical

Babcock & Wilcox states that fretting wear is of no consequence because of (1) the low probability that rod-rod contact will occur, (2) the small amount of relative motion and (3) the low contact force in the case contact does occur.

2.3.3 Thermal-Hydraulics

For MK-B and MK-C fuel with a gap closure corresponding to 40,000 MWd/MTU, B&W calculates DNBR reductions of a few percent. However, these penalties are considered insignificant and unnecessary, because the power production capability of fuel decreases with burnup. According to B&W analyses, fuel assemblies with burnups of 24,000 MWd/MTU or greater cannot produce sufficient power to achieve design limiting peaking values. At 24,000 MWd/MTU, the DNBR penalties calculated by B&W for MK-B and MK-C fuel are less than 1%. On this basis, B&W claims that a DNBR penalty due to fuel rod bowing does not have to be considered for reactor licensing.

3.0 Summary of Technical Evaluation

The bowing of fuel rods results in a deviation of fuel rod straightness and a subsequent variation in the fuel rod-to-rod spacing. The major concerns associated with fuel rod bowing are (1) the reduction in fuel rod-to-rod spacing and resulting decrease in margin to DNBR and (2) the increase in fuel rod-to-rod spacing and resulting increase in local power peaking. Also of concern are the potential effects of fuel rod fretting and corrosion which may arise as the fuel rod spacing is reduced to contact.

The B&W method for treating these effects is described in the fuel rod bowing topical report, BAW-10147P, described in the previous section. This topical report, the included references, associated NRC/B&W correspondence and submittals were the subject of this review. The more important questions that were raised during the course of the review together with the B&W responses are to be included as part of the approved version of the topical report. During the review several areas were identified as having high relative importance and/or a substantial degree of uncertainty and to some extent the review was focused on these areas. These included (1) the gap closure data base and its representation, (2) the measurement and determination of the DNBR penalty as a function of rod displacement, (3) the neutronics calculations of the bowing effects on local pin powers, and (4) the statistical method used to determine the 95/95 tolerance limits on DNBR and F_Q. The evaluation of these concerns is described in the following.

3.1 Gap Closure Data Base and Representation

The B&W gap closure data base and its representation were reviewed in detail. Areas of special concern included the methods used to measure the rod-to-rod spacings, the extent to which these measurements span the required (B&W et al.) fuel designs and expected operating conditions, and the interpretation and correlation of these measurements (vs. exposure, span length, etc.). The B&W response to questions raised as a result of these and related concerns (reference 9) has been evaluated and generally found to be satisfactory.

3.2 Determination of the DNBR Penalty

The B&W measurements and correlation of the DNBR rod bowing penalty vs. gap closure and the use of this penalty function in the determination of a DNBR penalty were reviewed in detail. Areas of special concern included the penalty threshold and contact penalty, and the interpretation of the DNBR penalty data. The B&W response to questions raised as a result of these and related concerns (reference 9) has been evaluated and generally found to be satisfactory.

3.3. Neutronics Calculations

The neutronics calculations of the bowing effects on local pin powers were reviewed in detail. Areas of particular concern included the calculational modeling (geometry, cross sections, numerical procedures and solution, etc.) and accuracy, the extent to which the calculated pin power sensitivities span the required fuel designs and operating conditions, and the correlation of the numerical results. The B&W response to questions raised as a result of these and related concerns (reference 9) has been evaluated and generally found to be satisfactory. However, the question of assembly bowing requires some discussion.

<u>ASSEMBLY BOWING</u> - Out-of-pile inspections (references 10, 11 and 12) at several plants have detected large fuel assembly bowing on the order of several hundreds of mils. Such large assembly bowing is an order of magnitude greater than that of fuel rod bowing and can primarily affect both DNB and loss-of-coolant accident(LOCA) margins of peripheral fuel rods.

The DNBR of peripheral rods is significantly higher than that of interior rods of equal power. This is because peripheral rods (a) have no adjacent unheated surfaces to enhance the reduction in DNBR and (b) are subjected to greater cooling. Also, peripheral rods are generally at lower power than central rods and a reduction in assembly gap will reduce the relative peripheral rod powers even further. Consequently, the interior fuel rods, which are essentially unaffected by fuel assembly bowing, will remain DNBR limiting.

The impact of assembly bowing on the LOCA margin arises due to the increased local neutron moderation and concurrent power increase in the peripheral rods that accompanies the widening of the inter-assembly gap.

Babcock & Wilcox has performed (reference 9) PDQ diffusion theory calculations of a 2x2 fuel assembly array in order to assess the effects of assembly bowing on local pin powers. The calculations considered two assembly configurations including assembly arrangement with nominal gaps and a perturbed configuration in which one fuel assembly is bowed diagonally away from its three adjacent neighbors. The central inter-assembly gaps adjacent to the displaced assembly were increased from 51 mils (nominal) to 102 mils while the outer adjacent gaps were reduced to zero. The specific assemblies selected were two 3.02% and two 2.06% enriched UO_2 MARK-3 assemblies representative of typical fresh/depleted reload assembly shuffle patterns.

The 51 mil increase in inter-assembly gap resulted in a 2.8% maximum increase in peripheral rod power. It is expected that this sensitivity is applicable to both the calculated diagonal assembly displacement as well as a lateral assembly displacement in which only one of the four central gaps is increased.

While assembly bow effects have not been incorporated in the F_Q peaking factor uncertainty, we believe that the conservatisms identified in response to question 6 together with the conservatisms listed below are sufficient to offset this deficiency when the 95/95 increase in inter-assembly gap is not significantly greater than ~50 mils.

a) Assembly bow measurements have been made out-of-pile under relatively unrestrained conditions. In pile, there are physical constraints imposed on the assembly by the upper and lower core plates as well as neighboring assemblies or the core shroud. These restraints are presently unquantified, though are probably very significant.

b) In the calculation of the F_Q rod bowing penalty, the worst span bow and a 95/95 closure is used (together with a 95/95 one-sided upper tolerance factor on the F_Q penalty) hence providing additional available conservatism.

c) Increased assembly gaps have their greatest impact on the rows of rods near the periphery of the assemblies. For geometries and core arrangements in which peak power rods are inboard from the gaps, the resultant assembly bow effects on peaking are very small.

d) Worst assembly bow peaking increases would occur in assemblies where corner rods are initially the peak rod with nominal gaps. This commonly occurs in assemblies with large numbers of poison rods. These assemblies usually have low burnup and actual rod bow effects are still small, even though the F_Q penalty typically calculated for rod bow is at a high burnup corresponding to relatively large bowing.

e) Power peaking perturbations tend to "heal themselves." In a given assembly, peak power increases in a corner rod will quickly decrease in magnitude as burnup accumulates allowing the peak power locations to move inboard.

f) The present calculation of the total peaking factor includes separate multipliers for the densification power spike penalty and the penalty representing the statistical combination of the nuclear reliability factor, the engineering hot channel factor and the rod bow peaking factor. If B&W were to include the spike factor in the statistical combination with the other three factors, the resulting factor would be less than the product of the original two penalties, thereby yielding a peaking credit.

g) Since the nuclear reliability factor described in the topical report BAW-10119-A, "Power Peaking Nuclear Reliability Factors," for the worst combination of peak power and assembly radial-local factors is less than the standard B&W analysis value of 1.075, there is a peaking credit available. This conservatism was recognized in the NRC topical report evaluation of BAW-10119-A.

h) The limiting location in the fuel assembly generally occurs between the 2- and 3-foot elevations. The amount of bow at these heights is less than the bow at the core midplane, resulting in a reduction in the effect of assembly bow on any associated power peaking increase in the region of greatest importance.

i) The limiting peak rod location in the core in the lumped burnable poison (LBP) shuffle scheme (used in all but one operating B&W reactor) is normally on the periphery of a fresh LBP-containing assembly and is sensitive to the effects of assembly bowing. However, since the assembly is in its first cycle of operation, the actual rod bow power peaking effects are zero or very small, compared to the conservative value used in topical report BAW-10147P. Thus the rod bow peaking allowance is available to offset peaking increases caused by assembly bow, since the maximum effects of fuel rod bowing on the limiting pin in the core are not expected to occur simultaneously with the effects of assembly bowing.

If the 95/95 inter-assembly gap increase exceeds 50 mils the effect of the assembly bow on F_Q may be offset by available power margin between the peripheral rods and the assembly peak rod. Based on neutronic sensitivity calculations, a gap increase of $\sim$ 10 mils may be offset by a 1% margin between the assembly peak rod power and the peripheral assembly rod powers. If sufficient margin between the peripheral and peak rod powers is not available to offset the expected inter-assembly gap increase, a detailed evaluation of the effects of assembly bow and local power peaking should be performed (including, e.g., the effects of burnup, burnable poison rods, water holes, margin to design limit peaking, core loading and the distribution of gap increases considering mechanical tolerances).

3.4 F_Q and DNBR Statistical Methodology

The B&W statistical methodology for determining the F_Q and DNBR 95/95 tolerance limits and rod bowing penalties has been reviewed in detail. Of particular concern are the methods for integrating over the individual rod bowing displacements, the determination of the mean and variance of bowing penalties, and the method for accounting for multiple rod displacements. The B&W response to questions raised as a result of these and associated concerns (reference 9) has been evaluated and generally found to be satisfactory. However, the statistical method for determining the DNBR penalty requires some discussion.

DNBR STATISTICAL METHODOLOGY - The statistical method used by B&W in determining the DNBR penalty is considered incomplete in that it does not properly account for the bowing of all eight rods surrounding the hot rod in the core. In fact, the proposed method is one-dimensional, considering the closure of only the two colinear gaps on the left and right of the hot rod and neglecting the closure of the remaining six gaps. Four of the remaining gaps are associated with "diagonal" neighbor rods which are ~ 2.5 times farther away than the closer neighbors. Consequently, the probability of the gap to one of these diagonal neighbors being smaller than the minimum gap to the closer neighbors is neglibible, and the effect of bowing of the four diagonal neighbors may be neglected. The increase in the DNBR penalty due to the inclusion of the remaining two closer gaps has been determined and results in an increase in DNBR penalty by a factor of ~ 2.

Also, B&W calculates an average DNBR rod bowing penalty, $\bar{\delta}$, and takes no additional penalty for uncertainty due to variability in gap closure as recommended in reference 2. This simplification is non-conservative and will result in an under-prediction of the DNBR penalty.

While these are significant deficiencies in the B&W rod bowing DNBR statistical methodology, we agree with B&W that there are several conservatisms in their treatment that provide sufficient margin to offset these deficiencies. That these conservatisms are sufficient to offset these deficiencies has been demonstrated quantitatively by performing DNBR-penalty sensitivity calculations. The conservatisms include the following:

a) The worst span bow for each assembly is used to obtain the gap closure correlations. In many cases the worst span is in the lower regions of the assembly, where minimum DNBR is not likely to occur.

b) The use of best estimate closure correlations rather than 95/95 correlations will reduce the DNBR penalty substantially. It should be noted that B&W uses an effective 95/95 upper tolerance factor explicitly in the calculation of the mean penalty to protect from DNBR. While it is standard practice to include this factor in determining the effects of uncertainties, it is conservative to use it in the calculation of the mean penalty.

c) The DNBR penalty will increase with burnup because of the associated reduction in gap spacing. Conversely, nuclear peaking tends to decrease with burnup. Babcock & Wilcox has conservatively not accounted for this fuel depletion effect.

d) The DNBR experiments, which employed a displaced rod and which were designed to assess the effect of bowing of one specific rod, had generalized bowing (though small) throughout on all of the other simulated fuel rods. The bowing was attributable to two factors; (a) the simulated fuel rods were not manufactured perfectly straight and (b) when power was applied to the ferromagnetic cartridge inserts, magnetic forces between rods were induced thus creating widespread bowing of small magnitudes. Hence, the DNB experiments and the respective analyses of the DNBR penalties are not strictly applicable to only situations involving one large bow. Rather, these penalties are more applicable to actual and more probable inpile situations and associated analyses involving a large bow in a field of several lesser bows. Consequently, this aspect, though unquantifiable, will partially compensate for the use of a 2 rather than an 8 bowed-rod DNBR penalty calculation in the DNBR methodology.

e) Cladding creepdown increases the nominal rod-to-rod spacing. This phenomenon was not modeled in the B&W analysis.

f) There is modeling conservatism in the treatment of reduction in DNBR as a function of gap closure. As shown in Figure 1, the proposed B&W licensing curve (depicted by the solid line) bounds the expected behavior (hypothesized by the dashed curve).

g) The use of a conservative penalty function in which the penalty threshold and contact penalty were selected in an extremely conservative manner provides additional conservatism.

h) The use of a gap closure distribution which allows negative rod-rod spacings (i.e., use of a normal distribution which is not truncated at contact) and a penalty function which contributes a DNBR penalty for these non-physical situations provides additional conservatism in the DNBR penalty calculation.

Other responses requiring some note or comment are the following. In response to question 12, B&W provided a detailed description of the methods used in the neutronic sensitivity calculations, and in response 28, the basis for the DNBR penalty function is provided. Conservative assumptions are made at several points in the development and application of the proposed methodology, and in response 6 B&W identifies the major sources of conservatism and provides estimates of the potential margin associated with each. While we have not performed an independent determination of these estimates, we have concluded that these effects do provide a substantial margin of conservatism in the B&W methodology and are more than adequate to compensate for other small non-conservatisms.

4.0 Technical Position

The B&W data base and calculational procedures proposed for the analysis of the effects of fuel rod bowing have been reviewed in detail. Consideration has been given to the basis and accuracy of the individual elements of the proposed methodology as well as the overall conservatism and adequacy of the resulting F_Q and DNBR penalties. Based on this review, we conclude that the proposed methodology provides an acceptable means for analyzing the effects of fuel rod bowing and determining the F_Q and DNBR rod bowing penalties.

This evaluation is limited to the fuel designs, exposures and conditions stated in the report and supporting documentation and is based, in part, on the B&W gap closure representation and the specific assumptions made in formulating this methodology. We recommend B&W perform continued fuel surveillance to ensure confidence in these assumptions and bases.

ACKNOWLEDGMENT

The author wishes to thank Drs. Dale A. Powers and Ralph O. Meyer of the Core Performance Branch of the NRC for guidance and several valuable discussions during the course of this review.

Thanks are also due to Drs. Wolfgang P. Barthold, Laurance Eisenhart and John R. Weeks for reviewing various sections of the topical reports and to Dr. Barthold for his contribution to the writing of the introductory section of this technical report.

References

1. Letter, C. Eicheldinger(W), to D.F. Ross (NRC), NS-CE-1161, August 13, 1976.

2. Letter, D. B. Vassallo (NRC), to J.H. Taylor (B&W), June 12, 1978 with enclosure, "Calculation of the Effect of Fuel Rod Bowing on the Critical Heat Flux for Pressurized Water Reactors," NRC, April 1978; revised by letter, D.B Vassallo (NRC) to J.H. Taylor (B&W), September 15, 1978.

3. Letter, J.H. Taylor (B&W)to D.B. Vassallo (NRC), "Determination of Fuel Rod Bow DNB Penalty," with enclosures, December 13, 1978.

4. Letter, J.H. Taylor (B&W) to S.A. Varga (NRC), enclosure 1, Appendix A, (Rev. March 26, 1979), "The Analysis of the Bowed and Unbowed CHF Test Data," March 27, 1979.

5. Letter,J.H. Taylor (B&W) to S.A. Varga (NRC), "B&W Rod Bow Penalty Calculations," June 22, 1979.

6. Letter, L.S. Rubenstein (NRC) to J.H. Taylor (B&W), "Evaluation of Interim Procedure For Calculating DNBR Reductions Due to Rod Bow," October 18, 1979.

7. "The DOT-IV Two-Dimensional Discrete Ordinates Transport Code with Space-Dependent Mesh and Quadrature," Oak Ridge National Laboratory report ORNL/TM-6529, August 15, 1978.

8 "ANISNBW- A One Dimensional Discrete Ordinates Transport Code," Rev. 2. Babcock & Wilcox report NPGD-TM-491, October, 1980.

9. "Responses to the First and Second Round Questions on BAW-10147P," Letter J.H. Taylor (B&W) to James R. Miller (NRC) dated May 17, 1982. "Supplementary Response to Second Round Question-26 on BAW-10147P," letter, J.H. Taylor (B&W) to Carl Berlinger (NRC), July 23, 1982.

10. "Interim Report: Surry Unit 2 End-of-Cycle 2 Onsite Fuel Examination of 17x17 Demonstration Assemblies After One Cycle Of Exposure," Westinghouse report WCAP-8873, January 1978.

11. "Pool Side Examination of PWR Demonstration Fuel Assemblies and Creep Specimens: End-of-Cycle 2," Babcock & Wilcox report LRC-4733-5, August 1978.

12. "Examination of Calvert Cliffs 1: Test Fuel Assembly After Cycle 3," CE/EPRI report RP 586-1, September 1979.

Figure 1

DNBR PENALTY DEPENDENCE ON ROD BOW

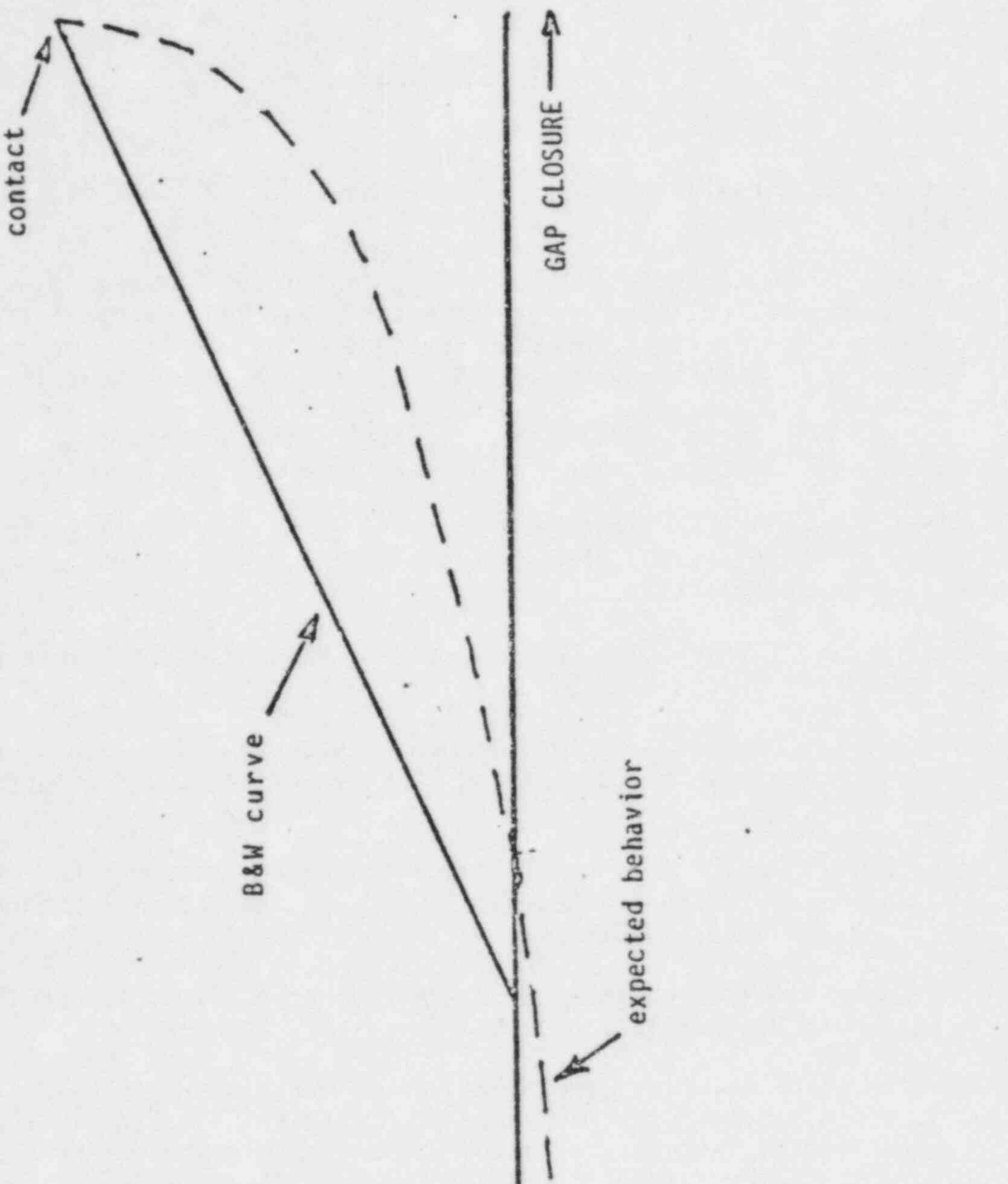

Babcock & Wilcox
Utility Power Generation Division
Lynchburg, Virginia

Topical Report BAW-10147A, Rev. 1

May 1983

Fuel Rod Bowing in Babcock & Wilcox Fuel Designs

Project Engineer: J. C. Moxley

Principal Contributing Authors: E. J. McGuinn, A. S. Heller
D. A. Farnsworth, J. C. Moxley

Key Words: Gap Closure, DNBR, Burnup, Power Peaking

ABSTRACT

The report describes an evaluation of the extent and effects of fuel rod bowing in Babcock & Wilcox fuel assemblies during irradiation. The correlation of an extensive data base of rod bow measurements has resulted in a method of predicting the magnitude of rod bow as a function of burnup. The results of bowed rod critical heat flux tests along with the rod bow prediction equation are incorporated into a correlation to be used for predicting departure from nucleate boiling ratio penalty as a function of burnup. The effects of rod bow on power peaking uncertainty and on the mechanical performance of the cladding are also addressed.

NOMENCLATURE

AEC	U.S. Atomic Energy Commission, now U.S. Nuclear Regulatory Commission
A	Area to adjust probability distribution to unity
a, a_L	Penalty at full closure, upper limit of penalty at full closure
Bu	Burnup
C, C_o	Gap closure, nominal or as-built value
C_{Bu}	Statistical model correction factor
CHF	Critical heat flux
DNBR	Departure from nucleate boiling ratio
D'	Test of normality of a data distribution
d, d_i, d_j	Differential, constants of integration
e	Exponential function
f(*)	Function of variable in brackets
gap closure	The change in the water channel gap expressed as a ratio to the nominal gap
K	Gap closure value below which no DNBR penalty exists
ℓ_o	Limit of integration, a constant
Mark B	B&W designation for 15 by 15 array fuel assembly design
Mark C	B&W designation for 17 by 17 array fuel assembly design
PIE	Post irradiation examination
r	Coefficient of determination, measure of model adequacy
rhs	Right-hand side
rod bow	Lateral deviation of a fuel rod from its theoretical unbowed position in a given span (The standard deviation of the distribution of the water channel gaps within a span is used as a measurement of rod bow for that span.)
Span	Fuel rod axial region between spacer grids
Tolerance interval; global	An interval that brackets a portion of the population with a specified confidence; over the entire data range
w	Variable of integration

water channel	The gap between adjacent fuel rods or adjacent fuel rod and guide tubes
worst span	The span of a fuel assembly that exhibits the largest magnitude for the standard deviation of the distribution of water channel measurements for that assembly
Δc	Change in gap closure
δ, δ_c, δ DNBR	Reduction — at closure, for DNBR
σ_j, σ/C_o	Bow, standard deviation of gap closures, relative to as-built
σ_a	Uncertainty in penalty at full closure
σ_e	Standard error of estimation
$\sum$	Notation of summation
π	pi
$\phi(*)$	Normal integral of variable integrated to upper value in brackets

CONTENTS

CONTENTS (Cont'd)

List of Tables

List of Figures

Figures (Cont'd)

1. INTRODUCTION

1.1. Summary

The phenomenon of fuel rod bowing was reported to the Atomic Energy Commission (AEC) in 1973 as a result of observations in Westinghouse pressurized water reactors (PWRs). The term rod bowing refers to the deviation in the straightness of a fuel rod caused by irradiation effects. The immediate concerns of fuel rod bow were the potential effects on bundle power distribution and on the margin of the fuel rods to departure from nucleate boiling (DNB).

In June 1974, the AEC requested that Babcock & Wilcox (B&W) review an analytical model developed to predict the magnitude of rod bowing and evaluate the B&W fuel design with the analytical model. In September 1974, B&W met with the AEC to discuss the unique features of the B&W fuel design that would preclude significant bowing. At this meeting, B&W reviewed its plans for post-irradiation examination (PIE) of fuel assemblies, which would measure fuel rod bow.

The continuing AEC concerns regarding fuel rod bow subsequently resulted in the imposition of a DNBR penalty on design analyses, which was based on conservative equations used to predict the magnitude of the bowing. The penalty equation assumed that the DNBR reduction due to rod bow varied linearly with bow (gap closure). The results of critical heat flux (CHF) tests performed for bundles containing rods bowed to partial and full contact were reported to the Nuclear Regulatory Commission (NRC) and were made available to all fuel manufacturers. The NRC evaluation of the results concluded that DNBR penalty at rod-to-rod contact was not being predicted conservatively by existing techniques.

On September 10, 1976, B&W submitted a report to the NRC presenting the results of rod bow measurements of B&W fuel. the results indicated a small amount of bow evident on the measured fuel assemblies, which had been irradiated to a burnup up to 20,000 MWd/mtU. Included in this report was a conservative method of predicting the magnitude of rod bow. As part of a total program addressing rod bow, B&W met with the NRC staff on February 25, 1977, to discuss plans for CHF tests to determine the effect of rod bow on the B&W Mark C 17×17 fuel assembly.

In June 1978, the NRC provided to B&W a method of conservatively calculating the magnitude of rod bow and the corresponding DNBR penalty.[1] The NRC suggested that B&W use this procedure to predict rod bow penalty as an interim measure until B&W submitted and received approval on a topical report on rod bow. In December 1978, B&W submitted an interim method for calculating DNBR penalty based on the NRC procedure.[2] The interim calculational method incorporated gap closure data from the B&W PIE program and preliminary CHF test data for a bundle containing a rod bowed to 55% closure, which was a significantly greater gap closure than had been measured in the PIE program. Final CHF test data were submitted to the NRC in March 1979[3], and the test results were incorporated into a final submittal of an interim DNBR penalty calculational method in June 1979[4]. This submittal received NRC approval in October 1979.[5] To date, the B&W rod bow measurement program has produced more than 125,000 measurements, including 26 fuel assemblies from eight manufacturing batches, two basic fuel assembly designs, two reactors, and fuel assembly average burnups to 40,000 MWd/mtU.

1.2. Conclusions

The magnitude of rod bow, or rod-to-rod gap closure, has been determined as a function of fuel assembly burnup. Equations developed from a statistical analysis of the rod bow data conservatively predict the increase in rod bow with burnup for B&W fuel designs. The results of the CHF tests conservatively indicated that no DNBR penalty is applicable for gap closure up to for B&W fuel designs.

The statistical combination of the rod bow measurement data and the CHF test data resulted in a DNBR penalty equation as a function of fuel assembly burnup. This equation is represented by the curves shown in Figures 7-1 and 7-2 for Mark B and Mark C fuel. The penalty curves are illustrated for fuel assembly burnup to 40,000 MWd/mtU and show a penalty that varies from at MWd/mtU to DNBR reduction (Mark B) and (Mark C) at MWd/mtU.

This penalty is considered to be insignificant and unnecessary because the power production capability of fuel assemblies diminishes with irradiation to the extent that fuel assemblies with burnups of 24,000 MWd/mtU or more cannot produce enough power to achieve design limit peaking values. Therefore, no DNBR reduction due to fuel rod bow need be considered in reactor licensing.

2. FUEL ASSEMBLY DESIGN — GENERAL DESCRIPTION

This section describes the design characteristics of B&W 15×15 Mark B and 17×17 Mark C fuel assemblies. Both fuel assembly types have the same basic design configuration and employ similar manufacturing techniques and assembly fabrication procedures. Table 2-1 is a design comparison of the assemblies.

The Mark B fuel assembly is shown in Figure 2-1 with its major components identified. It consists of Zircaloy-clad fuel rods, Zircaloy guide tubes, Inconel spacer grids, and stainless steel end fittings.

The upper and lower end fittings are rigidly connected to the guide tubes. The two end grids are attached to the end fitting through a reinforced extension of the outside grid strip. The six intermediate spacer grids are not attached rigidly to the guide tubes. There is a slight interference between the guide tubes and the spacer grid cell saddles. This interference ensures proper positioning and support of the guide tubes and allows the intermediate grids to move axially with fuel rod growth. This design reduces both the number of rods that experience axial restraint and the magnitude of the restraint loads that arise from fuel rod-to-guide tube differential expansion or growth.

During fabrication, keys hold the grid cells in the open position so that the fuel rods can be inserted freely without axial force. After all rods are in place, the keys are removed, closing the cells. This technique eliminates residual axial forces in the rods.

The assemblies are fabricated with the fuel rods in contact with the lower end fitting and with a clearance between the rods and the upper end fitting to accommodate fuel rod thermal expansion and irradiation growth throughout the life of the assembly.

The configuration of the 17×17 Mark C assembly is similar to that of the 15×15 Mark B design, as shown in Figures 2-1 and 2-2. The major differences are that the fuel rod diameter, thickness, and pitch have been proportionally reduced to accommodate the 17×17 matrix within the same assembly envelope. The design features of the fuel rod/spacer grid/guide tube interface are identical to those of the Mark B design.

The data reported for the Mark C assemblies were obtained from two sets of demonstration assemblies used to verify the design. These assemblies were fabricated with standard Mark C spacer grids and fuel rods except that the standard Mark C fuel rod cladding is 0.0005 inch thicker. The upper end fitting was modified to be compatible with both the fuel handling equipment and the reactor internals of the host Mark B reactor.

Table 2-1. Comparison of Fuel Assembly Designs

	Mark B	Mark C	Mark C 17×17 demonstration assemblies
Fuel Assembly			
No. of fuel rods	208	264	264
No. of guide tubes	16	24	24
No. of instrument tubes	1	1	1
No. of spacer grids	8	8	8
Rod pitch, in.	0.568	0.502	0.502
Rod-to-rod gap, in.	0.138	0.123	0.123
Fuel Rod			
Fuel stack length, in.	143	143	143
Cladding OD, in.	0.430	0.379	0.379
Cladding ID, in.	0.387	0.331	0.332
Cladding thickness, in.	0.0265	0.0240	0.0235
Guide Tube			
Tube OD, in.	0.530	0.465	0.465
Tube ID, in.	0.498	0.430	0.430

Figure 2-1. Mark B Fuel Assembly

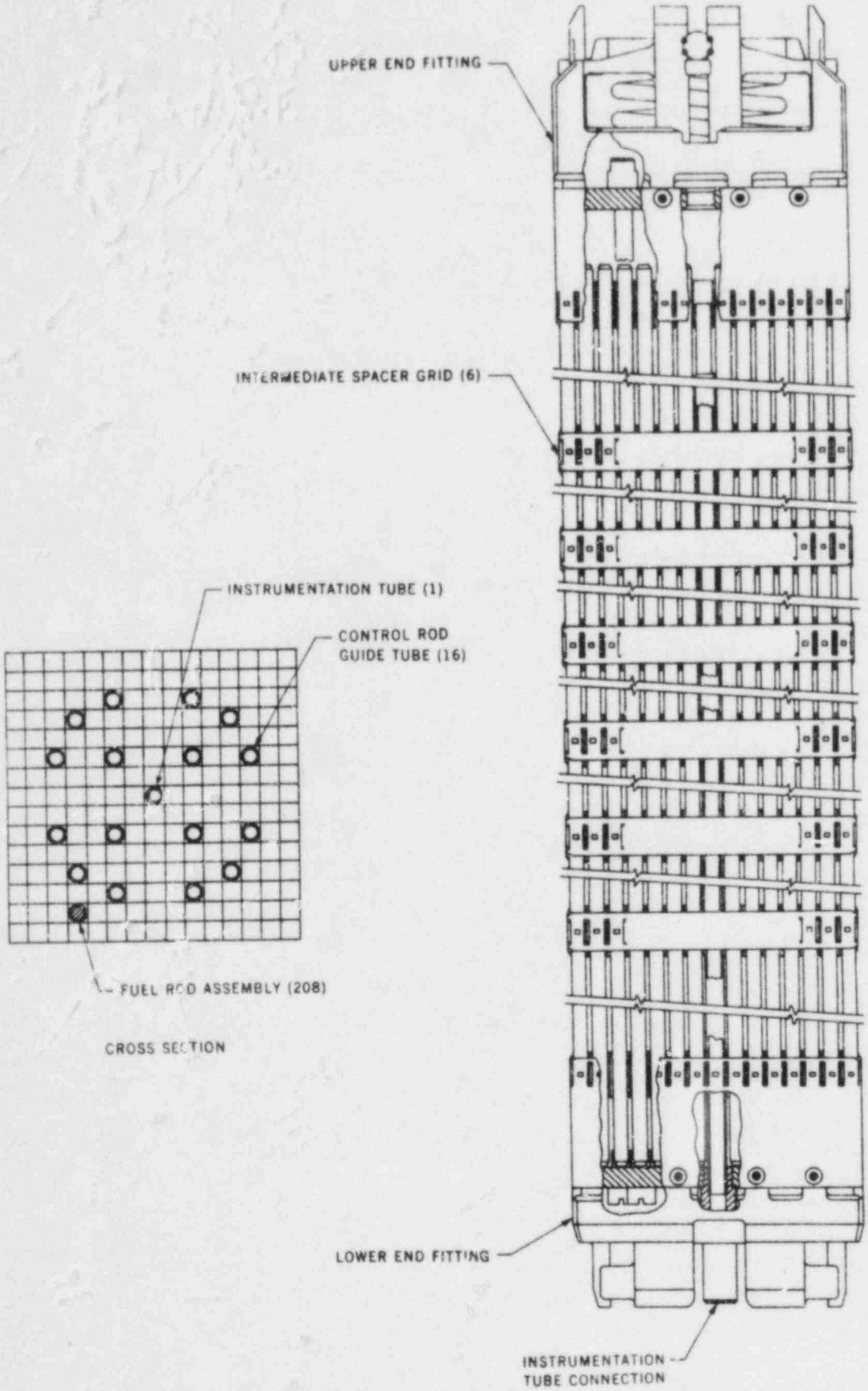

Figure 2-2. Mark C Fuel Assembly

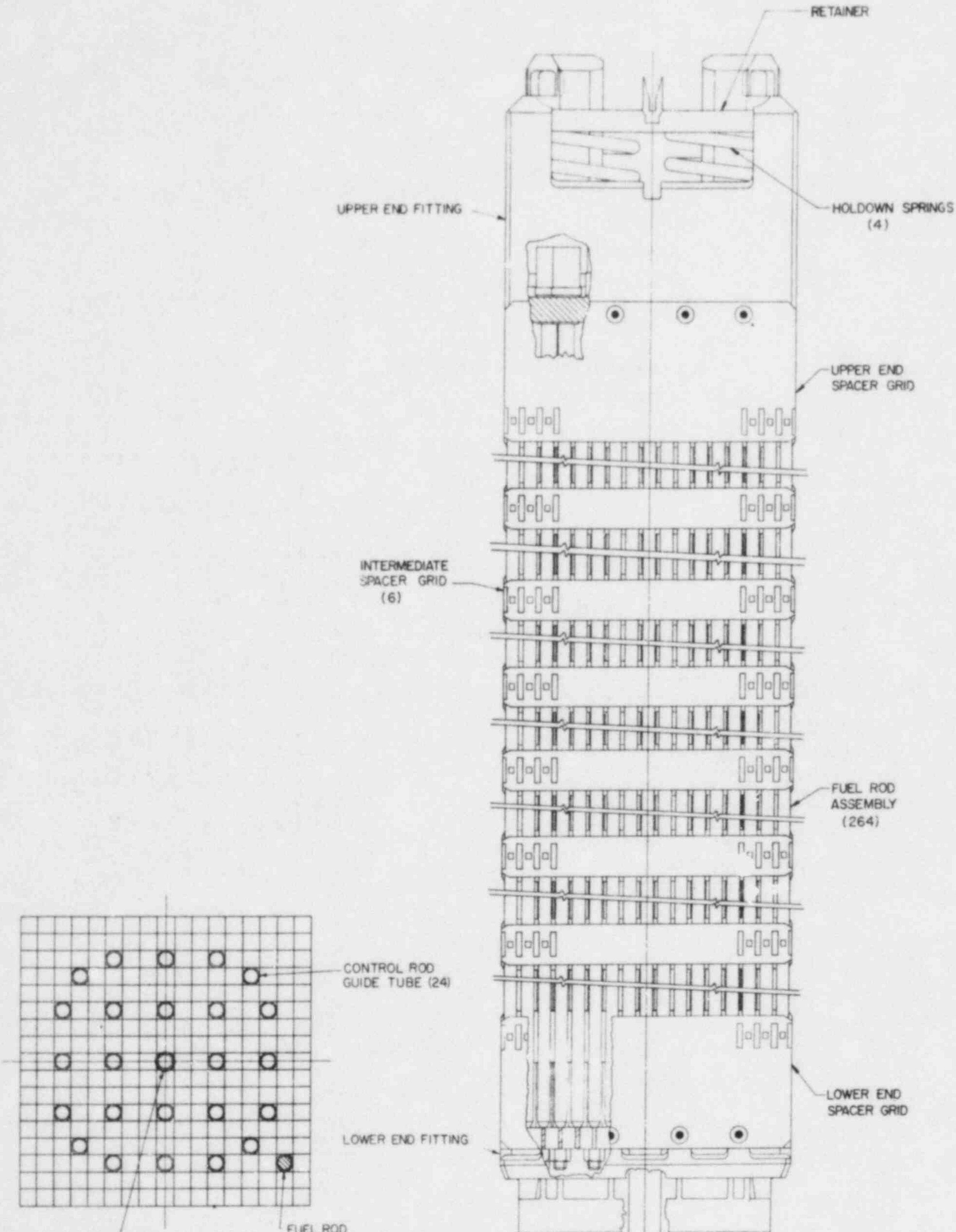

3. WATER CHANNEL MEASUREMENTS

The water channel gaps were measured in both irradiated and unirradiated fuel assemblies of the Mark B and Mark C designs. These data were reduced into a span by span summary for each assembly (Appendix B). The statistical summaries for the worst spans were combined into a data base for use in the development of a correlation relating rod bow to burnup as described in section 5.

The statistical analysis used to characterize the rod bow data is based on the assumption that the data follow a normal distribution as described in Appendix C.

3.1. Measurement Technique

Water channel spacing is the distance between adjacent rods in an assembly at the midplane between spacer grids. These spacings can be classified as rod-to-rod, rod-to-guide tube, or rod-to-instrument tube spacings. The nominal values for these spacings for both the 15×15 Mark B and the 17×17 Mark C assemblies are shown in Figure 3-1. Water channel measurements are usually taken between all rods, guide tubes, and instrument tubes in the two orthogonal directions at the midspan planes of the assembly as shown in Figure 3-2.

The water channel spacings are measured during post-irradiation examinations with the assembly in a test frame mounted on the side of the spent fuel pool at the reactor site. The water channel measuring device consists of a "Sulo" probe attached to a pneumatic plunger that inserts the probe through the water channel gaps between two rows of rods. The "Sulo" probe is a thin wand with strain gages attached to leaf springs that change their resistance proportionally when they are deflected. A special fixture is used to position the Sulo probe axially and transversely to the desired water channel of an assembly. The probe measures the distance between the pairs of rods on each insertion. A calibration signal for the probe is obtained before each insertion by passing the probe through two pairs of tungsten carbide pins with known separations (nominally 100 and 150 mils). The water channel measurements are determined by comparing the measured signal to these values. The data are recorded on a continuous time based chart recorder. Appendix A contains a complete description of the measurement techniques.

During the actual measurement of the water channel spacing, the Sulo probe spreads the fuel rods slightly, increasing the measured spacing and biasing the raw data. A linear correction is used to adjust all the individual water channel measurements of an assembly so that representative spacings can be obtained. This correction is proportional to the amount the leaf springs are deflected during measurement. The procedure for this correction is given in Appendix A.

The corrected midspan gap measurements are used to calculate the rod bow statistics. The standard deviation of gap, often referred to as rod bow, was determined for each plane, using the following equation:

$$\sigma = \left[\sum_{i=1}^{N} \frac{(X_i - \bar{X})^2}{N - 1}\right]^{\frac{1}{2}} = \left[\frac{\sum_{i=1}^{N} (X_i)^2 - \frac{1}{N}\left(\left(\sum_{i=1}^{N} X_i\right)^2\right)}{N - 1}\right]^{\frac{1}{2}} \tag{3-1}$$

where X_i = individual gap measurements,

$\bar{X}$ = average of measurements,

N = number of measurements in the data set.

3.2. Data Base

The data base used to develop the rod bow prediction model was obtained from an extensive measurement program on irradiated and unirradiated assemblies. Water channel measurements were taken on assemblies of both the 15×15 and 17×17 configurations. These assemblies are representative of a wide range of manufacturing and operational variations.

Table 3-1 is a listing of the rod-to-rod water channel gap measurements used to develop the rod bow to burnup correlations (section 5) for the Mark B and Mark C assemblies. These data are for the worst span of the assembly, which is defined as the span that exhibits the largest magnitude for the standard deviation of rod-to-rod measurements. Considering only the worst-span gaps ensures that the correlation developed from these data bounds the span-to-span variations that may exist within an assembly.

A complete summary of all the water channel measurements for each midspan measured is presented in Appendix B. The data are presented in statistical form for 26 assemblies from eight manufacturing batches and represent over 125,000 individual rod-to-rod gap measurements for fuel assemblies with burnups up to 40,000 MWd/mtU.

Table 3-1. Rod-to-Rod Water Channel Measurements

Fuel assembly			Rod-to-rod gap for worst span			
FA ident	EOC[a]	Assembly avg Bu, 10^3 MWd/mtU	Worst span location, span No.	No. of measurements	Mean[b] gap, mils	Std[c] dev'n mils
Plant A, 15×15 Mark B Assemblies						
1A16	1	10.6		352		
1B04	0	0.0		352		
	2	19.8		176		
1B05	0	0.0		352		
	2	19.7		352		
1B29	0	0.0		352		
	2	20.0		352		
1C04	3	22.0		350		
1C30	1	6.4		311		
	2	15.9		352		
	3	24.6		352		
1C63	0	0.0		352		
	1	7.6		352		
	2	16.6		352		
	3	25.1		352		
1C66	0	0.0		335		
	1	9.8		352		
	2	18.5		352		
	3	26.5		352		
1D13	3	31.2		352		
	4	39.8		298		
1D26	3	31.2		351		
	4	39.8		280		
1D40	0	0.0		352		
	1	13.1		341		
	2	24.8		352		
1D42	3	28.2		348		
	4	36.0		226		
1D45	3	31.2		344		
	4	39.8		273		
1D55	3	31.2		352		
	4	39.8		301		

Table 3-1. (Cont'd)

Fuel assembly			Rod-to-rod gap for worst span			
FA ident	EOC[a]	Assembly avg bu, 10^3MWd/mtU	Worst span location, span No.	No. of measurements	Mean[b] gap, mils	Std[c] dev'n, mils
Plant B, 15×15 Mark B Assemblies						
2B15	1	17.2		352		
	2	24.3		352		
2B40	0	0.0		352		
	1	17.2		52		
	2	24.3		352		
NJ008K	1	5.4		352		
	2	16.5		313		
NJ008L	1	5.4		352		
	2	16.5		352		
NJ008M	1	5.4		352		
	2	16.5		352		
NJ008N	1	5.4		352		
	2	16.5		352		
NJ00P7	1	11.0		352		
NJ00PG	1	10.8		352		
Plant B, 17×17 Mark C Assemblies						
NJ0059	0	0.0		310		
	1	5.4		310		
	2	12.1		310		
	3	24.6		310		
NJ005A	0	0.0		380		
	1	5.4		380		
	2	12.1		380		
	3	24.6		380		
NJ00MZ	0	0.0		444		
	1	9.4		444		
	2	22.3		333		
NJ00N	0	0.0		444		
	1	9.4		444		
	2	22.3		444		

Table 3-1. (Cont'd)

Footnotes

(a) EOC: end of cycle; end of cycle zero (0) refers to "as-built."

(b) Mean gap is the mean value for the distribution of gaps as determined from the water channel measurements:

mean gap $= \frac{1}{N} \sum$ gap where N = number of measurements.

(c) Standard deviation is defined as

$$\sigma = \left\{\frac{1}{N - 1} \left[\sum (\text{gap})^2 - \frac{1}{N} \left(\sum \text{gap}\right)^2\right]\right\}^{\frac{1}{2}}$$

where gap = water channel measurement.

Figure 3-1. Nominal Gap Dimensions

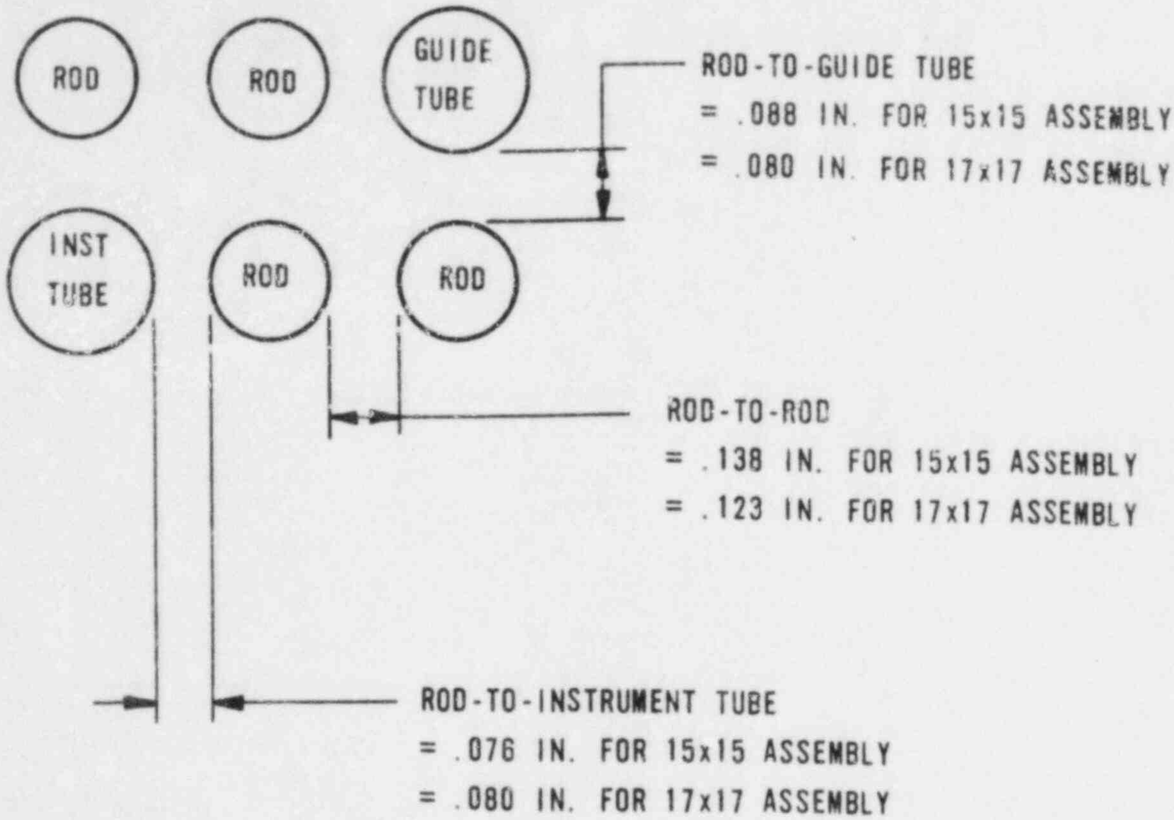

Figure 3-2. Fuel Assembly Span Lengths

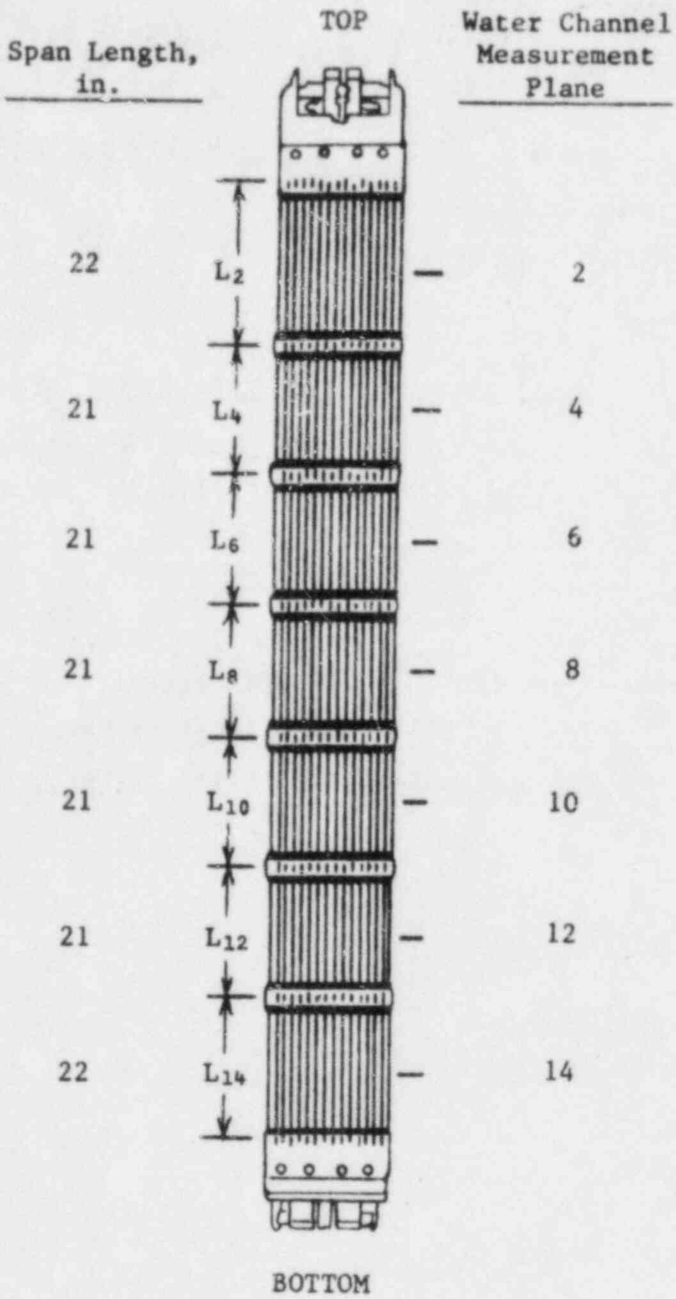

4. VARIABLES AFFECTING ROD BOW

Fuel rod bowing is a phenomenon that is affected by design configuration, manufacturing methods, and fabrication techniques as well as the fuel assembly burnup. To evaluate the importance of assembly variables, statistical techniques were used to investigate water channel gap measurement variations.

An empirical equation was developed to predict the magnitude of rod bow for an assembly as a function of the assembly average burnup. This correlation, described in section 5, is based on the variation of rod bow within an assembly. The correlation was adjusted to conservatively bound the batch-to-batch variations.

4.1. Variation of Rod Bow Within an Assembly

Variation of rod bow within an assembly may be characterized in the following categories:

- Rod-to-rod variation within a span.
- Row-to-row variation within a span.
- Span-to-span variation within the assembly.

The data base (section 3) used in the development of the correlation between rod bow and burnup contains all the rod-to-rod measurements for the worst span. Therefore, the rod-to-rod variations are inherently included in the statistical analysis.

A summary of the rod-to-guide tube water channel measurements is tabulated in Appendix B. The statistical data for the worst-span rod-to-guide tube gaps are presented in Table 4-1. As shown in Figure 4-1, the standard deviation of the rod-to-guide tube data is less than the standard deviation of the rod-to-rod data (presented in Table 3-1). Therefore, the rod-to-rod data used in the development of the rod bow correlation conservatively bounds the rod-to-guide tube data.

To determine whether a significant row-to-row variation exists within a span, the worst-span rod-to-rod data were divided into two categories: gaps involving peripheral rods and those involving only interior rods. The data in this form are presented in Table 4-2 and Figure 4-2. In a majority of the spans, there is no difference between the two categories at the 95% confidence level using the standard "F" test.

$$\sigma_A^2/\sigma_B^2 \leq F_{5\%} \tag{4-1}$$

where

σ_A and σ_B = standard deviations for peripheral and interion gaps within a span,

$F_{5\%}$ = F distribution at 5% significance level.

The water channel measurements tabulated in Appendix B were reviewed to identify the span-to-span variation in rod bow. In general, the spans below the core midplane had the largest magnitude of the standard deviation of the distribution gap measurements. Table 4-3 presents the distribution of the location of the worst spans for the Mark B and Mark C assemblies. Only the data from the worst span are used in developing the rod bow correlation.

4.2. Assembly Configuration Parameters

Fuel assembly design variations were evaluated for their effects on rod bow by incorporating specific changes into otherwise standard fuel assemblies. The water channel gaps were monitored after each cycle and compared to data from standard assemblies. The gap measurements from these assemblies are included in the data base (section 3.2) used to determine the rod bow/burnup correlation.

4.2.1. Rods-Lifted Assemblies

A standard B&W assembly is fabricated with the fuel rod contacting the lower end fitting. As described in section 2.1, the fuel rods are supported laterally along their lengths by the intermediate spacer grids, which can move axially with the rods relative to the guide tubes. This configuration limits the accumulation of axial strains in the rods.

The effect of contact between the fuel rods and the lower end fitting on rod bow was investigated by fabricating two Mark B assemblies with lifted rods, that is, with a gap between the rod and both the lower and upper end fittings.

Water channel gaps measured on the rods-lifted assemblies after each cycle of operation did not vary significantly from gaps measured for standard assemblies, as shown in Figure 4-3.

4.2.2. Spiral Eccentricity of the Cladding

In theory, when a fuel rod with a large wall thickness eccentricity is subjected to an axial strain, the rod will bow to equalize the eccentric force. The manufacturing processes used to fabricate the fuel rod cladding result in a spiral variation of the wall thickness. The eccentricity of the cladding (E_w) is defined by

$$E_w = \frac{t_{max} - t_{min}}{t_{avg}} \tag{4-2}$$

where t_{max}, t_{min}, and t_{avg} are the maximum, minimum, and average wall thicknesses, respectively. The magnitude of bow may also be affected by the axial spacing of the supports (spacer grids) relative to the spiral pitch of the eccentricity.

To evaluate the effects of spiral eccentricity, two standard Mark B fuel assemblies were fabricated using cladding selectively chosen from a typical manufacturing lot. The selection criterion would theoretically minimize rod sensitivity if spiral eccentricity were a significant consideration in the B&W design. A review of the data shows that the water channel gaps measured on the irradiated spiral eccentricity assemblies did not vary significantly from the gaps measured on other assemblies, as shown in Figure 4-3.

4.3. Fabricated As-Built Rod Bow

As discussed in section 2, the B&W fuel assembly design and manufacturing procedures incorporate several features that tend to reduce both as-built rod bow and rod bow during operation. The as-built water channel measurements were taken at B&W's nuclear fuel fabrication facility using a gang arrangement of Sulo probes. The as-built data are included in section 3.2.

The magnitude of the as-built rod bow is small when compared to rod bow of irradiated assemblies. A review of the data trends for the Mark B assemblies with both as-built and irradiated data shows no clear correlation between initial and end-of-cycle (EOC) values.

4.4. Summary

The following observations were made from the statistical analysis of the gap data. The standard deviation of all the rod-to-rod water channel gaps in the worst span bounds the distribution of all the gaps within the fuel assembly. The difference within the span between the peripheral and the interior gaps is not significant. In general, the standard deviation of rod-to-guide tube gaps is less than the standard deviation of rod-to-rod gaps. In addition, gap measurements from rods-lifted assemblies and spiral eccentricity assemblies did not vary significantly from the standard configuration assemblies. Therefore, the gap between the fuel rod lower end cap and the lower assembly end fitting is not a major factor in the rod bow response of the B&W assembly. The spiral pitch of the fuel rod cladding eccentricity relative to the spacer grid positioning is also not a major factor in rod bow response.

Table 4-1. Rod-to-Guide Tube Water Channel Measurements

FA ident	Assembly avg Bu, 10^3 MWd/mtU	Rod-to-guide tube gaps: Worst span, No.	No. of measurements	Mean gap, mils[a]	Gap[b] std dev'n, mils
1A16	10.6		64		
1B04	0.0		64		
	19.8		32		
1B05	0.0		64		
	19.7		64		
1B29	0.0		64		
	20.0		64		
1C04	22.0		64		
1C30	6.4		60		
	15.9		64		
	24.6		64		
1C63	0.0		64		
	7.6		64		
	16.6		64		
	25.1		64		
1C66	0.0		64		
	9.8		64		
	18.5		64		
	26.5		64		
1D13	31.2		64		
1D26	31.2		64		
1D40	0.0		64		
	13.1		60		
	24.8		64		
1D42	28.2		63		
1D45	31.2		61		
1D55	31.2		64		
2B15	17.2		64		
	24.3		64		
2B40	0.0		64		
	17.2		34		
	24.3		64		
NJ008K	5.4		64		
	16.5		58		
NJ008L	5.4		64		
	16.5		64		

Table 4-1. (Cont'd)

FA ident	Assembly avg Bu, 10^3 MWd/mtU	Rod-to-guide tube gaps: Worst span, No.	No. of measurements	Mean gap,[a] mils	Gap[b] std dev'n, mils
NJ008M	5.4		64		
	16.5		64		
NJ008N	5.4		64		
	16.5		64		
NJ00P7	11.0		64		
NJ00PG	10.8		64		
NJ005A	0.0		84		
	5.4		84		
	12.1		84		
	24.6		84		
NJ0059	0.0		66		
	5.4		66		
	12.1		66		
	24.6		66		
NJ00MZ	9.4		96		
	22.3		72		
NJ00ND	9.4		96		
	22.3		96		

(a) Mean gap is the mean value for the distribution of gaps as determined from the water channel measurements:

mean gap = $\frac{1}{N} \sum$ gap, where N = number of measurements.

(b) Standard deviation is defined as

$$\sigma = \left\{\frac{1}{N - 1} \left[\sum (\text{gap})^2 - \frac{1}{N} \left(\sum \text{gap}\right)^2\right]\right\}^{1/2}$$

where gap = water channel measurement.

Table 4-2. Rod-to-Rod Water Channel Measurements — Periphery Vs Interior

		Peripheral gap			Interior gap		
Assembly ident	Assembly avg Bu, 10^3 MWd/mtU	No. of measurements	Mean[(a)], mils	Std dev'n[(b)], mils	No. of measurements	Mean[(a)], mils	Std dev'n[(b)], mils
1A16	10.6	108			244		
1B04	0.0	108			--		
	19.8	54			122		
1B05	0.0	108			--		
	19.7	108			244		
1B29	0.0	108			244		
	20.0	108			244		
1C04	22.0	107			243		
1C30	6.4	76			--		
	15.[illegible]	108			244		
1C63	0.0	108			244		
	7.6	108			244		
	16.6	108			244		
	25.1	108			244		
1C66	0.0	108			--		
	9.8	108			244		
	18.5	108			244		
	26.5	108			244		
1D13	31.2	108			244		
	39.8	89			209		
1D26	31.2	108			243		
	39.8	81			199		
1D40	0.0	108			--		
	13.1	106			235		
	24.8	108			244		
1D42	28.2	107			241		
	36.0	[illegible]			157		
1D45	31.2	107			237		
	39.8	80			193		
1D55	31.2	108			244		
	39.8	85			216		
2B15	17.2	108			244		
	24.3	108			244		
2B40	0.0	108			244		
	17.2	21			31		
	24.3	107			244		

Table 4-2. (Cont'd)

Assembly ident	Assembly avg Bu, 10^3 MWd/mtU	Peripheral gap: No. of measurements	Peripheral gap: Mean[a], mils	Peripheral gap: Std dev'n[b], mils	Interior gap: No. of measurements	Interior gap: Mean[a], mils	Interior gap: Std dev'n[b], mils
NJ008K	5.4	108			244		
	16.5	89			244		
NJ008L	5.4	108			244		
	16.5	108			244		
NJ008M	5.4	108			244		
	16.5	108			244		
NJ008N	5.4	108			244		
	16.5	108			244		
NJ00P7	11.0	108			244		
NJ00PG	10.8	108			244		
NJ0059	0.0	124			186		
	5.4	124			186		
	12.1	124			186		
	24.6	124			186		
NJ005A	0.0	124			256		
	5.4	124			256		
	12.1	124			256		
	24.6	124			256		

[a] Mean gap is the mean value for the distribution of gaps as determined from the water channel measurements:

Mean gap $= \frac{1}{N} \sum$ gap, where N = number of measurements.

[b] Standard deviation is defined as

$$\sigma = \left\{\frac{1}{N-1}\left[\sum (\text{gap})^2 - \frac{1}{N}\left(\sum \text{gap}\right)^2\right]\right\}^{1/2}$$

where gap = water channel measurement.

Table 4-3. Distribution of Worst-Span Locations

Location	Frequency of worst span, %
Top	
2	
4	
6	
8	
10	
12	
14	
Bottom	

Figure 4-1. Rod-to-Rod Vs Rod-to-Guide Tube Gaps

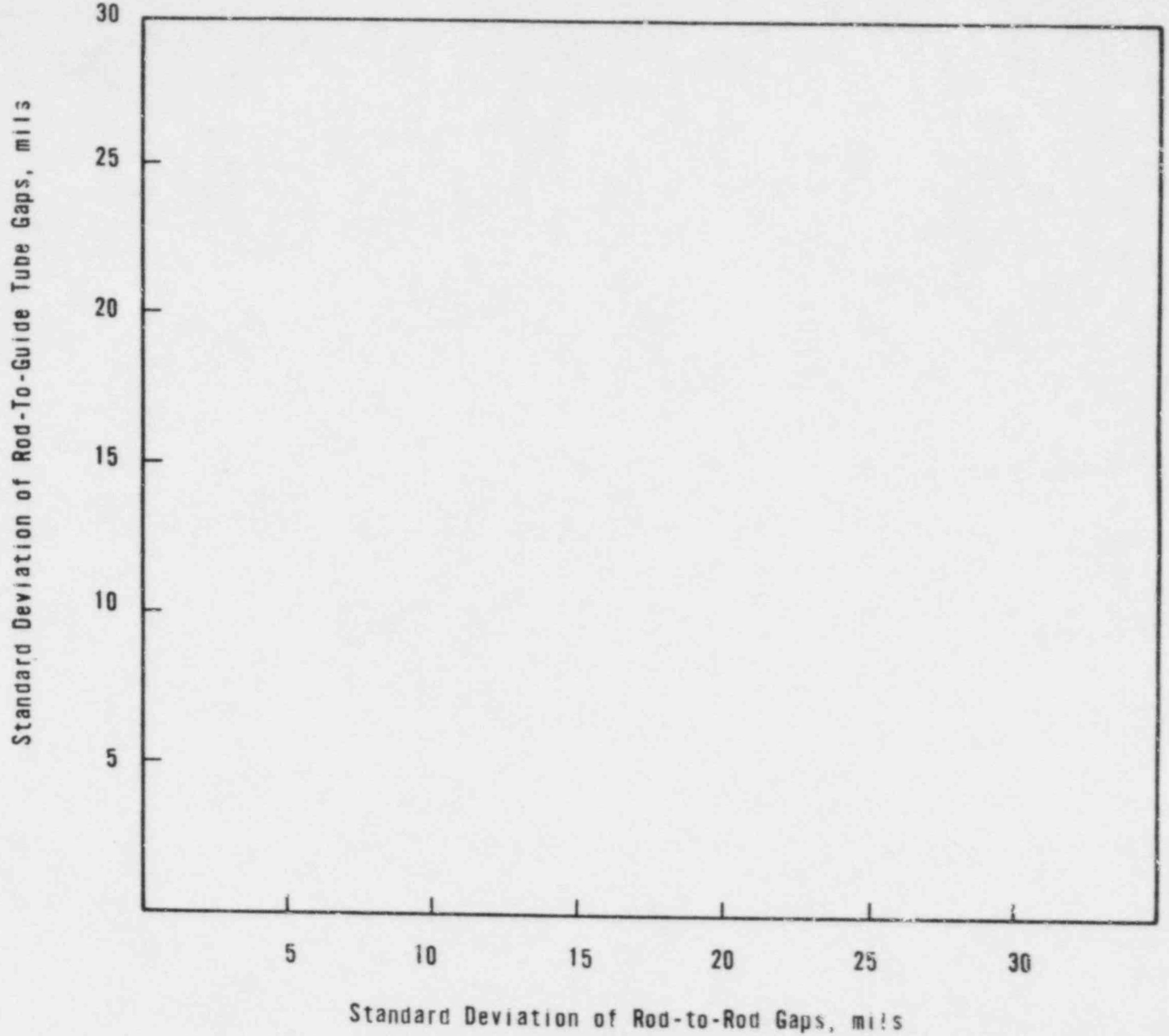

Figure 4-2. Interior Vs Peripheral Gaps for Mark B Assemblies

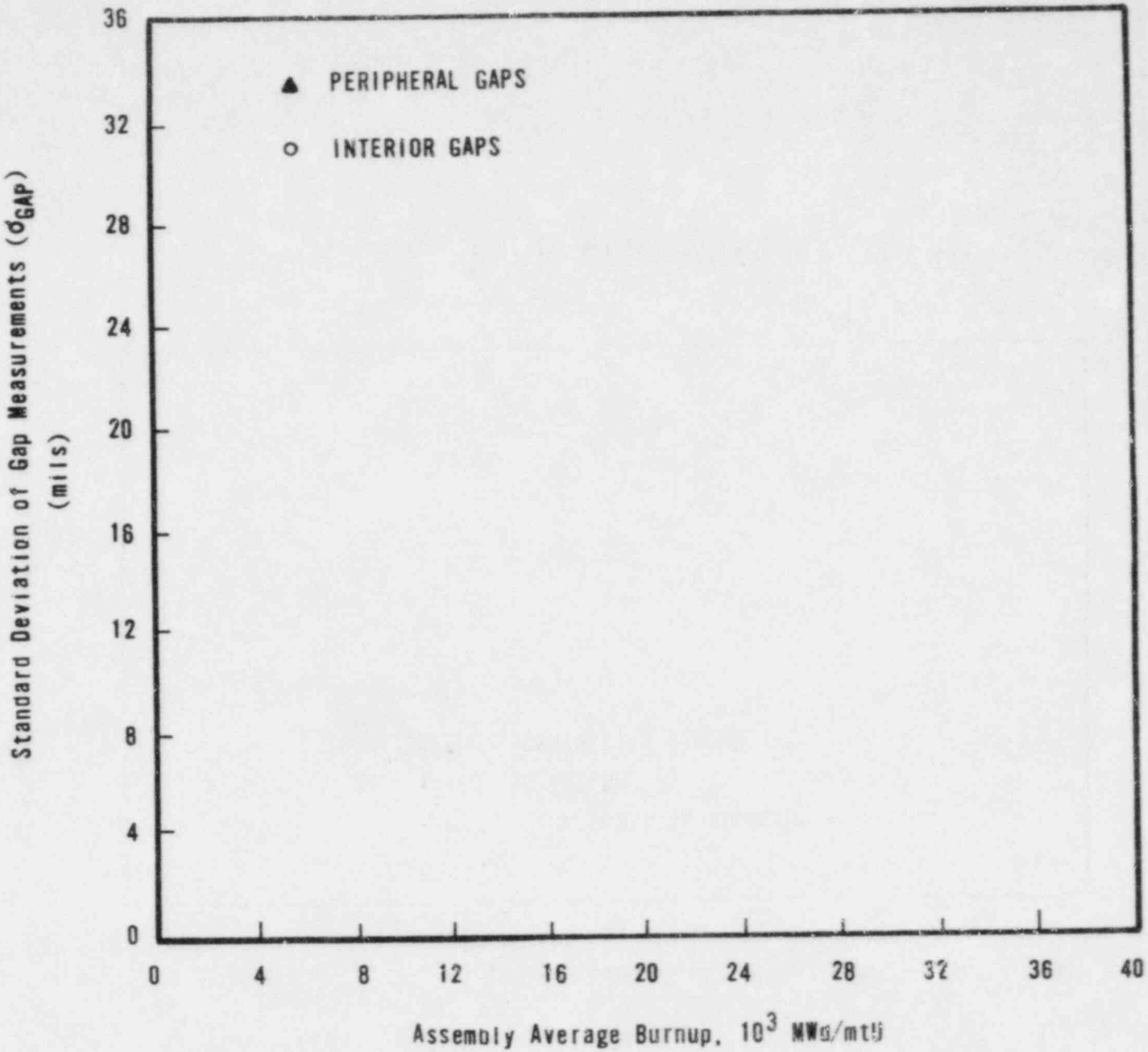

Figure 4-3. Comparison of Gap Measurements for Lifted Rod, Spiral Eccentricity, and Standard Configuration Assemblies

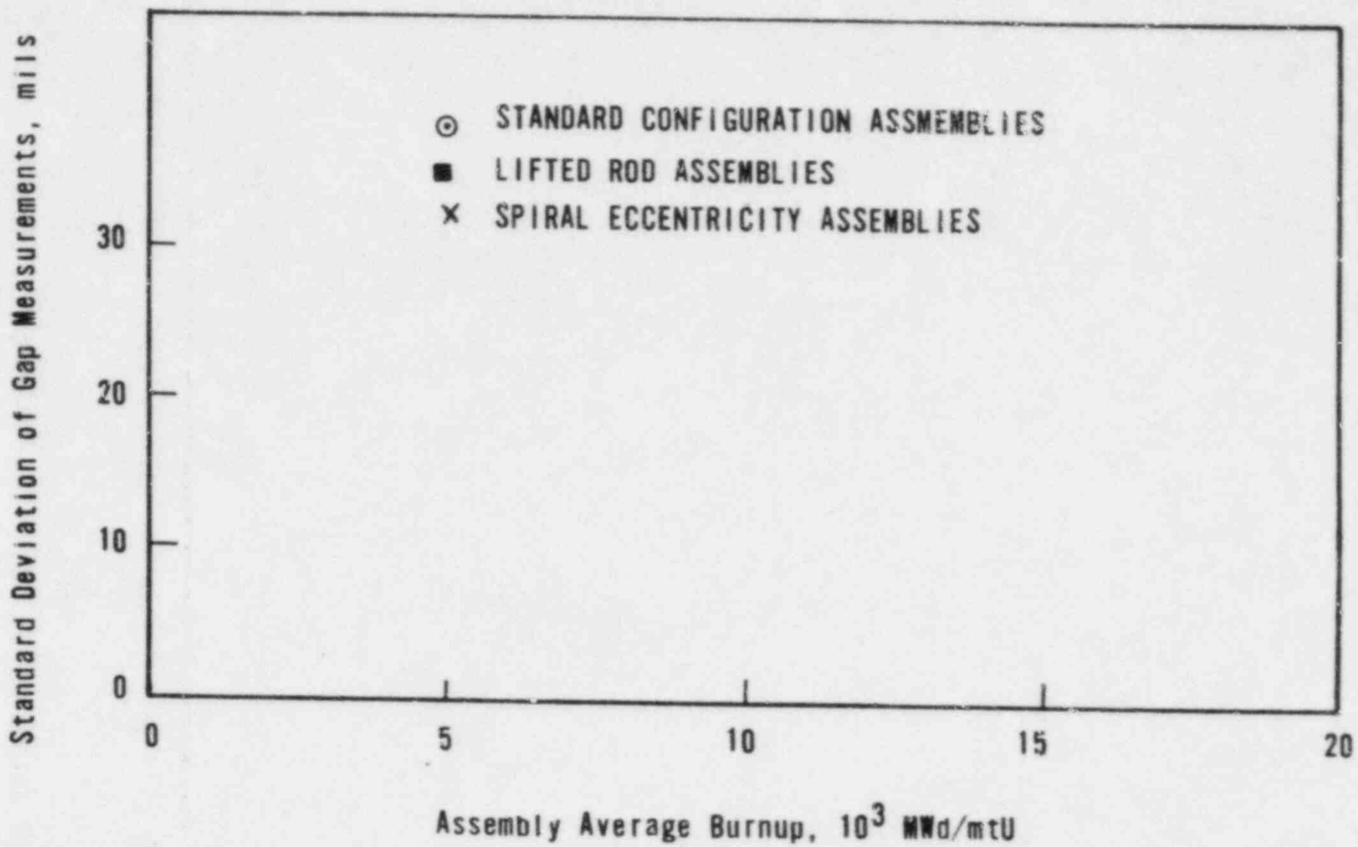

5. ROD BOW CORRELATION

The relationship between bowing of the fuel rods and fuel burnup is expressed by an empirical equation correlating the water channel gap measurements to assembly average burnup. This equation was developed by a statistical analysis of the gap measurements summarized in section 3.2, following the guidelines presented in reference 1.

The distribution of rod-to-rod measurements in the span with the largest standard deviation was used to bound all the gaps within an assembly. The data are assumed to be characterized by a normal distribution. A complete discussion of the data normality is included in Appendix C.

A global tolerance multiplier is used to ensure that the gap predicted by the empirical equation bounds 95% of all the gaps within an assembly at a specific burnup with a 95% confidence level. A cold-to-hot factor is used to adjust the predicted gap to the incore environment.

5.1. Empirical Equation for Water Channel Gap

The rod-to-rod data base (section 3.2) was statistically evaluated using standard regression techniques as described in Appendix D. The empirical equation was determined to be

$$\sigma_{gap} = \tag{5-1}$$

where

σ_{gap} = best estimate of the standard deviation of rod-to-rod gaps for the worst span, mils,

Bu = fuel assembly average burnup, 10^3 MWd/mtU.

A plot of the equation and data base is presented in Figure 5-1. The equation predicts the best estimate of the standard deviation of the water channel gap in the worst span of a fuel assembly at a specified level of burnup. The gap standard deviation is used as a relative measure of the amount of rod bow, which is defined as the lateral deviation of a rod from its theoretical unbowed position. A review of the data base shows a trend for the rod bow behavior to saturate at the high levels of burnup (>35,000 MWd/mtU) with the magnitude of the standard deviation of gap measurements remaining constant or decreasing.

The pertinent variable for calculating the effects of fuel rod bowing on the margin to DNB is gap closure, which is related to the difference between the nominal and the measured or predicted values for the rod-to-rod gap. It is expressed as percentage of the nominal gap. Therefore, the standard deviation of gap closure is

$$\sigma_{\text{gap closure}} = \frac{\sigma_{\text{gap}}}{\text{nominal gap}} \times 100 \qquad (5\text{-}2)$$

where σ_{gap} is the measured or predicted standard deviation of gaps, and the nominal gap is defined by the assembly configuration.

The derivation of the bow equation was based on only the measurements from Mark B assemblies. Figure 5-1 compares the Mark B and Mark C data. In general, the trend in the relationship between the rod-to-rod σ_{gap} and burnup is the Mark C σ_{gap} is Therefore, to predict the magnitude of the water channel gaps in a Mark C assembly. The value of gap closure expressed as a percentage of the nominal gap will differ between Mark B and Mark C by

5.1.1. Tolerance Factor

Fuel rod bowing causes a reduction in CHF as determined by the DNB within an assembly. The guidelines specify that for correlations affecting the DNB, there should be a 95% probability, at the 95% confidence level, that the core meets its design criterion, including the effects of rod bow.[1]

The empirical equation (5-1) predicts the best estimate values for the amount of change in the rod-to-rod gaps of the worst span. These values are adjusted by a global tolerance factor at the 95% confidence level using the following relationship.

$$\sigma_{95/95} = \sigma_{bow} + \sigma_t \quad (5\text{-}3)$$

where $\sigma_{95/95}$ = 95% tolerance level of the standard deviation of rod bow (mils), worst span,

σ_{bow} = predicted best estimate of the standard deviation of rod bow (mils) = σ_{gap} (equation 5-1), worst span,

σ_t = factor that includes the effects of model correction and standard error of prediction σ_e (mils) and its uncertainty.

Appendix D gives details of these derivations.

The results of the global tolerance calculations are given in Table 5-1. The ratio of the global tolerance to predicted values is burnup-dependent. The values presented in Table 5-1 are conservative when compared to the 1.5 factor suggested in reference 1. The ratio can be approximated by

$$\text{ratio} = \frac{\sigma_{95/95}}{\sigma_{bow}} = \quad (5\text{-}4)$$

where Bu is the assembly average burnup, 10^3 MWd/mtU.

5.2. Cold-to-Hot Correction Factor

To adjust the rod bow prediction to reflect the actual core operating conditions, the cold-to-hot correction factor of 1.2 is used, suggested in reference 1:

$$\sigma_{hot} = 1.2\ \sigma_{cold}$$

This cold-to-hot factor is used to adjust all predicted rod-to-rod gap closure values included in the calculation of rod bow effect on DNBR.

Table 5-1. Rod Bow Predictions

Burnup, 10^3 MWd/mtU	Rod bow, mils Best estimate	95% global tolerance	Ratio
5.4			
8.0			
12.0			
16.5			
18.0			
20.0			
25.0			
30.0			
35.0			
39.8			

Figure 5-1. Rod Bow Prediction Model

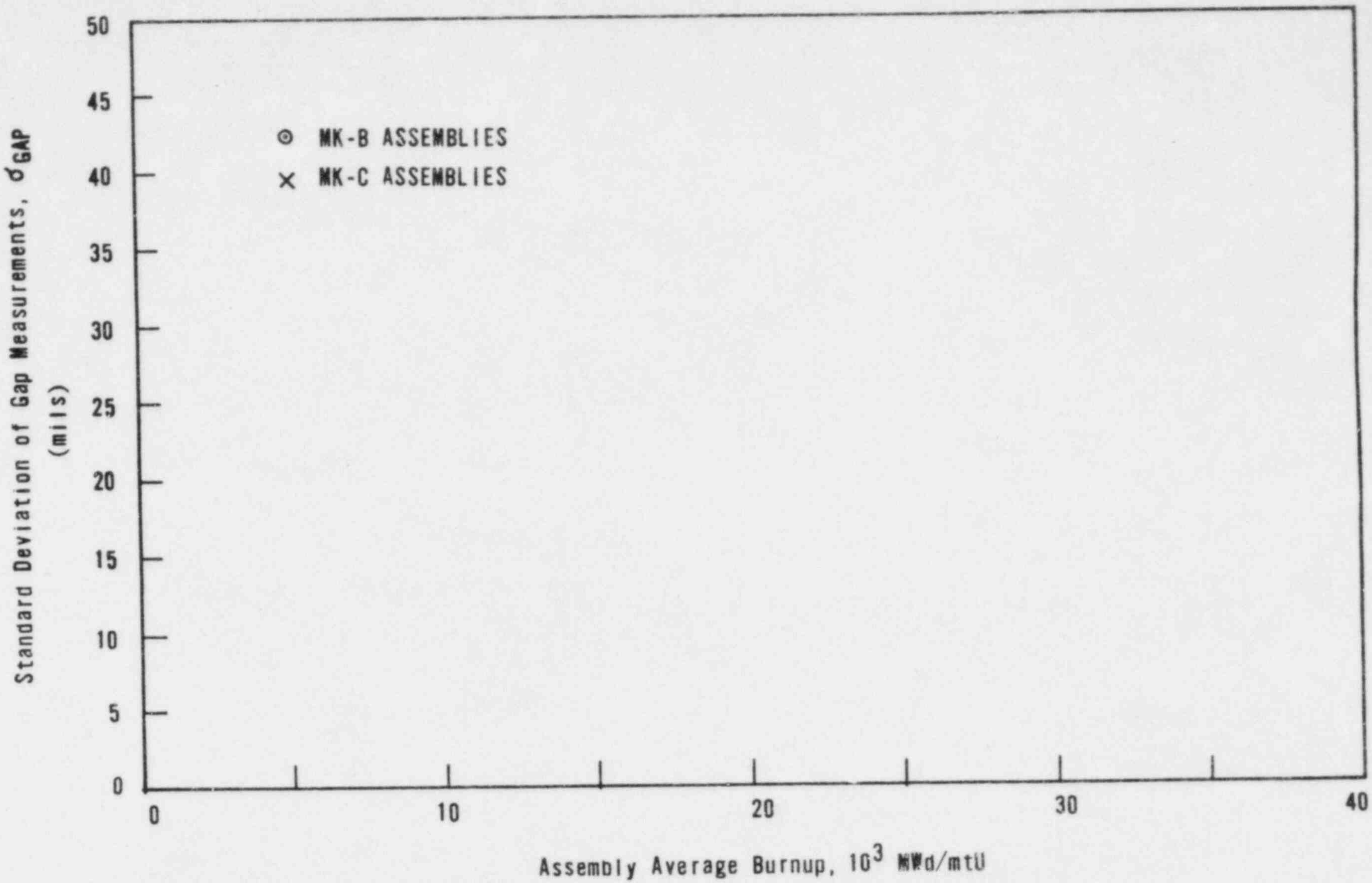

6. ROD BOW EVALUATION

Fuel rod bowing affects PWR design and operation in two ways: (1) effects on thermal-hydraulic design criteria in preventing DNB and (2) the effect on the mechanical integrity of the fuel cladding.

6.1. Thermal-Hydraulic Consideration

A major thermal-hydraulic design criterion for PWRs is the prevention of DNB during normal operation and during incidents of moderate frequency classified as Condition I or Condition II events.[6] For any of these events, the reactor core is assured of meeting the design criteria by demonstrating that the predicted minimum DNBR is greater than the corresponding design limit DNBR.

The effects of rod bow on DNBR have been determined from CHF tests performed on two Mark C geometry rod bundles. Both bundles were identical in geometry and heated rod design except that one bundle contained a heated rod bowed to 55% closure with adjacent heated rods in a guide tube subchannel location, while the other contained all unbowed rods. The results of these tests were submitted to the NRC and are included in Appendix E.[2,3]

The data obtained from these tests were used to establish a threshold for the amount of fuel rod bowing below which there is no reduction in DNBR. Above this threshold value, the reduction in DNBR can be calculated using a formula that includes the threshold value. Although these tests were performed for Mark C geometry fuel, the results are also judged valid for Mark B fuel. This judgement is based on comparisons of subchannel velocity profiles for the Mark C and Mark B geometries which show lower velocities (as a percentage of average velocity) in Mark C rod-to-rod gaps than in Mark B rod-to-rod gaps.

6.1.1. Evaluation of DNBR Reduction Due to Bow

The amount of DNBR reduction, δ_{DNBR}, is related to the amount of fractional gap closure, $\Delta c/C_o$, as illustrated with the straight line in Figure 6-1. The equation that relates gap closure to DNBR reduction is obtained from reference 1:

$$
\delta_{DNBR} = \begin{cases} \dfrac{\delta c}{1 - K}\left(\dfrac{\Delta c}{C_o} - K\right) & \text{for } K \le \Delta c/C_o \le 100\text{, percent} \\ 0 & \text{for } 0 \le \Delta c/C_o < K\text{, percent.} \end{cases} \tag{6-1}
$$

The empirical estimates of δ_c, DNBR reduction at full gap closure, and K, the threshold value of zero DNBR penalty, define the slope of the line. The value of $\Delta c/C_o$ vary from zero to 100% since gap closure is complete at 100%, or contact. The values of the DNBR reduction vary from zero to δ_c. The parameter δ_c is denoted in this report as "a," penalty at full closure. The DNBR limit (DNBRL) including bow is obtained from the DNBR limit without bow, using:

$$
DNBRL_{bow} = \frac{DNBRL_{no\ bow}}{1 - \delta_{DNBR}} \tag{6-2}
$$

The $DNBRL_{no\ bow}$ value is equivalent to the design limit and corresponds to the appropriate CHF correlation limit value.

6.1.2. The Penalty Model

As outlined above, the values of K and δ_c are empirical and their estimates determine the slope and intercept of the penalty line. B&W has performed bowed rod CHF tests to establish the basis of the value of K.[2,3] Appendix E gives details of this experiment. Analysis of variance and significance tests indicated that an average difference of between bowed and unbowed data is negligible at the $\alpha = 0.01$ level but not at the 0.05 level.[2,3] This statistically inconclusive result prompted the NRC to recommend a penalty of 5.2% at 55% closure.[4,5] This was accepted by B&W on the basis that a lower, more conservative estimate of K results, as Figure 6-2 illustrates, i.e., the position of K_2 relative to K_1 or 55%, is closer to zero. The method of determining this penalty is provided in Appendix E, part 5.

The value of the parameter δ_c, or a, penalty at full closure, was provided in ref. 7. A best estimate value of a = 0.3353 was used with an uncertainty of 0.1. The 10 data points (N_c = 10) that yielded these results were used to calculate a_L, the 95% upper limit value of the penalty at full closure as follows:

$$a_L = \qquad + t_{0.05,9} \frac{0.01}{\sqrt{10}} = \tag{6-3}$$
$$=$$

Finally, the equation for predicting the DNBR penalty is given as

$$\delta_{DNBR} = \begin{cases} \dfrac{a_L}{1 - \qquad} \left(\dfrac{\Delta c}{C_o} - \qquad \right), & \qquad \le \Delta c/C_o \le 1.0, \\ 0, & 0 \le \Delta c/C_o \le \qquad . \end{cases} \tag{6-4}$$

This equation would define the penalty, δ_{DNBR}, if the value of $\Delta c/C_o$ were known. Equation 6-4 denotes the conditional penalty.

The approach above accounts for the uncertainty in the estimates of the parameters K and a and does so conservatively in their implementation. Since the uncertainty in the model coefficients (or the resultant slope of the line) have thus been accounted for, equation 6-4 will give conservative estimates of the penalty δ_{DNBR} for fixed values of $\Delta c/C_o$.

The only unknown still to be evaluated is the value of $\Delta c/C_o$ for which δ_{DNBR} is to be calculated. $\Delta c/C_o$ is a random variable with an assumed distribution. The development of the method used to predict the unconditional DNBR penalty is presented in Appendix F. Figure 6-3 illustrates the half-normal distribution with two different bow estimates. The boundary of the penalty region is available from equation 6-4.

6.2. Mechanical Evaluation

The mechanical consideration with respect to rod bow is the possibility of fretting on the outer surfaces of the fuel rod cladding at 100% gap closure. Fretting is a surface wear phenomenon resulting from small relative movements between two surfaces in contact with each other.

Based on a large number of rod-to-rod gap measurements, the empirical equation (5-1) predicts a very low probability that rod-to-rod contact will occur in B&W fuel assemblies. In the unlikely event that such contact should occur, the depth of wear would be insignificant because of the small amount of relative motion and low contact force. Therefore, rod bow-related fretting wear is not a concern in the B&W fuel assemblies.

Figure 6-1. Model — DNBR Reduction Vs Gap Closure

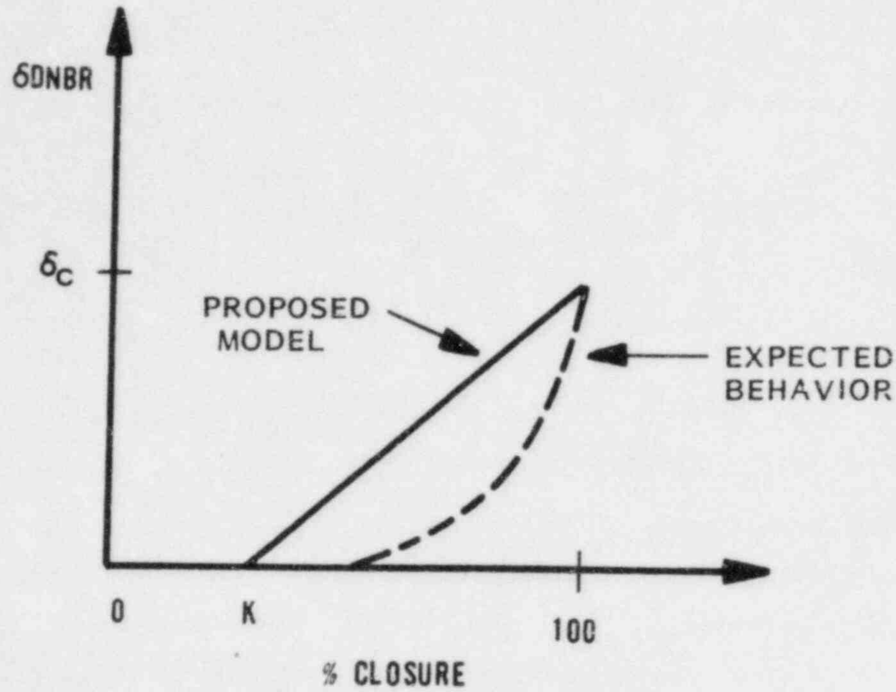

Figure 6-2. Penalty Vs Closure Relationship

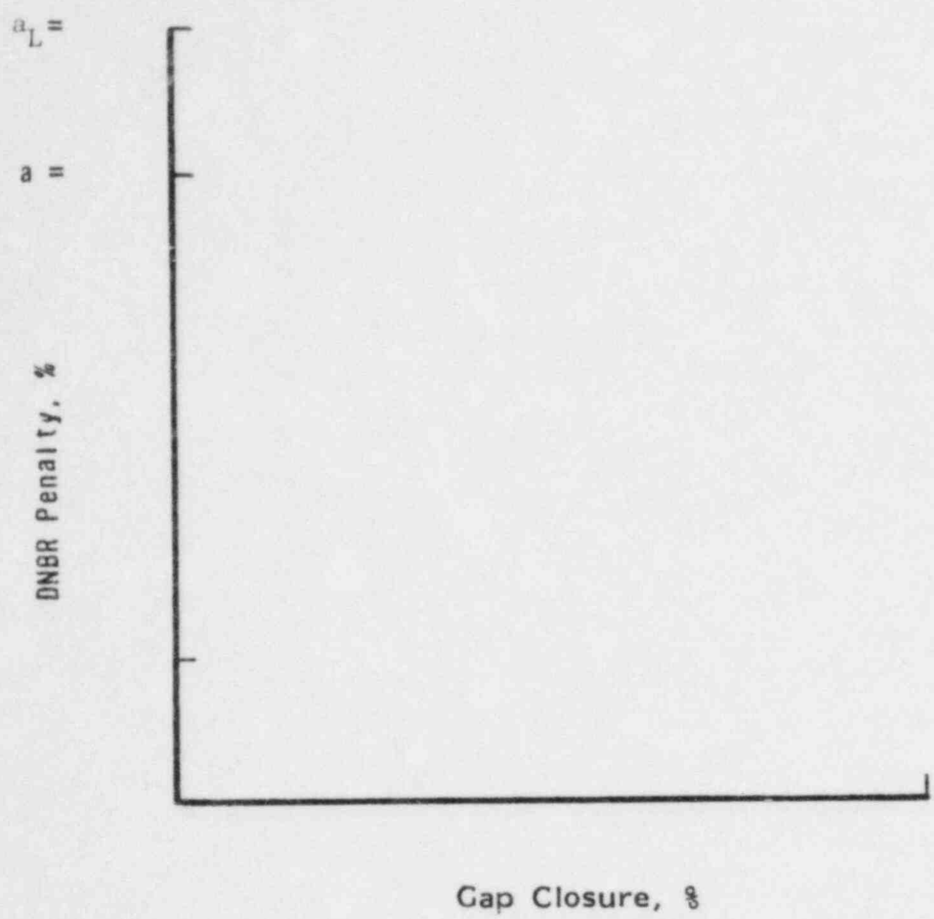

PENALTY = 0 Gap Closures < K

$$\text{PENALTY} = \frac{a\left(\frac{\Delta C}{C_0} - K\right)}{1-K}, \text{ CLOSURES BETWEEN K, 100}$$

Figure 6-3. Illustration of the Penalty-Bow Relationship

7. ROD BOW EFFECTS ON PLANT PARAMETERS

7.1. DNBR Considerations

A procedure for conveniently evaluating the DNBR reduction for plant-specific analyses was developed from the methods presented in sections 5 and 6. A method of calculating DNBR penalty due to rod bow was developed as a function of fractional gap closure and is presented in section 6. Since gap closure is related to the core operating parameter of burnup, the correlation of gap closure versus burnup (section 5) was used in conjunction with the correlation of DNBR penalty versus gap closure (section 6) to establish a method of calculating DNBR penalty as function of fuel assembly average burnup. A detailed description of the development of the calculational procedure is presented in Appendix F. The application of this conservative calculational procedure results in the DNBR penalty curves shown in Figures 7-1 and 7-2 for Mark B and Mark C fuel.

Plant-specific analyses include an evaluation of the DNBR reduction due to rod bow. DNBR margins existing from conservatisms used in evaluating core DNBR may be used to offset reductions due to rod bow. A generic conservatism used in such evaluations that results in a 1% DNBR credit used to offset rod bow DNBR penalty is a flow area (pitch) reduction factor. This credit has been approved by the NRC.[8] The flow area reduction factor represents the uncertainties associated with intrabundle flow area due to manufacturing variations and as-built fuel rod bow.

The penalty curves are illustrated in Figures 7-1 and 7-2 for fuel assembly burnup to 40,000 MWd/mtU. They show a penalty that varies from at MWd/mtU to DNBR reduction (Mark B) and DNBR reduction (Mark C) at MWd/mtU. This penalty is considered to be insignificant and unnecessary because the power production capability of fuel assemblies diminishes with irradiation to the extent that fuel assemblies with burnups of 24,000 MWd/mtU or more cannot produce enough power to achieve design limit peaking values.

Therefore, no DNBR penalty due to fuel rod bow need be considered in reactor licensing.

7.2. Power Peaking Consideration

Local power peaking effects due to local neutron moderation variations are a result of fuel rod bowing. The magnitude of peaking changes was evaluated for a range of geometries and fuel enrichments; the results are presented in Appendix G. The impact of these local peaking changes on core design peaking factors is accounted for by a peaking factor uncertainty.

A value of the rod bow-related peaking uncertainty was determined that would be bounding for any burnup since the local peaking change is dependent on gap closure as described in Appendix G, and since gap closure is dependent on burnup as described in section 5. Combining these data yields a local peaking change of for a burnup of 40,000 MWd/mtU. A maximum peaking uncertainty of is conservatively bounding for any gap closure predicted to occur in B&W fuel designs. This maximum peaking uncertainty was statistically combined with other independent uncertainties into an overall peaking uncertainty, which is used to establish core peaking limits in plant-specific analyses. The method of combining these uncertainties has been submitted to the NRC.[9] This technique is very conservative when the actual bow prediction and corresponding peaking increases presented in this report are considered. Since local peaking changes are burnup-dependent at the beginning of life (BOL) and early in the life of the fuel, the rod bow effect on peaking is negligible.

Figure 7-1. Mark B Rod Bow DNBR Penalty Vs Burnup

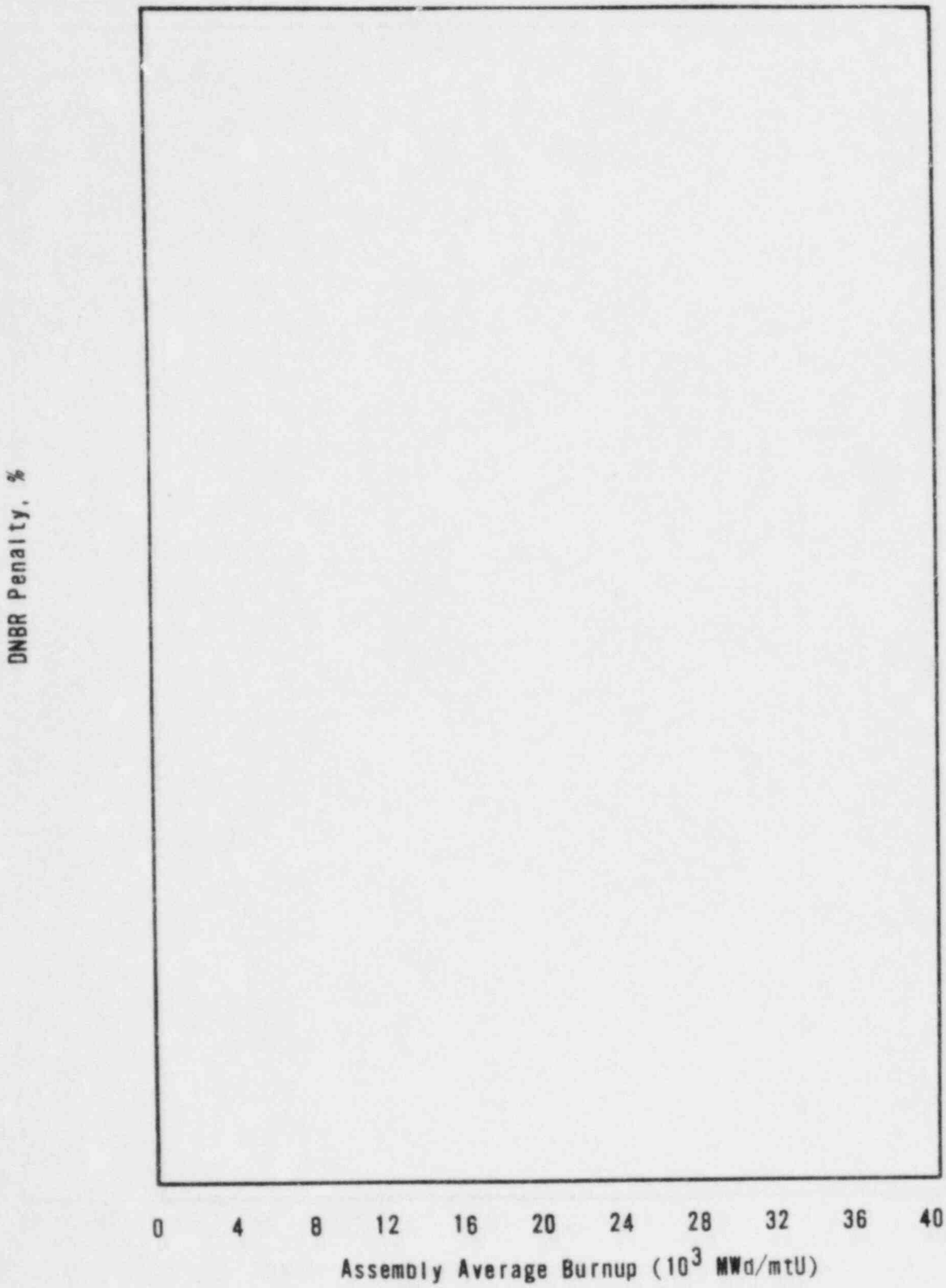

Figure 7-2. Mark C Rod Bow DNBR Penalty Vs Burnup

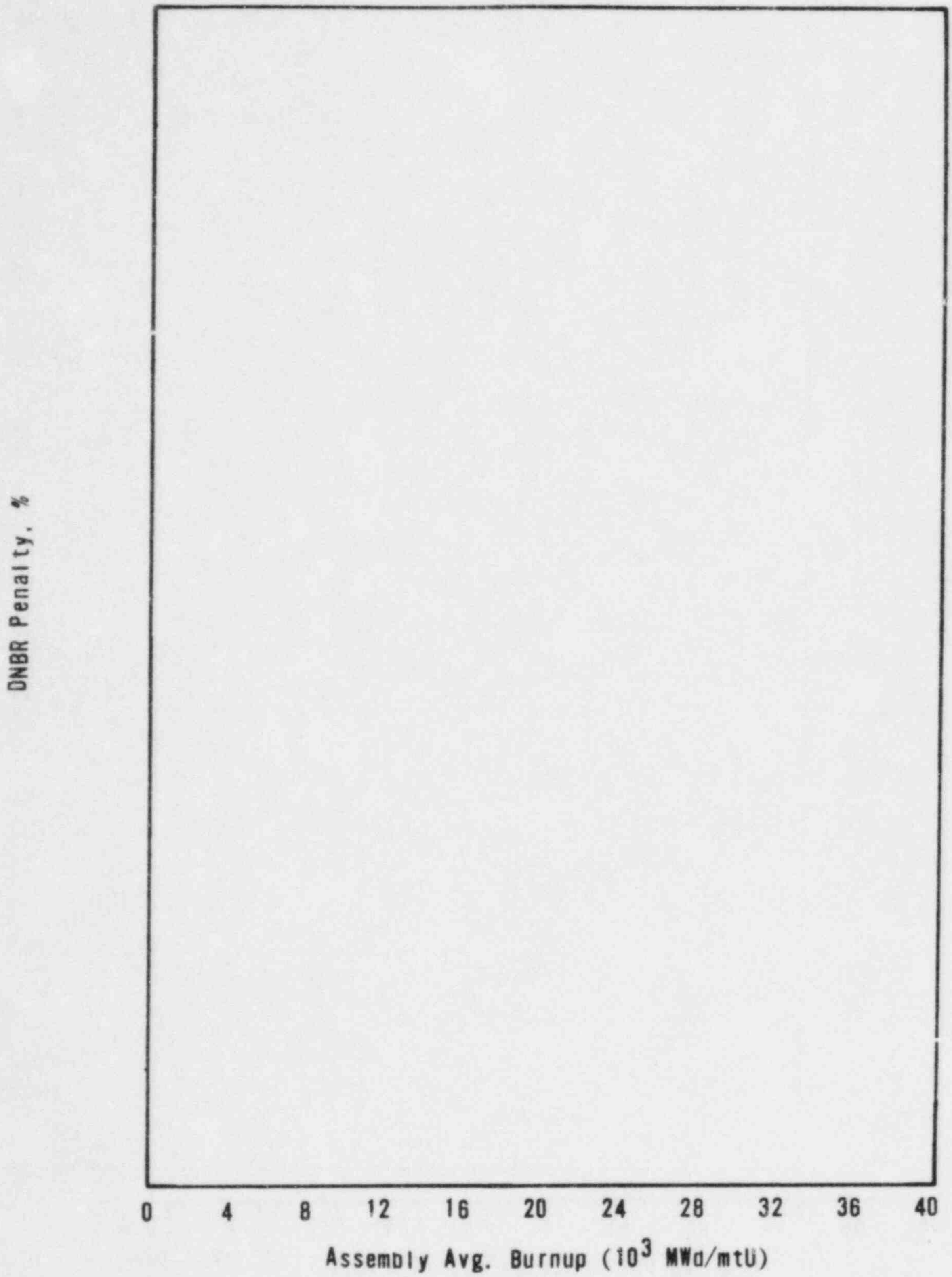

APPENDIX A

Water Channel Measurements

1. Introduction

The method of water channel measurements and the subsequent data analysis were discussed in section 3.1 of this report. This appendix discusses additional details of the water channel measurement technique and addresses errors that affect the reproducibility and the accuracy of the data.

Water channel measurements are made using a "Sulo" probe (Figure A-1). The probe consists of a thin wand with a leaf spring attached to either side. Strain gages are bonded to the inside of the leaf springs. The resistance of the strain gages is proportional to the amount the leaf springs are deflected. The probe is inserted into the channel between two planes of fuel rods and measures the distance between adjacent fuel rods in the direction perpendicular to the insertion. The probe is calibrated before each insertion by passing it through two sets of calibration pins (nominally 100 and 150 mils), shown in Figure A-1. The water channel data are scaled to these values. The measurement range of the probe is limited to the thickness of the wand (nominally 50 mils) and the relaxed dimension of the leaf springs (170 to 200 mils, depending on the probe).

The water channel data are obtained as a continuous, time-based voltage output of the probe during the insertion. The amplitude of the voltage peaks represents the minimum spacing between rods. A computer was used to digitize the calibration peaks and data peaks from the strip charts and to store them on magnetic tape. These data are corrected for measurement bias called probe spreading. The following sections discuss in detail the potential and real errors encountered in the measurement and the analysis of the water channel data and describes the corrections made to the data account for the errors.

2. Error Analysis

This section assesses the major errors that could occur during the taking and analyzing of water channel data. The areas discussed are inaccuracies of the probe, inaccuracies due to geometry, and errors in the recording and reduction of data.

The range of the Sulo probe used in water channel measurements is limited. A typical probe has a measurement range from 50 to 200 mils. If a significant number of points are outside that range, both the mean and standard deviations of the spacing distribution are biased. There is also a nonlinear region of the probe in the first 10 mils of deflection from the relaxed dimension. The nonlinear region has the effect of reducing the upper limit of the probe. If a significant number of data points on a given assembly are missed or biased, a computer program is used to correct their biases.

During measurement of each water channel spacing, the springs on the probe displace the rods so that the measured spacing is larger than the actual spacing. This measurement bias is called probe spreading. A linear correction applied to the data corrects each spring in proportion to the amount the leaf springs were deflected. Second, the fuel rods have an associated ovality that may be as large as mils. The effect of fuel rod ovality is included in the measurement of the water channel spacings and is assumed to be randomly orientated.

The water channel data are recorded on a time-based strip chart. The accuracy of the reduction of these data is determined by the strip chart readability, which is estimated at ±0.5 mil. Once the data are stored in the computer, no other experimental errors are encountered. Calculational errors are kept to a minimum by using standardized computer programs to analyze the water channel data, which have been checked for data manipulation errors.

3. Correction of Water Channel Spacing Data for Probe Spreading Effect

The contact type of Sulo probe, used to measure the spaces between fuel rods, causes the fuel rods to bow slightly. This results in measurements larger than the actual spaces. The amount of increase caused by the probe depends on the size of the gap to be measured; the characteristics of the probe, fuel rods and guide tubes; the amount of spring relaxation in the spacer grids; and some lesser effects. The probe spreading correction is important because the distribution of spacings is contracted causing the standard deviation to decrease as much as 10% (see Figure A-2). The standard deviation is the parameter used to determine rod bow using the water channel technique.

The correction to the measured spacing can be determined using an equation of the following form:

$$X_a = \qquad \text{(A-1)}$$

where

X_a = actual spacing,

X_m = measured spacing,

h = relaxed dimension,

K_p = spring rate of probe,

K_r = spring rate of rod.

Equation A-1 assumes that the probe and rod have linear spring characteristics and that the rods are effectively cantilevered at each grid. This equation requires that the probe spring rate and relaxed dimension and the rod (guide tube) spring rates be known.

The spring rates have not been measured; therefore, the K_p/K_r factor must be determined empirically. The K_p/K_r factor is determined from the relaxed dimension of the probe and the amount of deflection that occurs at a known spacing as shown in Figure A-2. The average deflection for a plane is the difference between the measured and actual spacing (Figure A-3). This can be obtained by subtracting the average as-built and the amount of cladding creepdown from the average measured spacing:

$$\bar{d} = \tag{A-2}$$

where

$\bar{d}$ = average midplane deflection,

$\bar{X}_m$ = average measured spacing,

$\bar{X}_a$ = average actual spacing,

$\bar{X}_{ab}$ = average as-built spacing,

CD = average creepdown.

Once the average deflections are calculated, equation A-1 can be solved for K_p/K_r. The difference between the measured and actual value is the deflection.

$$\frac{K_p}{K_r} = \tag{A-3}$$

Thus, K_p/K_r is calculated for each plane. All of these K_p/K_r values are averaged for the assembly and used in equation A-1 to correct the data. A similar correction factor is calculated for rod-to-guide tube measurements, which are treated independently.

The correction method has been verified on assemblies that were precharacterized during manufacture and at poolside.

Figure A-1. Sulo Probe Being Inserted Between Two Calibration Pins

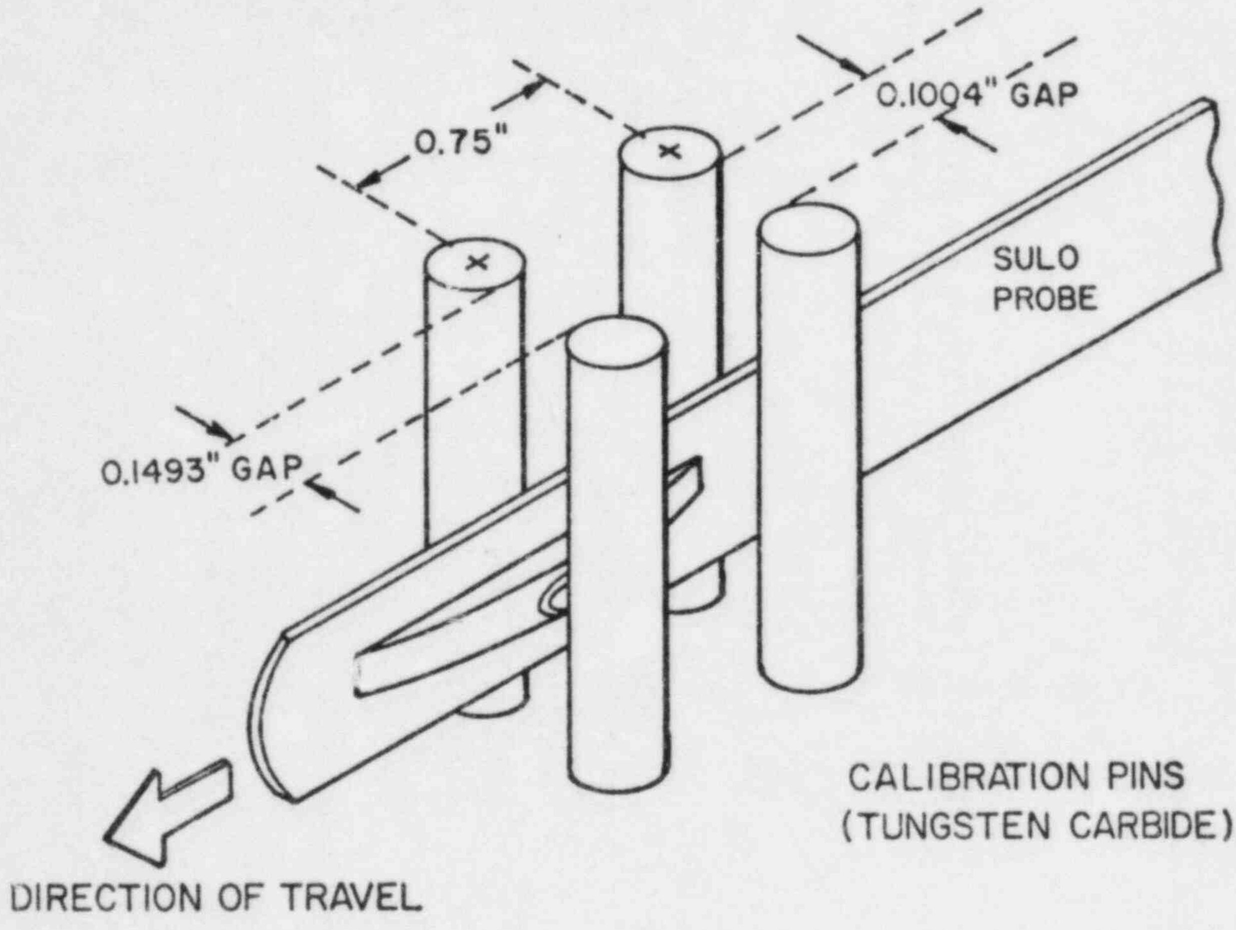

Figure A-2. Typical Probe Deflection Characteristics

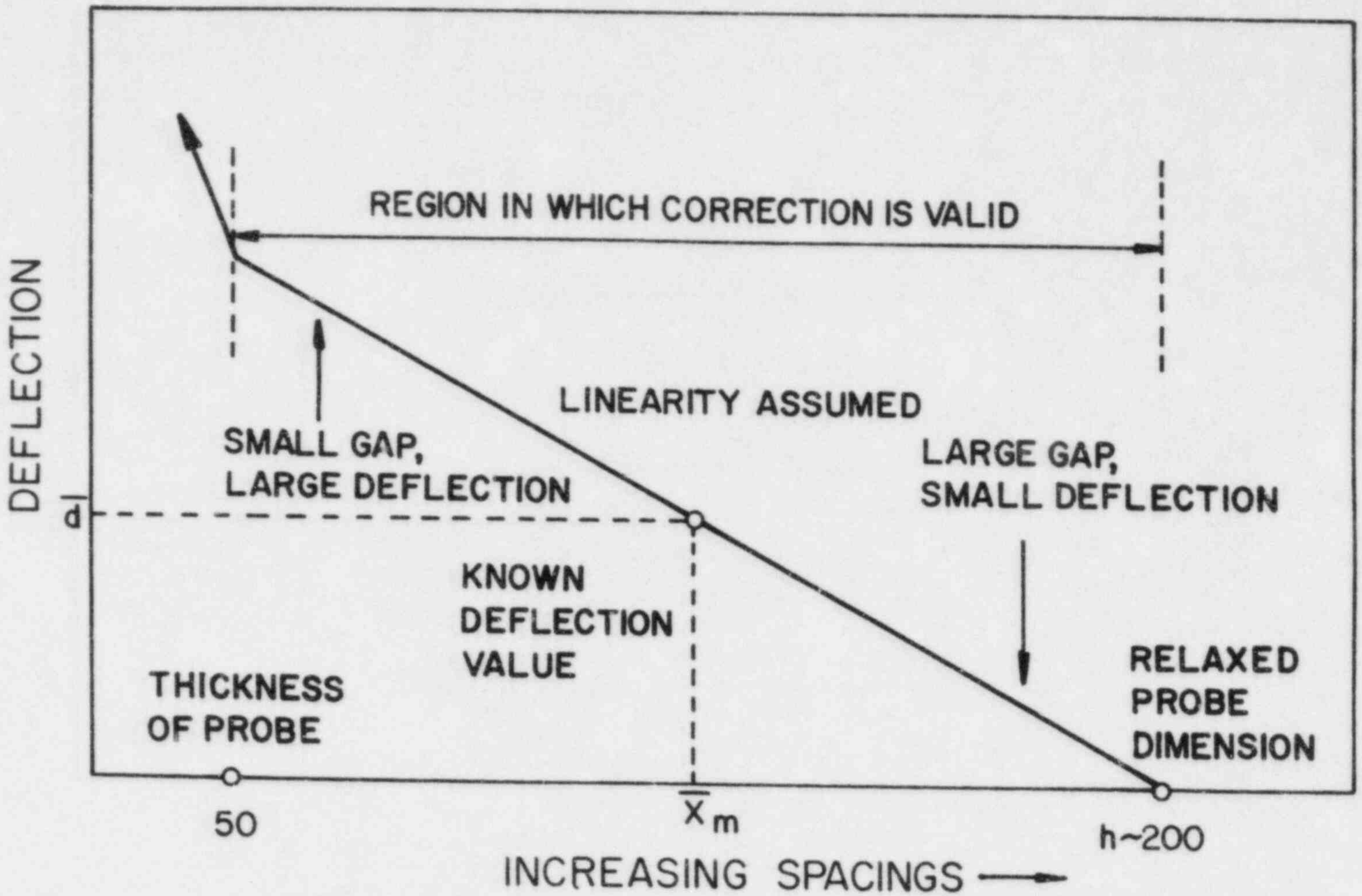

Figure A-3. Effect of Probe Spreading on Frequency Distribution

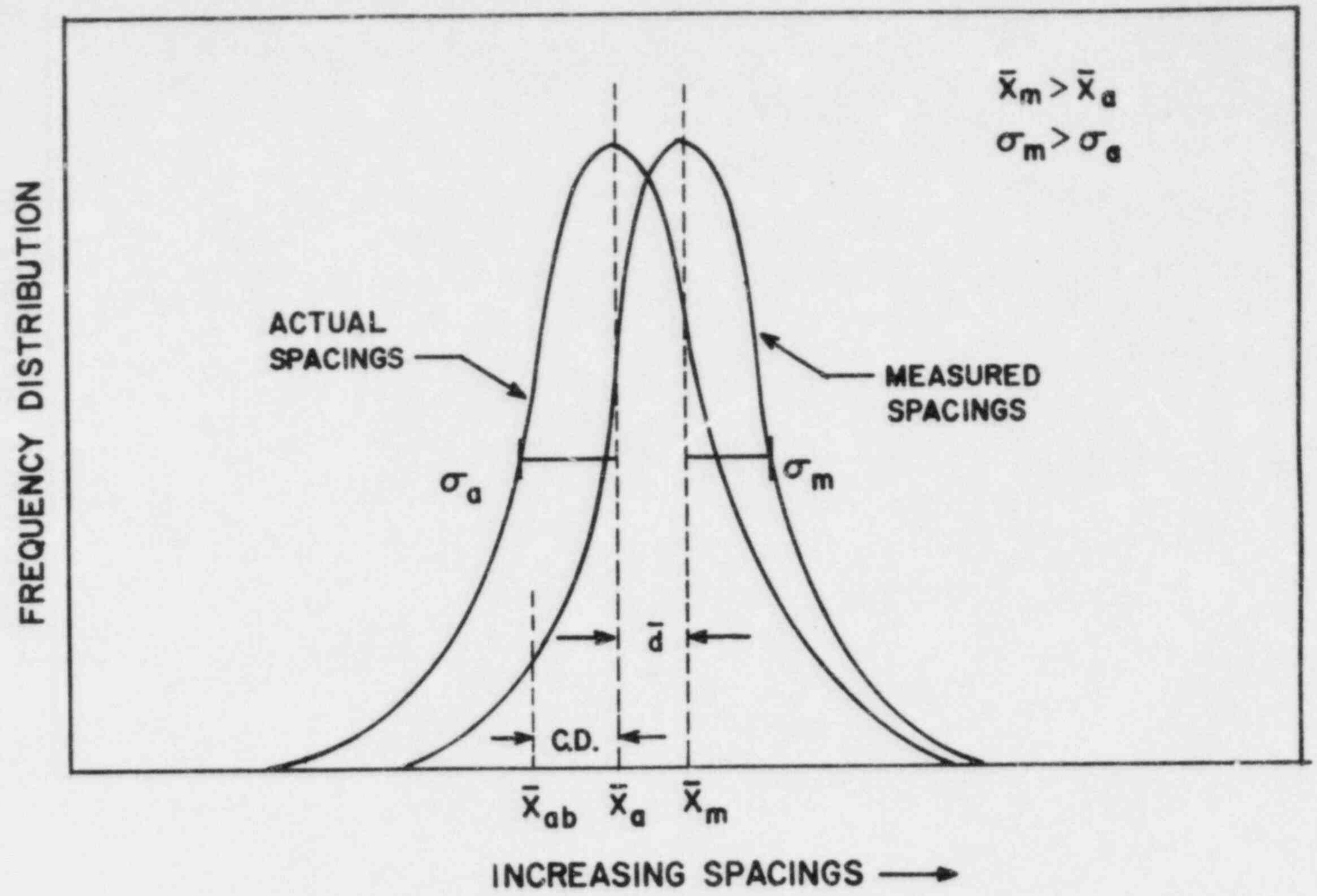

APPENDIX B

Water Channel Gap Measurement
Data Base

This appendix presents the span-by-span statistical summaries of the PIE water channel gap measurements. These data were obtained from an extensive measurement program on both the 15×15 Mark B and the 17×17 Mark C assemblies, which are representative of the range of manufacturing and operational variations. The data represent over 125,000 individual measurements that have included 26 fuel assemblies from eight manufacturing batches, two basic fuel assembly designs, two reactors, and fuel assembly average burnups to 40,000 MWd/mtU.

Table B-1. Water Channel Measurements

						Rod-to-rod gaps, mils									Rod-to-guide tube, mils		
						Interior + Periphery			Periphery			Interior					
Plant	Batch	Fuel assy ident	EOC(a)	Assembly avg burnup, 10^3 MWd/mtU	Measurement plane	Mean(b) gap, $\bar{y}_{R/R}$	Stand.(c) dev'n, $\sigma_{R/R}$	No. of meas'nts, $N_{R/R}$	Mean(b) gap, $\bar{y}_P$	Stand.(c) dev'n, σ_P	No. of meas'nts, N_P	Mean(b) gap, $\bar{y}_I$	Stand.(c) dev'n, σ_I	No. of meas'nts, N_I	Mean(b) gap, $\bar{y}_{R/GT}$	Stand.(c) dev'n, $\sigma_{R/GT}$	No. of meas'nts, $N_{R/GT}$

APPENDIX C

Normality of Data Distributions

A test of normality was performed on the gap measurements described in Appendix B using the D' equations prescribed by the American National Standards Institute[10] and recommended by NRC Regulatory Guide 5.22. The assumption of normality was checked on the spacing distribution of each individual plane. A test statistic was calculated and compared to critical values at the 95% confidence level. The interpretation of the test is that, if passed, the data do not exhibit enough evidence for the rejection of normality. The test results are summarized below.

Percent of Spacing Distribution Passing D' Normality Assessment

FA type	No. of reactor cycles 0	1	2	3	Total, %
Mark B	44	45	58	71	54
Mark C	44	55	12	50	38

It should be noted that the normality of the spacing distribution generally increases with irradiation. After three cycles of operation, 71% of the spacing distributions passed the normality test. This indicates that as the standard deviations of the spacing distributions increase, they become more normal.

The term "worst span" refers to spans in an assembly whose gap measurements have the largest variation, i.e., their standard deviation is largest. For these worst spans, the D' test results indicate that 66% of the Mark B spans and 50% of the Mark C spans passed. In most of the cases the test statistic was lower than the critical values, implying that there is more than normal curtosis, that is, the distribution is more peaked.[10] Under such circumstances, the assumption of normality is conservative.

Random samples of comparisons bore out this fact. It was found that the 84th percentile value from the normal distribution yields larger estimates and is thus more conservative than the same estimate for the data. Figure C-1 is a typical illustration given for one of the comparisons.

Figure C-1. Frequency Plot of Measured and Calculated Gap Values

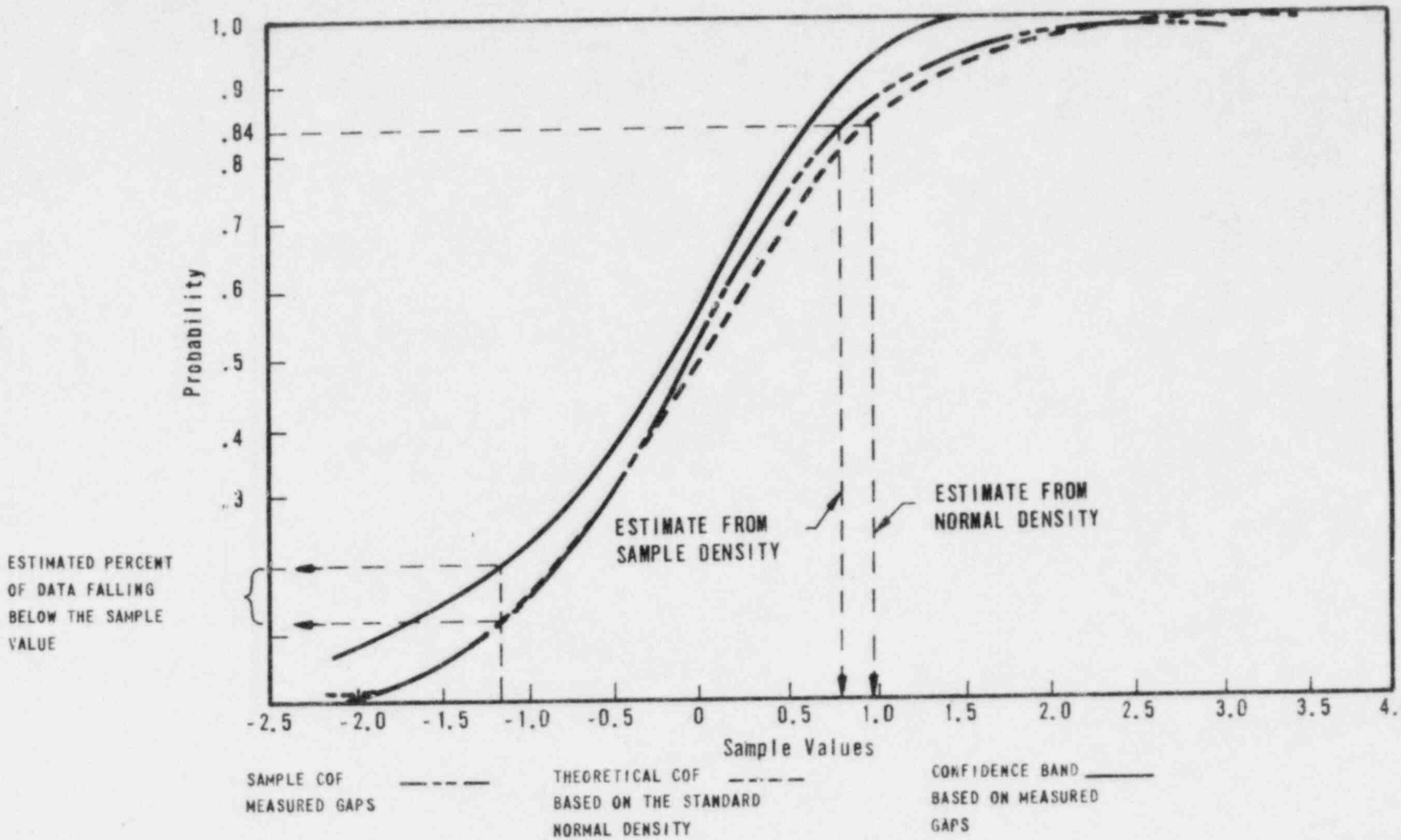

APPENDIX D

Rod Bow Correlation

1. Data Description

The rod-to-rod data described in section 3 were used to form the points from which the prediction equation for bow was developed. It was found that the frequency distribution of worst-span gap closures can be characterized by the normal distribution in 62% of the worst spans analyzed. It is shown in Appendix C that in the cases where the data contradict the normality assumptions, the results are biased in the conservative direction. Thus, the use of normality is justified and the standard deviation of worst-span gap closure measurements is assumed to estimate the 84th or larger percentile value of a standard normal distribution.[1] The population percentage of gap closure is related to the worst-span percentage by the relationship

$$P_{worst} = (P_{population})^N. \qquad \text{(D-1)}$$

Therefore, the 97.5 percentile of the population is expected to be represented by the 84th percentile estimates of the worst span. The seven spans measured equal the N value.

2. Model Description

The data were reduced to the common assembly average burnup. It can be seen from Figure 5-1 that for some values of burnup there are several data points, but for others only one value is available. The relationship of bow to burnup was evaluated empirically using standard (L.S) regression techniques. The best model was found to be

$$\text{bow} = \qquad \text{(D-2)}$$

which for practical purposes may be used as a linear model. This model satisfies both statistical and physical conditions of the bow phenomenon.

A plot of the data and the model of equation D-2 fitted to the data are shown in Figure 5-1. The regression coefficients of equation D-2 were obtained from the linearly transformed model,

$$\ell n \qquad = \qquad \text{(D-3)}$$

The estimates of the regression coefficients of equation D-3 yield a coefficient of determination r = 0.839 and a standard error σ_ε = , which indicate a statistically satisfactory result.

3. Tolerance Calculations on Bow

In order to validate the linearization procedure, a weighted regression was performed based on the G. P. Box technique of reference 11. The results indicated that the ℓn transformation, equation D-3, does not violate the homoscedasticity assumptions on the residuals. The weighted regression coefficients were found to be very close to those of the unweighted estimates of equation D-3. A more detailed comparison is available in paragraph 4. The predicted values from equation D-2 were used as the basis for defining a 95% tolerance level using the following relationship:

bow tolerance (at 95/95) =

(D-4)

with $C_{Bu} = \sqrt{X_0'(X'X)^{-1}X_0}$ the model correction factor.

Table D-1 shows the results of calculating the upper tolerance level using this relationship. It may be seen that the ratio of the global tolerance values to the predicted values is extremely conservative when compared to the 1.5 factor suggested in reference 1.

The burnup-dependent ratios can be calculated by the approximating relationship

ratio = (D-5)

over the range of the burnup data.

As pointed out in reference 12, the upper bound calculated with equation D-4 is expected to bracket the population, with at least 95% confidence, simultaneously over the range of burnup values (restricted to the data range). Because of the statistical properties of this upper bound and the extreme conservatism it represents, no further uncertainty of bow will need to be implemented. The results from equation D-4 will be directly applicable in the CHF penalty calculation after the adjustment of "cold to hot" variation is made.

All empirical estimates shown in Table D-1 are based on the Mark B data. An thus adding to the conservatism of the meth... applied to the Mark C fuel design.

4. Rod Bow Modeling

The L.S regression estimates of the coefficients were calculated with and without the weighting technique. Since the results of the two techniques compare well, only the unweighted coefficients were subsequently implemented. The weighted L.S using techniques of reference 11 yielded

(D-6)

or in the form

(D-7)

As the best model, this compares favorably with equation D-2,

Table D-2 shows calculations for the same inputs using each model.

Table D-1. Rod Bow Predictions

Burnup, GWd/mtU	Best estimate bow, mils	95% global tolerance bow, mils	Ratio	Hot, % as-built[a] Mark B	Mark C[b]
5.4					
8.0					
12.0					
16.5					
18.0					
20.0					
25.0					
30.0					
35.0					
39.8					

[a] Rod-to-rod as-built = 138 mils Mark B, 123 mils Mark C; hot-to-cold ratio = 1.20 for both.

[b] Mark C = [Mark B(138)]/123 = Mark B(1.122).

Table D-2. Bow and Burnup Values

Point ident	Burnup, GWd/mtU	Observed bow, mils	Predicted bow, mils	
			Unweighted	Weighted
1	5.4			
2	5.4			
3	5.4			
4	5.4			
5	6.4			
6	7.6			
7	9.8			
8	10.6			
9	10.8			
10	11.0			
11	13.1			
12	15.9			
13	16.5			
14	16.5			
15	16.5			
16	16.5			
17	16.6			
18	17.2			
19	17.2			
20	18.5			
21	19.7			
22	19.8			
23	20.0			
24	22.0			
25	24.3			
26	24.3			
27	24.6			
28	24.8			
29	25.1			
30	26.5			
31	28.2			
32	31.2			
33	31.2			
34	31.2			
35	31.2			
36	36.0			
37	39.8			
38	39.8			
39	39.8			
40	39.8			

APPENDIX E

CHF Test of Bowed Rod Bundle

1. Introduction

As part of a continuing 17×17 geometry test program on a new 7-MWe heat transfer facility at the Alliance Research Center (ARC), B&W has tested two 5×5 nonuniform guide tube bundles. The bundles (C9 and C10) were identical in geometry and heated design effects except that in the C10 bundle one of the hot rods was bowed into the guide tube channel to achieve approximately 55% closure in the rod-to-rod gaps.

This pair of tests presents an excellent opportunity to observe the effects of a bowed rod on CHF under reactor operating conditions at an upper value of the bow (closure) actually expected to occur. Analysis of the data from these tests is approached on both subchannel and bundle-average bases.

The analysis shows that the bowed rod results are within the uncertainty inherent in CHF testing and correlation. Consequently, no bow penalty is indicated for B&W fuel assemblies for predicted closures of up to 55%.

2. Test Description

2.1. Facility

The ARC 7-MWe heat transfer facility is a sophisticated, computer-controlled arrangement with the capability of testing full-length (12 ft) CHF bundles under pressures of up to 2600 psia, flows of up to 4 million lbm/h-ft^2, and inlet enthalpies approaching saturation.

2.2. Bundles

The two bundles (C9 and C10) were identical in design except for the C10 bowed rod. Figures E-1 and E-2 show the C9 (unbowed) and C10 (bowed) bundle cross sections and dimensions. An axial representation of the bundles along with the tested axial heat distribution of the bundles along with the tested axial heat distribution (a symmetric 1.67 peak-to-average flux shape) is shown in Figure E-3.

Spacer axial locations and subchannel form loss coefficients are given in Tables E-1 and E-2, respectively. The location of maximum closure (bow) in bundle C10 was 96.1 in. axially from the beginning of the heated length. An intermediate spacer was [illegible] at this location to maintain the required gap reduction. The spacer is a simple, chemically etched minimum turbulence grid

0.2 in. long. Its main purpose in CHF testing is to maintain spacing between electrically heated rods subjected to induced magnetic forces.

2.3. CHF Detection

The onset of the transition from nucleate to film boiling (the CHF point) was determined using acoustical sensors with continuous 4.5-in. temperature sensing zones (16 zones per sensor) over the last 6 ft of the bundle. Each of the 24 tubes had a separate sensor. The sharp temperature rise associated with CHF could thus be detected at any radial position over any of the 16 axial zones on any of the 24 heated tubes (or at a total of 384 possible CHF locations). This essentially universal coverage for CHF detection by acoustical sensors is a significant advance in nonuniform CHF testing (versus the use of thermocouples) and is reported in depth in reference 13.

3. Analysis

3.1. Subchannel Basis

CHF is traditionally correlated as a function of local (subchannel) geometry, mass velocity, pressure, and quality. A correlation of this form requires the use of a subchannel computer code to predict these local conditions within the bundle. For this analysis the LYNX2 code[14] was used in conjunction with the final B&W Mark C CHF correlation (BWC). The results were then compared in the form of measured to predicted CHF ratios. The results of this comparison are shown in Tables E-3 and E-4 and Figure E-4. On the average, the C-10 measured-to-predicted CHF ratios were 3 to 4% below those of C9.

3.2. Bundle Average

Since geometry, heat and flow conditions were nearly equal between bundles, further comparison is pertinent. The observed bundle average heat fluxes to CHF can be plotted versus inlet subcooling in parameters of mass velocity. These plots exhibit linear trends; thus, any difference in bundle performance should be obvious.

This was done for both bundles; the plots of the raw data are shown in Figures E-5 and E-6 for bundles C9 (unbowed) and C10 (bowed). A direct comparison of these two figures is possible if the tested mass velocities are equal. This was not the case since the C9 mass velocities averaged approximately 4% greater than those of the C10 bundle. Consequently, a one-to-one correction of power to flow (at each mass velocity) was made to both bundles to correct the observed CHF heat fluxes to correspond to exact mass velocities of 1.5 through 3.5 million lbm/h-ft.[14] A linear least-squares regression was then performed on both sets of data in parameters of these mass velocities.

The results are shown in Figure E-7 as a comparison of the bundle average CHF conditions. The average differences obtained in this manner in parameters of mass velocity are shown in Table E-5. The results here show the C10 bundle average CHFs to be approximately 2% below those of C9.

In CHF correlation, measured/predicted CHF ratios (M/P) are of primary interest. A 1% increase in measured CHF leads to about a 2% increase in M/P CHF ratio since not only does the measured value (M) increase, but the predicted value (P) decreases because of the increased severity of local conditions (mainly a higher local quality). Thus, the observed 2% difference in bundle average CHFs translates to a difference of approximately 4% in average M/P CHF ratios.

4. CHF Uncertainty

4.1. Areas of Uncertainty

Uncertainty in CHF testing and correlation can be divided into three areas:

1. The ability to repeat a CHF point within a bundle test at the same conditions of pressure, flow, and inlet temperature. This type of uncertainty is due to parameter measurement error as well as the local uncertainty inherent in the CHF phenomenon.
2. The ability to repeat CHF points between like bundles. This uncertainty is due to test modeling uncertainties, such as deviations in bundle as-built dimensions, heated effects, facility differences (if any), etc.
3. The correlational uncertainty inherent in any empirical CHF correlation (i.e., the "fitting" uncertainty), especially one dependent on calculated (versus observed) local conditions.

4.2. Uncertainty Analysis

Data from seven rod bundles were used to develop the BWC CHF correlation. On each bundle, "repeat" data points were taken at a specified midpoint in the pressure, flow, and inlet temperature test matrix. Statistics for the repeats are shown in Table E-6, and statistics for the BWC data base are shown in Table E-7. The following insights can be drawn from analysis of these statistics:

1. σ_p can be considered to be the uncertainty of the within bundle repeatability. σ_m can be considered to be the uncertainty of the between bundle repeatability (between the means of similar bundles). Considering both within and between uncertainties, the uncertainty associated with all repeat points as a group (σ_R) should be

   $$\sigma_R = (\sigma_p^2 + \sigma_m^2)^{1/2} = 0.048.$$

   This value compares well with the observed value of 0.046.

2. The total uncertainty of the BWC correlation (σ_T) is 0.070. Defining the correlational (fitting) uncertainty as σ_c, it follows that

   $$\sigma_T = (\sigma_p^2 + \sigma_m^2 + \sigma_c^2)^{1/2},$$

   or

   $$\sigma_c = (\sigma_T^2 - \sigma_p^2 - \sigma_m^2)^{1/2} = 0.051.$$

   A 5% fitting uncertainty is reasonable considering the complexity and range of the BWC correlation.

3. Deviations between bundle means in the BWC correlational data base ranged from -4.8 to +2.9% with a standard deviation of 2.5%.

Based on a standard normal distribution, deviations between bundle means of roughly two standard deviations would be expected. In item 1 above, the standard deviation between repeat means was 3% and in 3 above, the standard deviation between bundle means was 2.5%. Thus, the deviation of approximately 5 to 6% can be expected.

5. Conclusions

The analysis of the data by two different methods shows average CHF ratio performance differences of 3 to 4% between bundles (paragraph 3). This is within the range of CHF test repeatability for similar bundles (paragraph 4).

The conclusion drawn from this analysis is that under typical reactor operating conditions and at rod bow configurations producing maximum closures of up to 55% of the nominal rod gaps, no bow penalty is indicated for B&W fuel assemblies.

However, if an upper limit bow penalty must be determined, the only basis for comparison of bowed and unbowed CHF values is that of bundles C9 and C10 since these are identical in every way except to the bow phenomenon. Comparison of the C10 bowed data with other bundles in the CHF data base would necessarily introduce excess variability due to factors entirely unrelated to rod bow effects. Therefore, it is suggested that a conservative value of CHF adjustment be based on these two bundle results alone.

We have one identically paired observation, i.e., C10 and C9. Both were tested in the same facility, had virtually the same axial and radial power distributions, the same geometry, and the same range of test conditions. Thus, in the absence of a series of paired observations, an upper confidence limit on the bias between the true means of these observations can be calculated. Of course, this value would not represent the actual expected bias (if any), but would represent the true upper limit of this bias at the given value of closure.

Let

μ = true mean measured/predicted CHF ratio,

$\bar{X}$ = observed mean measured/predicted CHF ratio,

n = number of observations, and

S = unbiased estimate of the standard deviation of X_i around μ.

Then the upper confidence value on the difference between the true means is

$$(\mu_{C9} - \mu_{C10}) \le (\bar{X}_{C9} - \bar{X}_{C10}) + Z_{0.05}\left(\frac{S^2_{C9}}{n_{C9}} + \frac{S^2_{C10}}{n_{C10}}\right)^{\frac{1}{2}} \times (C)$$

$$\text{where} \quad C = 1 + \frac{1 + Z^2_{0.05}\left(\dfrac{S^4_9}{n^2_9(n_9 - 1)} + \dfrac{S^4_{10}}{n^2_{10}(n_{10} - 1)}\right)}{4 \times \left(\dfrac{S^2_9}{n_9} + \dfrac{S^2_{10}}{n_{10}}\right)^2}$$

Using C9 and C10 values from reference 3,

$$(\mu_{C9} - \mu_{C10}) \le (1.006 - 0.973) + 1.645\left[\frac{(0.064)^2}{85} + \frac{(0.078)^2}{77}\right]^{\frac{1}{2}} \times (1.0063),$$

and

$$(\mu_{C9} - \mu_{C10}) \le 0.0517 \text{ (or } 5.2\%).$$

The F ratio for C10/C9 yields a value of 1.485, which is not significantly different from $F_{0.01,84,76}$ but is significantly different at the $\alpha = 0.05$ level. Thus, using the Aspin-Welch statistic as shown above is conservative[20], and at 55% closure the upper limit on the DNBR penalty due to rod bow is 5.2%.

Table E-1. Spacer Grid Axial Locations

Table E-2. Subchannel Form Loss Coefficients

Table E-3. Measured/Predicted CHF Ratios ($\bar{M}/P$) in Parameters of Pressure

Pressure, psia	$\bar{M}/P$ (Vs BWC) C9	C10	% Δ, (C9 Vs C10)
1600	1.010	0.967	4.3
1800	1.003	0.965	3.8
2000	1.025	0.997	2.7
2200	1.017	0.978	3.8
2400	0.975	0.946	3.0
All	1.006	0.973	3.3

Table E-4. Measured/Predicted CHF Ratios in Parameters of Mass Velocity

Mass velocity, 10^{-6} lbm/h-ft^2	$\bar{M}/P$ (Vs BWC) C9	C10	% Δ, (C9 Vs C10)
1.0	--	1.080	--
1.5	1.003	0.994	0.9
2.0	0.989	0.955	3.4
2.5	0.998	0.929	6.9
3.0	1.010	0.943	6.6
3.5	1.052	0.956	9.1
All	1.006	0.973	3.3

Table E-5. Adjusted Bundle Average Heat Fluxes to CHF ($\bar{q}''$) in Parameters of Mass Velocity

Mass velocity, 10^{-6} lbm/h-ft^2	$-\bar{q}''$, 10^{-3} Btu/h-ft^2 [(a)] C9	C10	% Δ, (C9 Vs C10)
1.0	--	280	--
1.5	380	373	1.8
2.0	469	462	1.5
2.5	552	540	2.2
3.0	634	625	1.4
3.5	719	697	3.1
Average			2.0

(a) At 200 Btu/lbm inlet subcooling.

Table E-6. Rod Bundle Repeat Point Statistics

Bundle	Number of repeats, n	$\bar{M}/P$ (Vs BWC)	Standard deviation, σ
C3	6	0.952	0.064
C6	7	0.942	0.036
C7R	6	1.022	0.039
C8	7	0.955	0.010
C9	3	0.972	0.049
C10	4	0.969	0.004
C11	--	--	--
C12	5	1.011	0.027
All	38	0.973	0.046

The weighted pooled standard deviation:

$$\sigma_p = \left(\frac{\sum (n_i - 1)\sigma_i^2}{\sum n_i - 7}\right)^{1/2} = 0.038$$

The standard deviation of the bundle repeat means

$$\sigma_m = \frac{\Sigma\left((M/P)_i - \frac{\Sigma(\bar{M}/P)_i}{7}\right)^2}{6} = 0.030.$$

Table E-7. Statistics for BWC Correlational Data Base

Bundle	No. of points	Mean M/P CHF	Standard deviation
C3	68	1.010	0.070
C6	92	0.951	0.072
C7R	95	1.017	0.069
C8	122	0.994	0.062
C9	85	1.006	0.064
C11	30	1.028	0.074
C12	109	1.009	0.061
All	601	0.999	0.070
C10[a]	77	0.973	0.078

[a] The bowed rod bundle C10 was not used in the BWC data base.

Figure E-1. C9 (Unbowed) Test Geometry

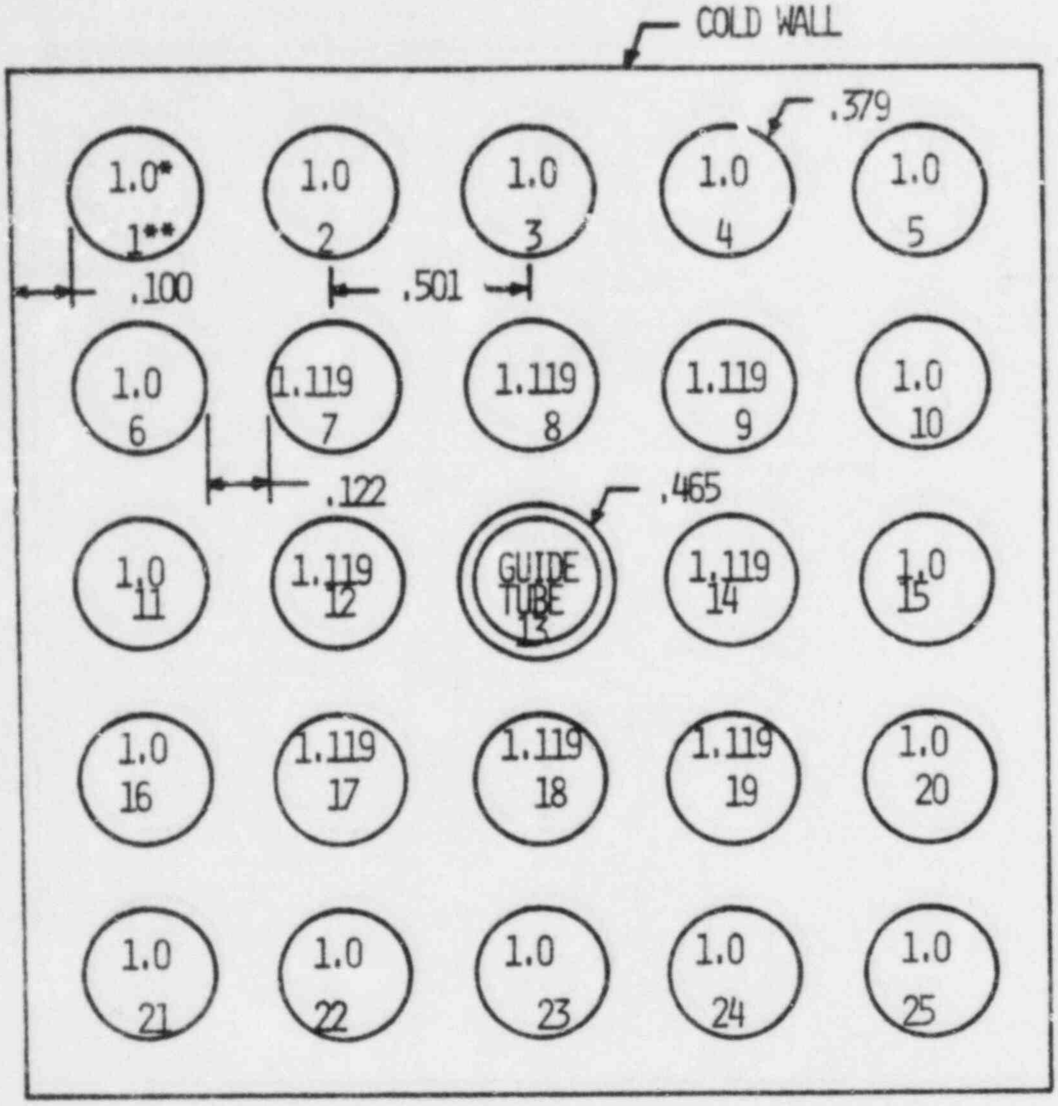

* RELATIVE HEAT FLUXES

** ROD NUMBERS

Figure E-2. C10 (Bowed) Test Geometry

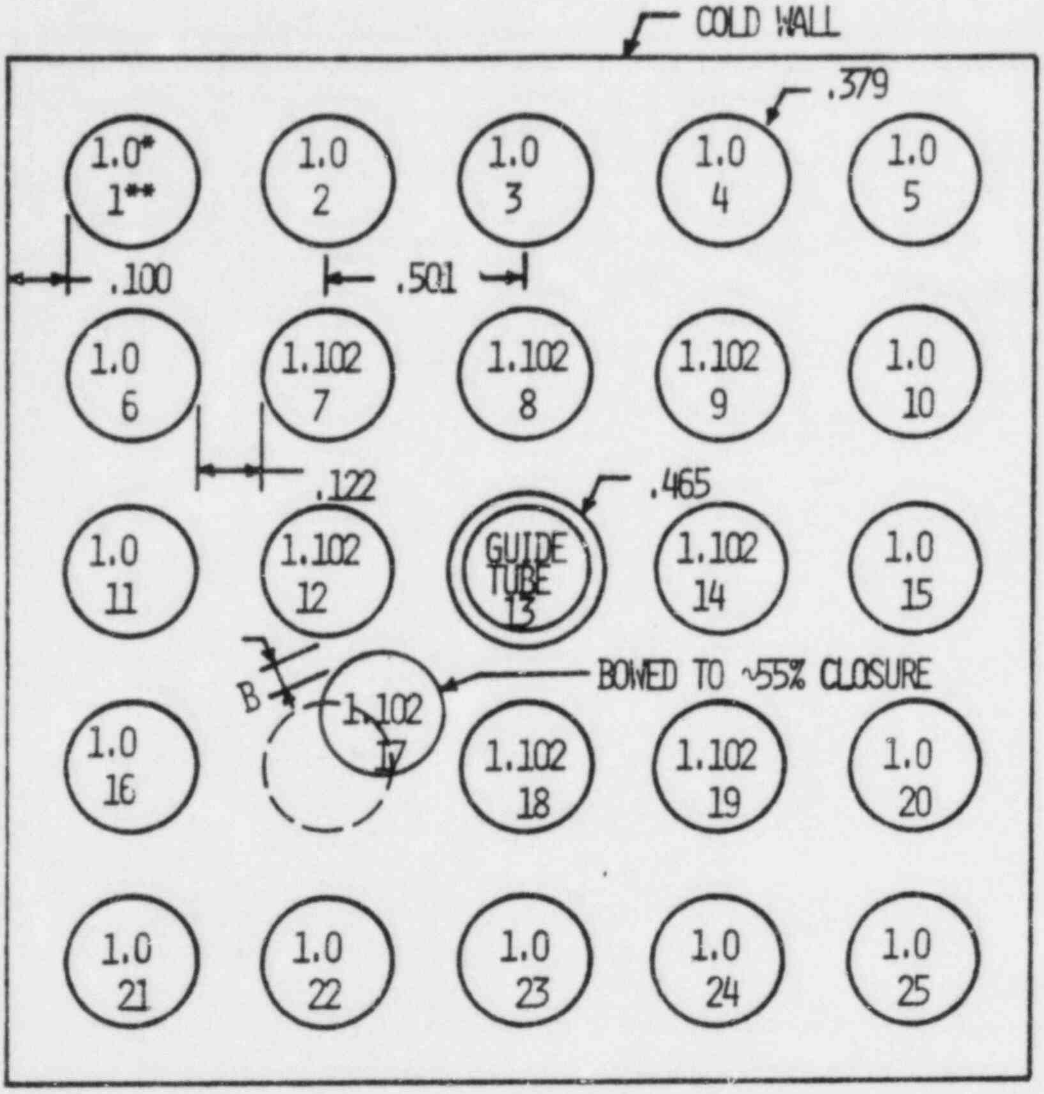

* RELATIVE HEAT FLUXES

** ROD NUMBERS

B = (1 - .55) x (.122) = .055" (BOWED MINIMUM GAP)

Figure E-3. Nonuniform Guide Tube Bundles

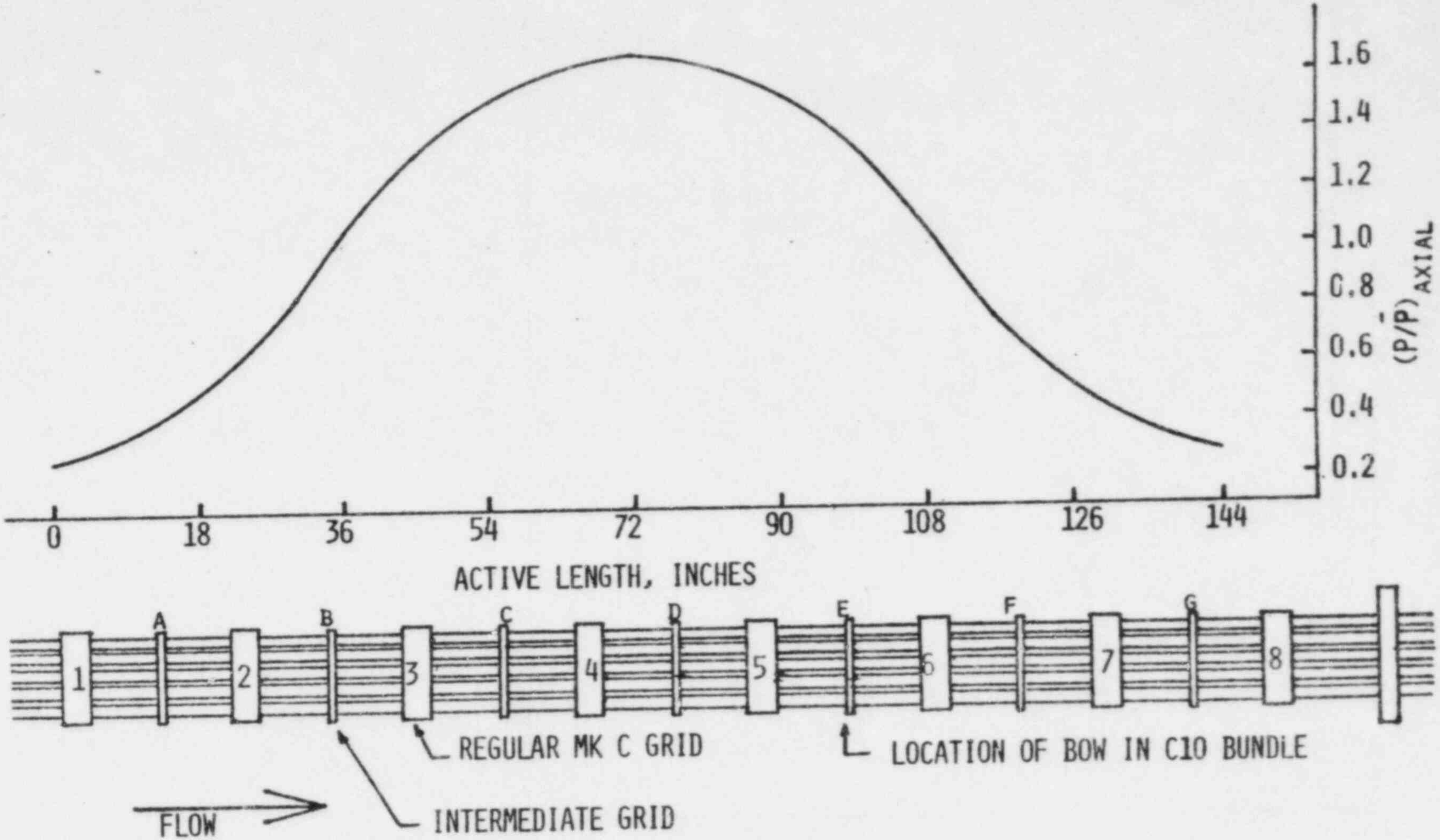

Figure E-4. C9 and C10 Data Compared to BWC CHF Correlation

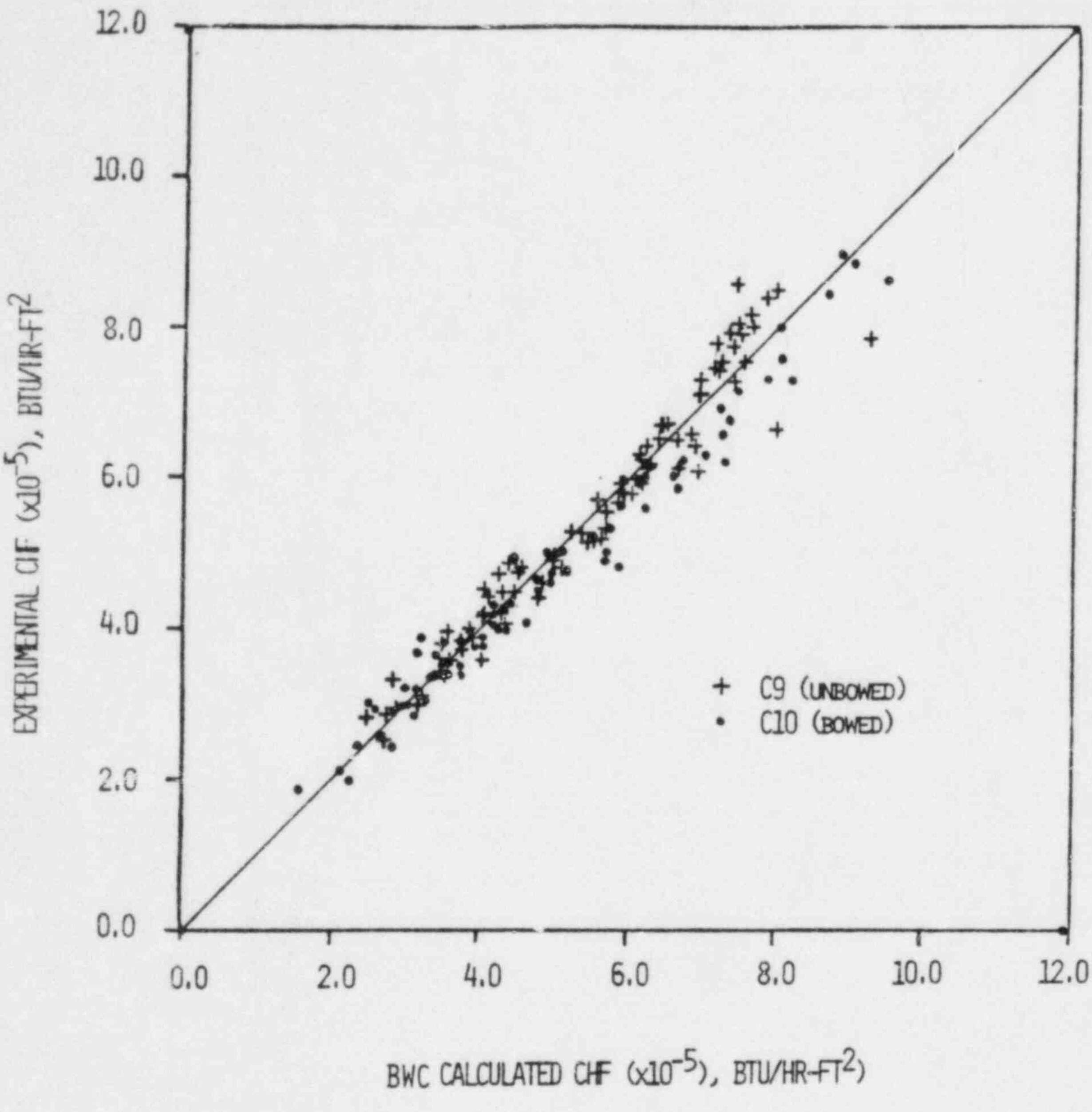

Figure E-5. C9 (Unbowed) Raw Bundle Data

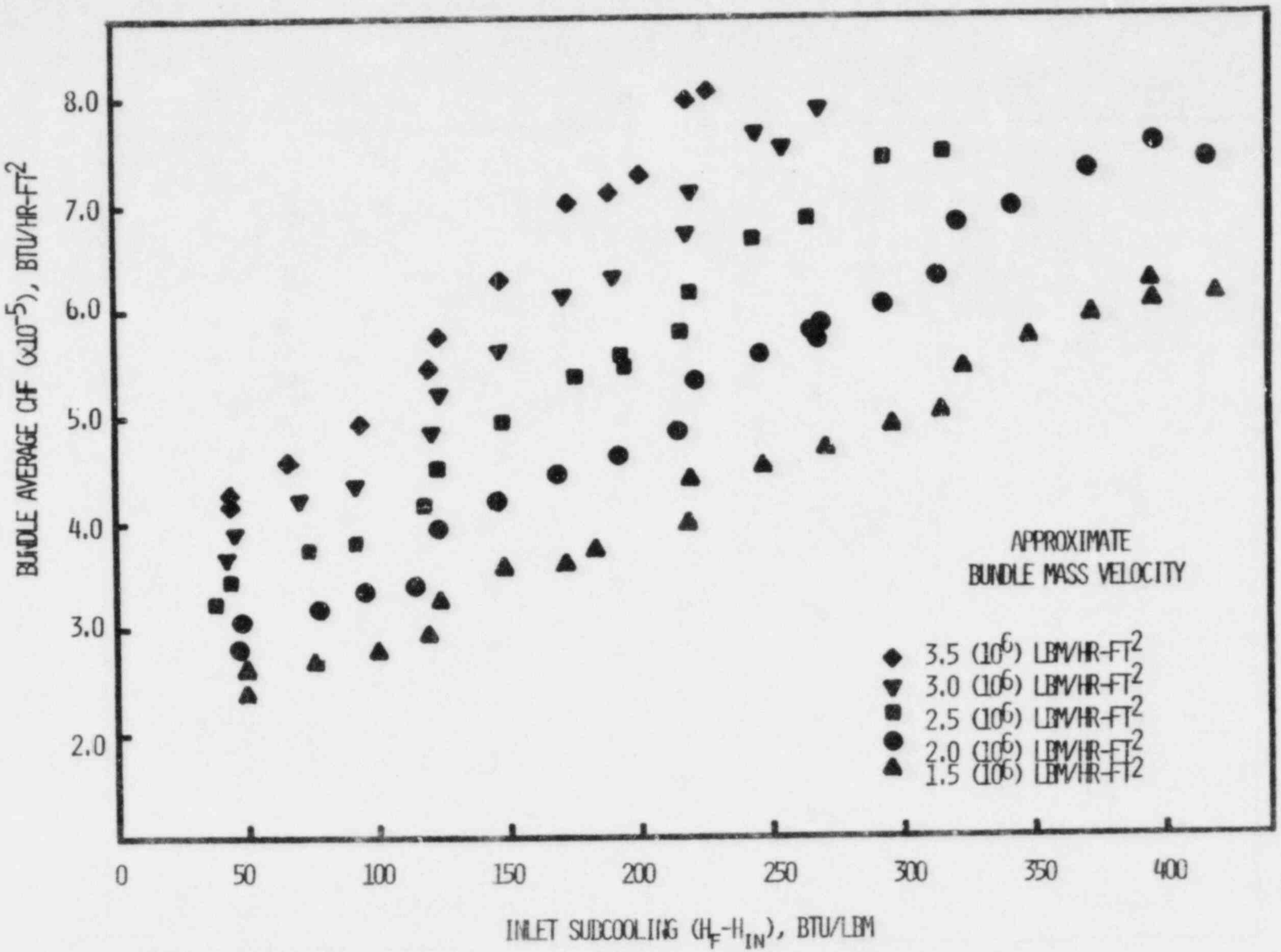

Figure E-6. C10 (Bowed) Raw Bundle Data

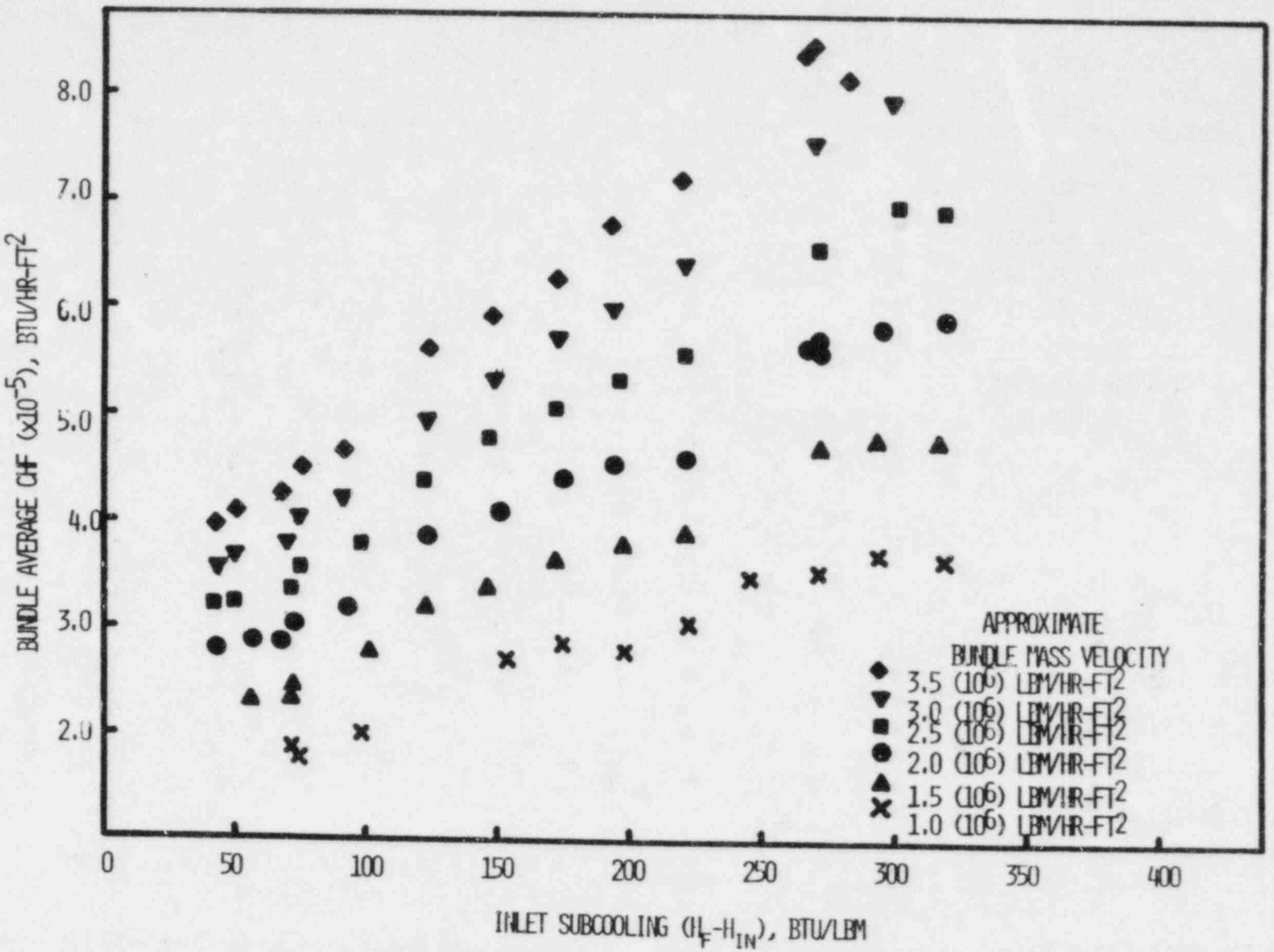

Figure E-7. Least-Squares Fit of Corrected C9 and C10 Bundle Data

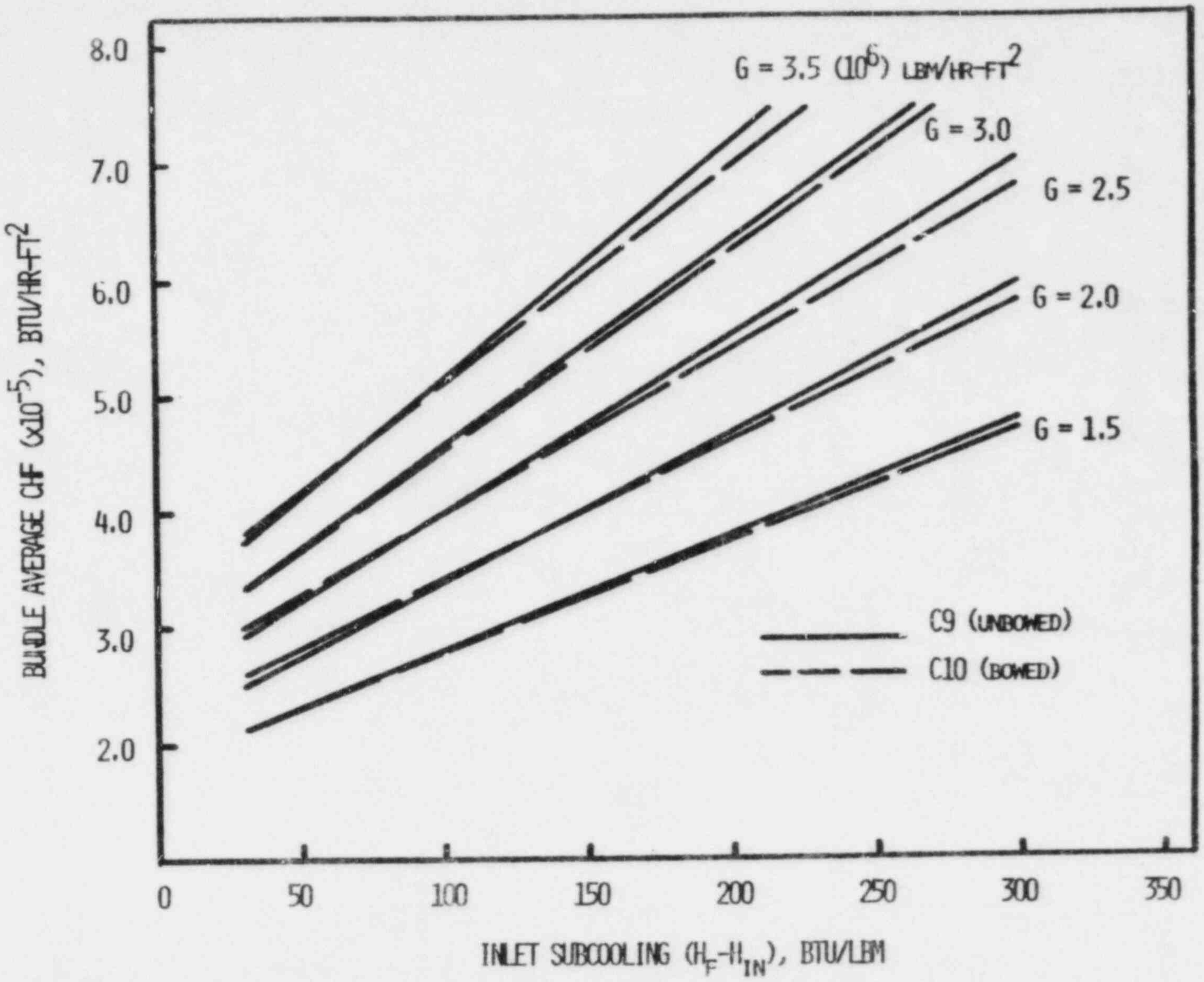

Attachment A — Data

Bundle average conditions for bundles C9 and C10 are shown in Tables E-8 and E-9, respectively. The axial power profiles for both bundles for both inner and outer rods are shown in Tables E-10 and E-11. Finally, the local condition results for bundles C9 and C10 are shown in Tables E-12 and E-13.

Table E-8. Bundle Average Conditions for C9

Run	Pressure, psia	Mass flux, 10^6 lbm/h-ft^2	Inlet enthalpy, Btu/lbm	Average heat flux, 10^6 Btu/h-ft^2	Primary rod No.	DNB length, in.
774						
775						
776						
777						
774						
779						
780						
781						
782						
784						
786						
787						
788						
789						
790						
791						
792						
793						
794						
795						
796						
797						
798						
800						
801						
802						
803						
804						
805						
806						

Table E-8. (Cont'd)

Run	Pressure, psia	Mass flux, 10^6 lbm/h-ft^2	Inlet enthalpy, Btu/lbm	Average heat flux, 10^6 Btu/h-ft^2	Primary rod No.	DNB length, in.
807						
808						
809						
810						
811						
812						
813						
814						
815						
816						
817						
818						
819						
820						
821						
822						
824						
825						
826						
827						
828						
829						
830						
832						
833						
834						
835						
836						
837						
838						
840						
843						
844						
845						
846						
848						
849						
850						
851						
852						

Table E-8. (Cont'd)

Run	Pressure, psia	Mass flux, 10^6 lbm/h-ft^2	Inlet enthalpy, Btu/lbm	Average heat flux, 10^6 Btu/h-ft^2	Primary rod No.	DNB length, in.
853						
854						
855						
856						
857						
858						
859						
860						
861						
862						
863						
864						
865						
866						
867						

Table E-9. Bundle Average Conditions for C10

Run	Pressure, psia	Mass flux, 10^6 lbm/h-ft^2	Inlet enthalpy, Btu/lbm	Average heat flux, 10^6 Btu/h-ft^2	Primary rod No.	DNB length, in.
885						
886						
887						
888						
889						
890						
891						
892						
893						
894						
895						
896						
897						
898						
899						
900						
901						
902						
903						
904						
905						
907						
908						
909						
910						
911						
912						
913						
914						
915						
916						
917						
918						
919						
920						
921						
922						
923						
924						
925						
926						
927						
928						

Table E-9. (Cont'd)

Run	Pressure, psia	Mass flux, 10^6 lbm/h-ft^2	Inlet enthalpy, Btu/lbm	Average heat flux, 10^6 Btu/h-ft^2	Primary rod No.	DNB length, in.
929						
930						
931						
932						
933						
934						
935						
942						
944						
946						
948						
950						
952						
955						
961						
963						
965						
967						
968						
969						
970						
971						
972						
973						
974						
975						
976						
977						
978						
979						
980						
981						
982						
983						

Table E-10. Axial Power Profiles for Bundle C9

Inner rod		Outer rod	
X, in.[a]	Norm. power ratio	X, in.[a]	Norm. power ratio
0.0	0.264	0.0	0.264
4.125	0.264/0.283[b]	4.000	0.264/0.283[b]
8.375	0.283/0.306[b]	8.000	0.283/0.301[b]
14.308	0.386	13.853	0.383
20.308	0.513	19.853	0.510
26.000	0.666/0.752[b]	21.500	0.541/0.611[b]
30.000	0.872	24.000	0.682
36.000	1.063	30.000	0.864
42.000	1.247	36.000	1.059
48.000	1.418	42.000	1.252
54.000	1.548	48.000	1.396
60.000	1.615	54.000	1.542
66.000	1.668	60.000	1.613
72.000	1.658/1.637[b]	66.000	1.646
78.000	1.647	72.000	1.663/1.642[b]
84.000	1.595	78.000	1.626
90.000	1.529	84.000	1.593
96.000	1.400	90.000	1.523
102.000	1.232	96.000	1.378
108.000	1.050	102.000	1.236
114.000	0.862	108.000	1.047
118.000	0.744/0.671[b]	114.000	0.854
123.692	0.518	120.000	0.675
129.692	0.390	122.500	0.605/0.548[b]
135.875	0.306/0.315[b]	124.147	0.515
139.375	0.315/0.276[b]	130.147	0.387
144.000	0.276	136.250	0.301/0.303[b]
		139.750	0.303/0.280[b]
		144.000	0.280

[a] Measured from start of heated length.

[b] Step in power profile.

Table E-11. Axial Power Profiles for Bundle C10

Inner rod		Outer rod	
X, in.[a]	Norm. power ratio	X, in.[a]	Norm. power ratio
0.0	0.295	0.0	0.271
6.0	0.300	5.82	0.273
8.422	0.301	12.0	0.339
12.0	0.344	18.0	0.445
18.0	0.451	23.57	0.585
24.0	0.593	26.0[b]	0.648/0.714
26.0[b]	0.649/0.718	30.0	0.841
30.0	0.848	36.0	1.034
36.0	1.042	42.0	1.223
42.0	1.230	48.0	1.397
48.0	1.378	54.0	1.542
54.0	1.522	60.0	1.636
60.0	1.621	66.0	1.707
66.0	1.698	72.0	1.719
72.0	1.720	78.0	1.707
78.0	1.698	84.0	1.636
84.0	1.621	90.0	1.542
90.0	1.522	96.0	1.397
96.0	1.379	102.0	1.223
102.0	1.230	108.0	1.035
108.0	1.042	114.0	0.843
114.0	0.849	118.0[b]	0.716/0.656
118.0[b]	0.719/0.655	124.0	0.491
124.0	0.506	130.0	0.372
130.0	0.383	135.75[b]	0.299/0.303
135.5[b]	0.305/0.317	139.75[b]	0.303/0.275
139.75[b]	0.317/0.273	144.0	0.275
144.0	0.273		

[a] Distance downstream of beginning of heated length.

[b] Step in power profile.

Table E-12. Local Condition Results for Bundle C9

ID.	DNB RATIO	CALCULATED HEAT FLUX	MASS VELOCITY	ENTERING ENTHALPY	PRES.	B.O. PT.	EQUI DIAM	QUALITY	F FACTOR	EXP. HEAT FLUX

Table E-13. Local Condition Results for Bundle C10

ID.	DNB RATIO	CALCULATED HEAT FLUX	MASS VELOCITY	ENTERING ENTHALPY	PRES.	B.O. PT.	EQUI DIAM	QUALITY	F FACTOR	EXP. HEAT FLUX

APPENDIX F

Rod Bow Effect on DNBR

As outlined in section 6, DNBR reduction is a function of gap closure, $\Delta c/C_o$, and gap closure is a function of burnup. Appendix F presents the development of the method used to determine the DNBR reduction as a function of burnup.

1. Relating Penalty to Burnup

The value of δ_{DNBR} is uniquely defined by equation F-1 once the value of $\Delta c/C_o$ is known. Formally, the value of the penalty is conditional on $\Delta c/C_o$ and can be denoted as

$$\delta_{DNBR}|\Delta c/C_o = \qquad \text{(F-1)}$$

Then unconditionally,

$$\delta_{DNBR} = \qquad \text{(F-2)}$$

for all values of the constant d_i between and 1.0 and d_j between 0 and , respectively. Equation F-2 is a weighted sum of possible penalties over the interval (0,1). Since $\Delta c/C_o$ is continuous over this interval, the sums in equation F-2 are replaced by integrals and combined. Thus,

$$\delta_{DNBR} = \qquad \text{(F-3)}$$

Being probabilities, the weights are positive and fall into the interval (0,1). If they sum (integrate) to unity, i.e., the probability function of $\Delta c/C_o$ is normalized to unity, the value obtained from equation F-3 will be the unconditional penalty of δ_{DNBR} at any given assembly burnup.

The penalty value from equation F-3 will be a function of the parameters of $\Delta c/C_o$, i.e., of its probability distribution parameters. These parameters govern the likelihood of a $\Delta c/C_o$ value falling above or below . As the proportion of values falling above increases, the value of δ_{DNBR} increases appropriately. This is clear from equation F-1, which shows that for those values of $\Delta c/C_o$ that fall below , no contribution to the integral of equation F-3 is made since the penalty function is zero. The illustration of Figure F-1 helps to clarify this point.

In the next section, it will be shown that it is σ, the parameter of the $\Delta c/C_o$ distribution, that governs the size of δ_{DNBR}. In this context, σ is often equated with "bow" in the literature.[1,2,4,7] The relationship of burnup to bow and gap closures is evaluated in Appendix D.

2. Probability Distribution of Gap Closure

Traditionally, gap closures (C) have been assumed to be normally distributed.[1] If C has a mean of μ and standard deviation of σ, the notation $C \sim N(\mu,\sigma)$ is often used. The probability that C will be less than a value ℓ_0 is defined by

$$P(C \leq \ell_0) = \qquad \text{(F-4)}$$

The notation $\phi(*)$ refers to the integral from $(-\infty)$ to a value $(*)$ of a standard normal variable $[Z \sim N(0,1)]$. The value of the mean, μ, of equation F-4 is referred to as the "as-built gap" in previous sections and is denoted by C_o.

Normalization to unity over the interval (0,1) is achieved by evaluating equation F-6 from zero to one and dividing the density by this area. Performing this operation yields the normalized density of $\Delta c/C_o$ between the values ($0 \leq \Delta c/C_o \leq 1$). The form of equation F-6 thus becomes

(F-8)

and is valid for values of r between (0,1). The normalizing factor, A, is found to be

$$A = 2[\phi(1/\sigma^*) - 0.5]. \tag{F-9}$$

Substitution of equation F-8 and F-1 into equation F-3 yields the result that the unconditional penalty is

$$\delta_{DNBR} = \qquad \text{(F-10)}$$

with the constant A defined in equation F-9. The details of the integration are found in paragraph 3 of this appendix.

Figures F-2 and F-3 show bow, or σ^*, as a function of burnup, using the results of the analyses presented in section 5 and also the corresponding δ_{DNBR} - S calculated with equation F-10. The values of δ_{DNBR} can be readily substituted into equation 6-2 to yield the limit values of DNBR (bow) with the value of DNBR (no bow) = from reference 15.

3. Derivation of Penalty Equation, F-10

With a_L = and K = and σ replaced by σ*, equation F-10 is obtained.

Figure F-1. Penalty-Bow Relationship

Figure F-2. Mark B Percent Bow Predictions and Penalties

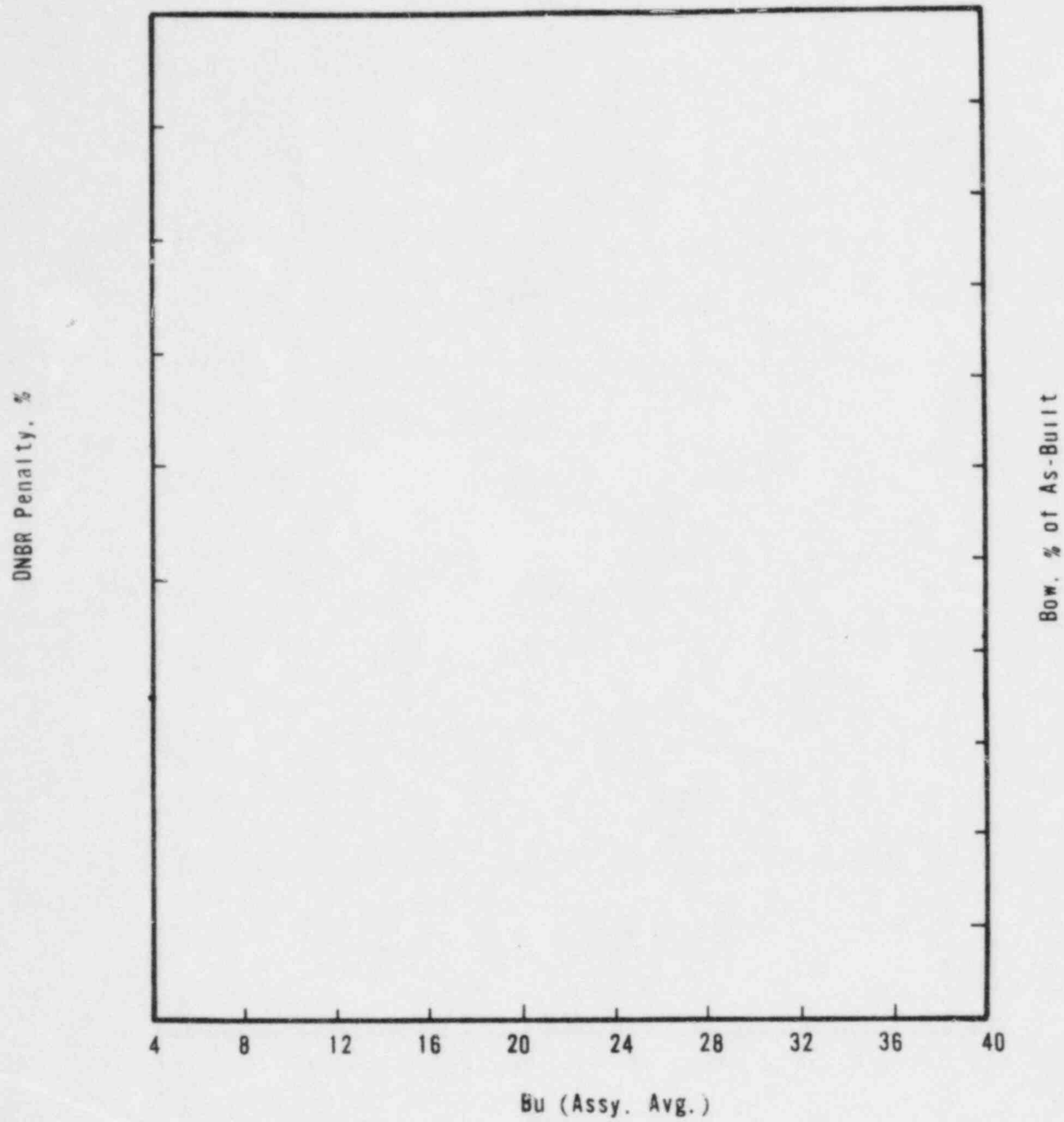

Figure F-3. Mark C Percent Bow Predictions and Penalties

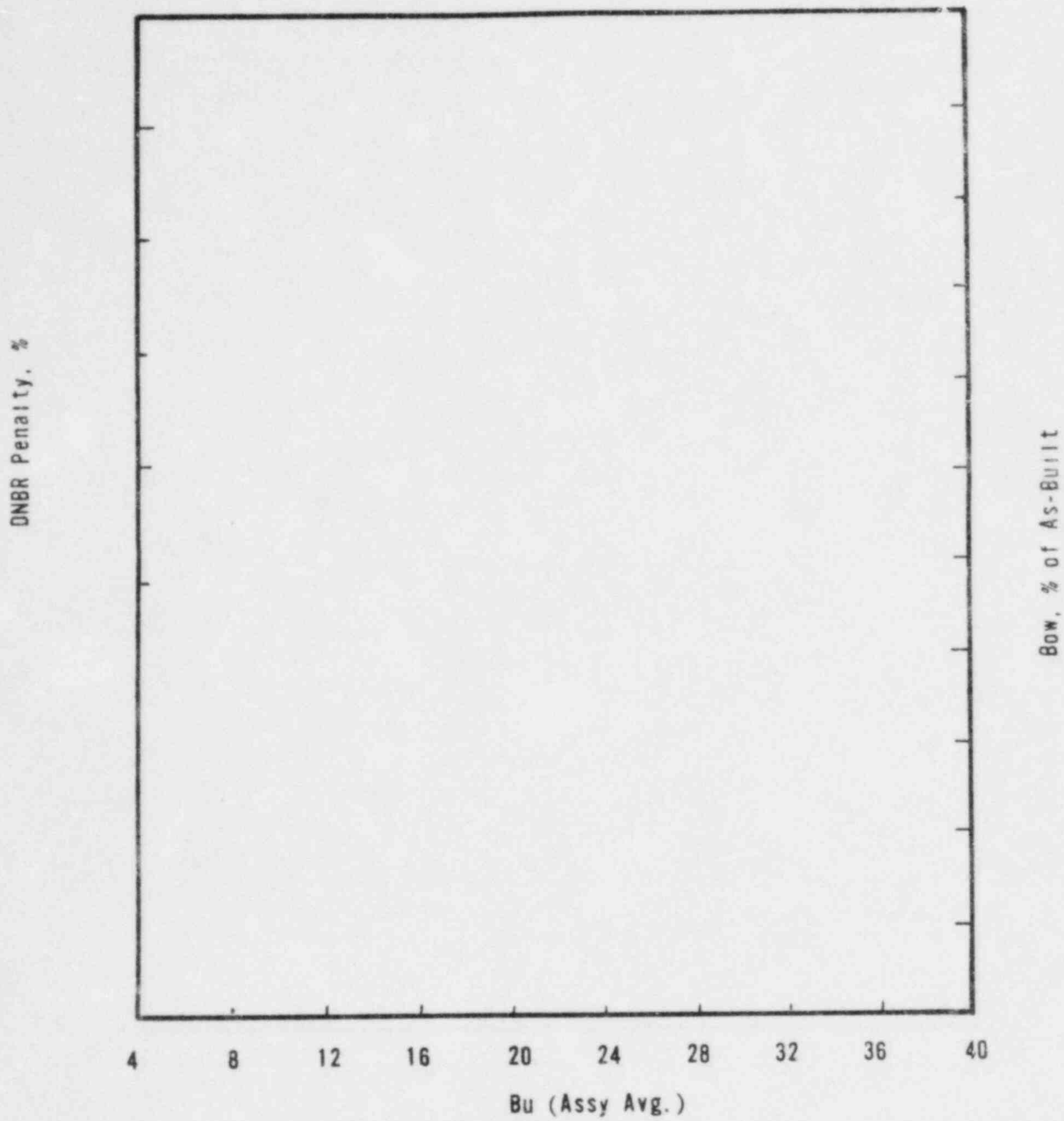

APPENDIX G

Rod Bow Effect on Power Peaking

Fuel rod bowing results in small local power changes in the vicinity of the bowed rod because of a change in neutron moderation. For example, a fuel rod located near a bowed rod will see a softer neutron spectrum if the direction of bow is away from its lattice location. The increase in neutron moderation will result in an increase in rod power because the nominal lattice is under-moderated. On the other hand, if the direction of bow is reversed, there will be a decrease in neutron moderation, resulting in a decrease in power.

The magnitude of this effect on power is a function of material properties and geometry, including the rod bow. This phenomenon has been investigated for the standard B&W 15×15 and 17×17 designs. The DOT code was used to calculate the power distribution for a 5×5 lattice array of fuel rods including a bowed rod as a function of the magnitude and azimuthal direction of bow.[16] The code modeled the neutron energy spectrum as six groups, divided into five thermal and one fast group. The cylindrical geometry of the individual rods was approximated in rectangular coordinates. A bowed rod was modeled at the center of a 5×5 array of fuel rod unit cells surrounded by a homogeneous fuel/moderator region (see Figure G-1). Macroscopic cross sections were calculated by the ANISN code.[17] Microscopic cross section data for input to ANISN were obtained from the NULIF[18] and PROLIB[19] codes for fast and thermal neutrons, respectively.

Figures G-2 and G-3 show the effects of bowing on bowed rod power for 15×15 and 17×17 lattices, respectively. The power change is always negative and is independent of azimuthal angle. Analyses also show that the power change in perturbed rods is independent of enrichment for enrichments from 2.75 to 3.20 wt % ^{235}U.

The power effect of a single bowed rod on other rods in the immediate vicinity is shown in Figures G-4 through G-13. Results for the Mark B lattice are shown in Figures G-4 through G-8 for a fuel enrichment of 3.00 wt % ^{235}U. Results for the Mark C lattice are shown in Figures G-9 through G-13 for a fuel enrichment of 3.45 wt %. The effect of enrichment-induced peaking is shown by Figures G-14 and G-15 for the Mark B lattice. Maneuvering analysis of fuel cycle designs includes the peaking uncertainty associated with rod bow.

Figure G-1. Dot Grid, 5 × 5 Discrete Fuel Rod Array, Constant Mesh Spacing

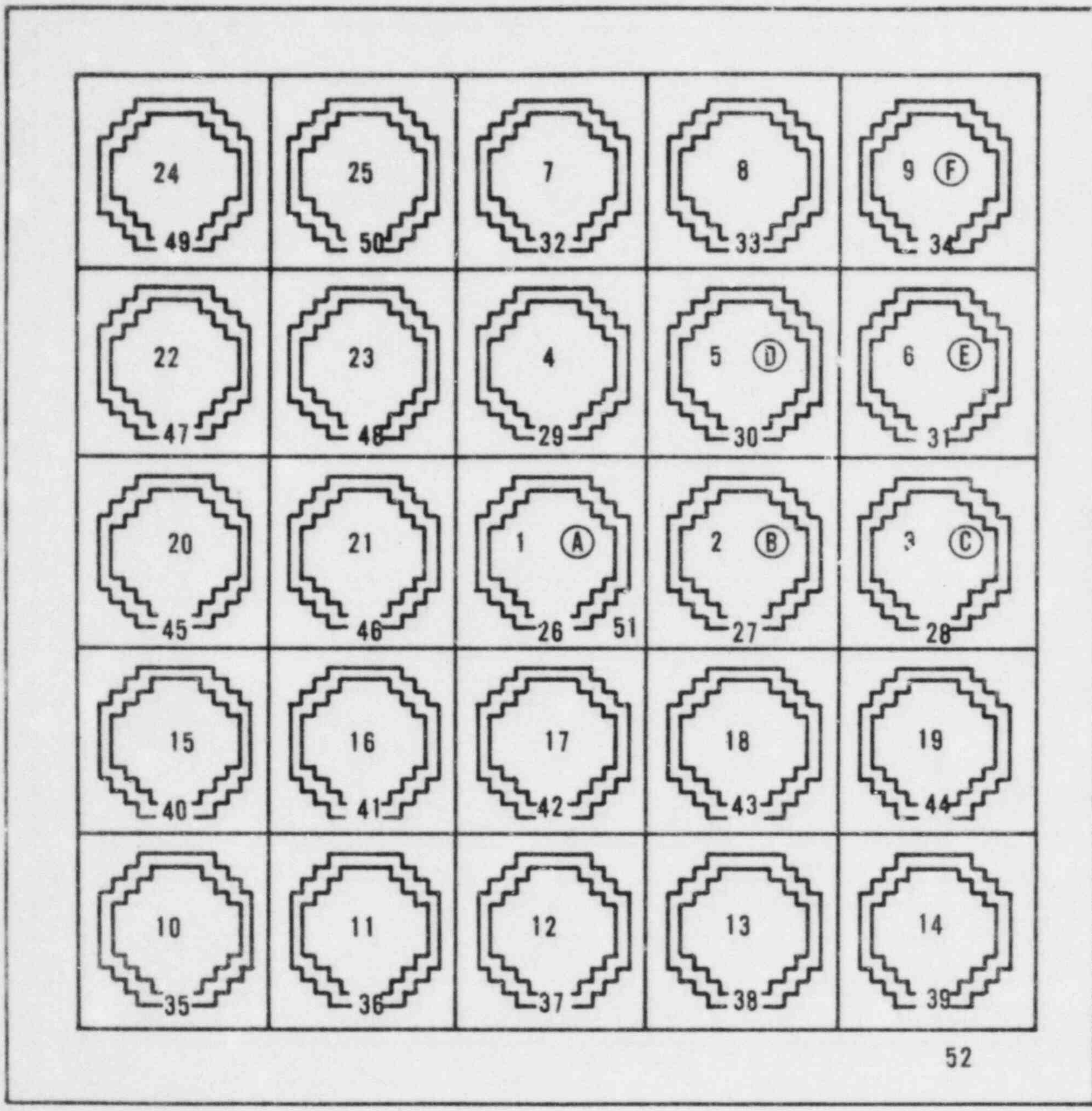

ZONE DESIGNATION

1-25 FUEL PELLET

26-50 CLAD & MOD.

51 MODERATOR

52 HOMO. FUEL

Figure G-2. Power Change in Fuel Rod A Due to Self Bow, Mark B Geometry

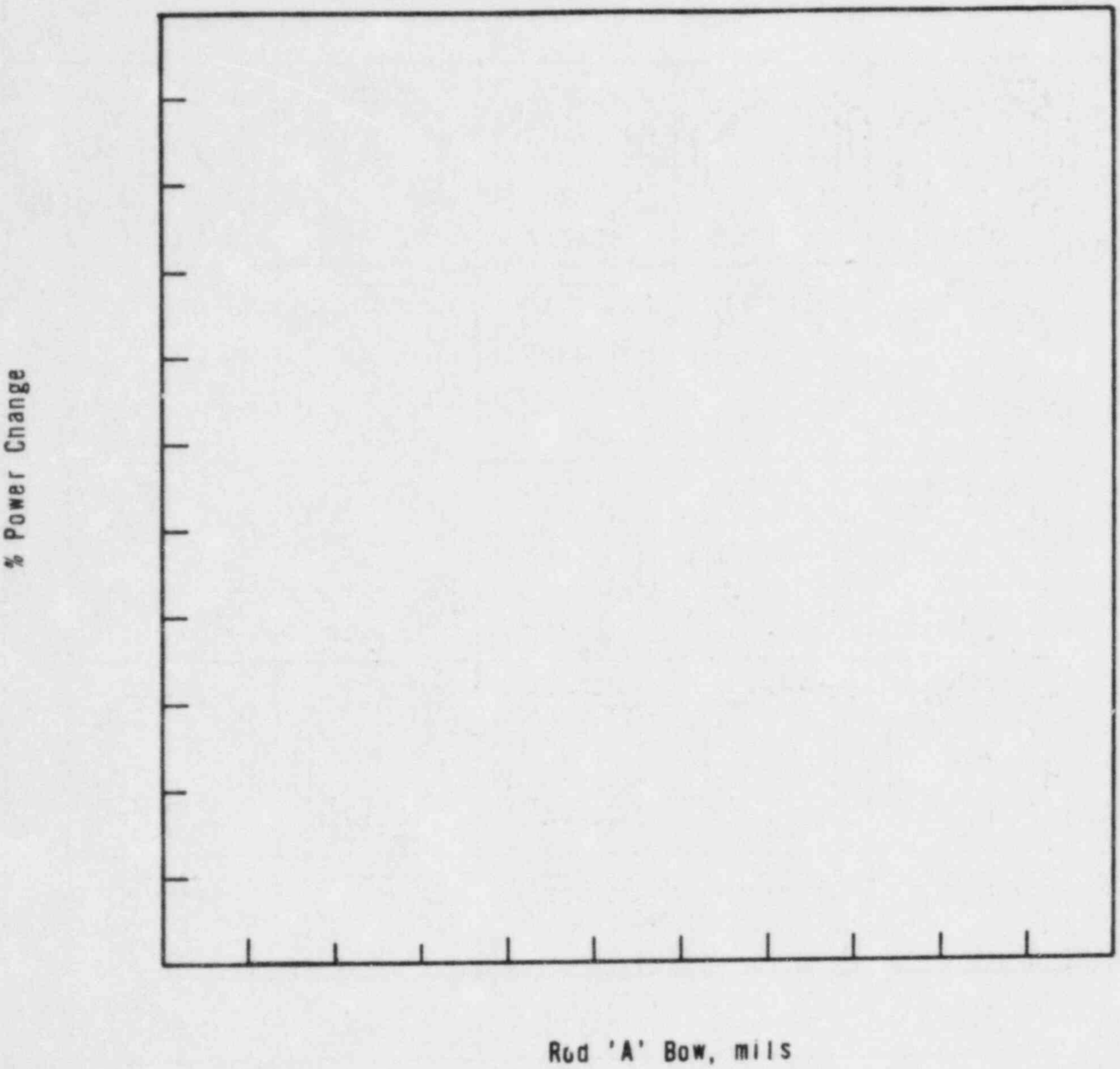

Figure G-3. Power Change in Fuel Rod A Due to Self Bow, Mark C Geometry

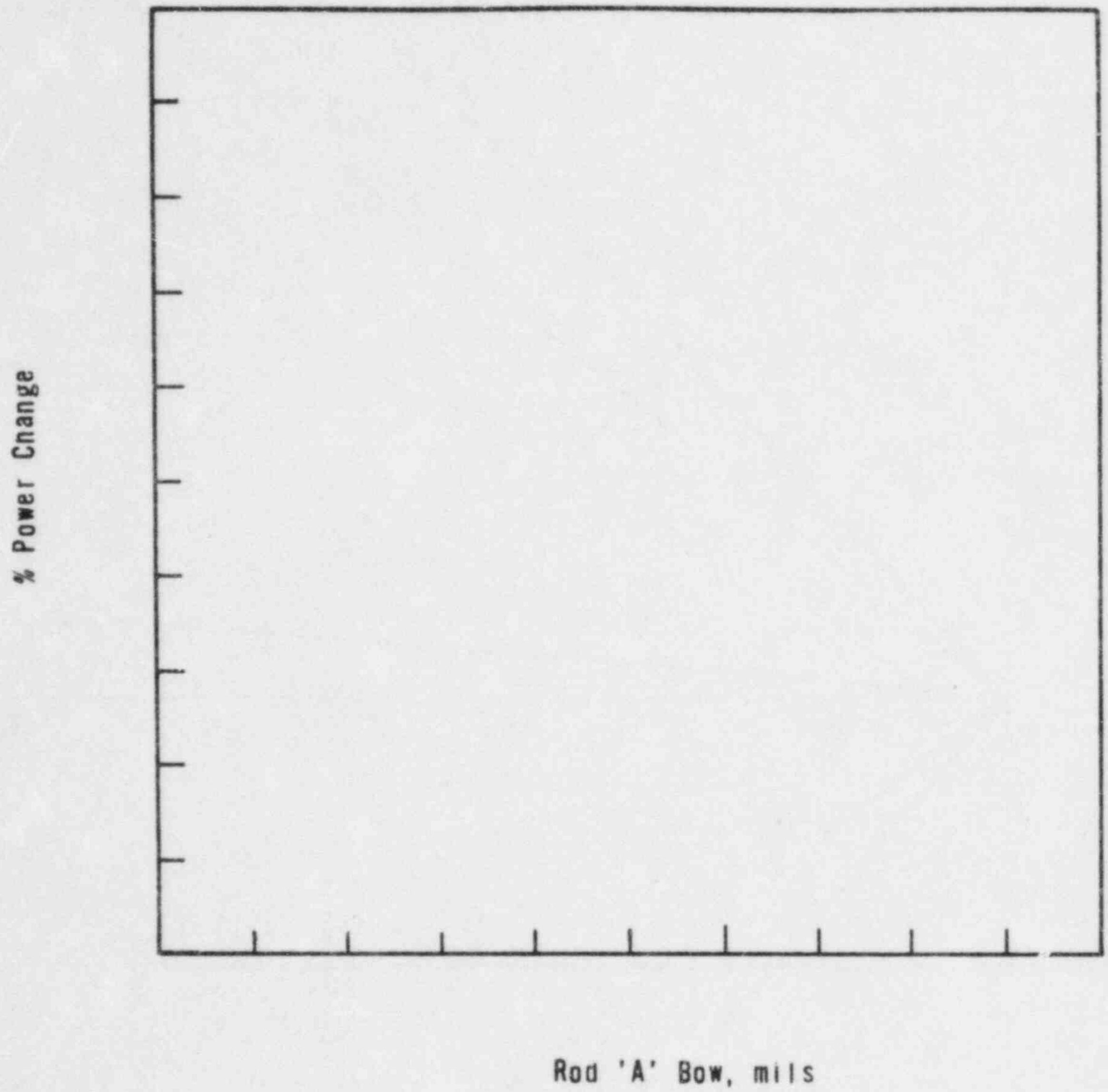

Figure G-4. Percent Power Change in Rod B Due to Rod A Bow, Mark B Geometry, E = 3.00 wt %

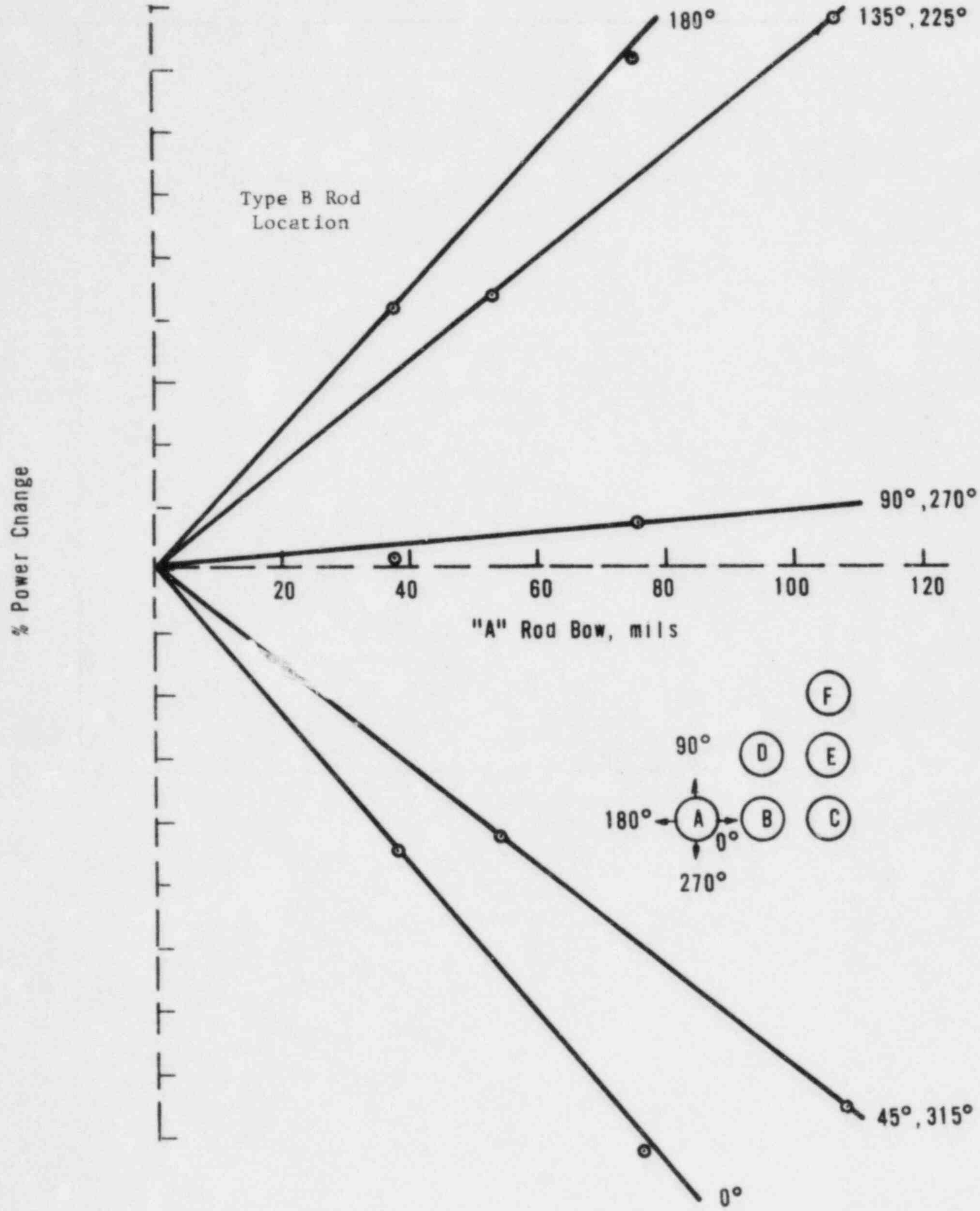

Figure G-5. Percent Power Change in Rod C Due to Rod A Bow, Mark B Geometry, E = 3.00 wt %

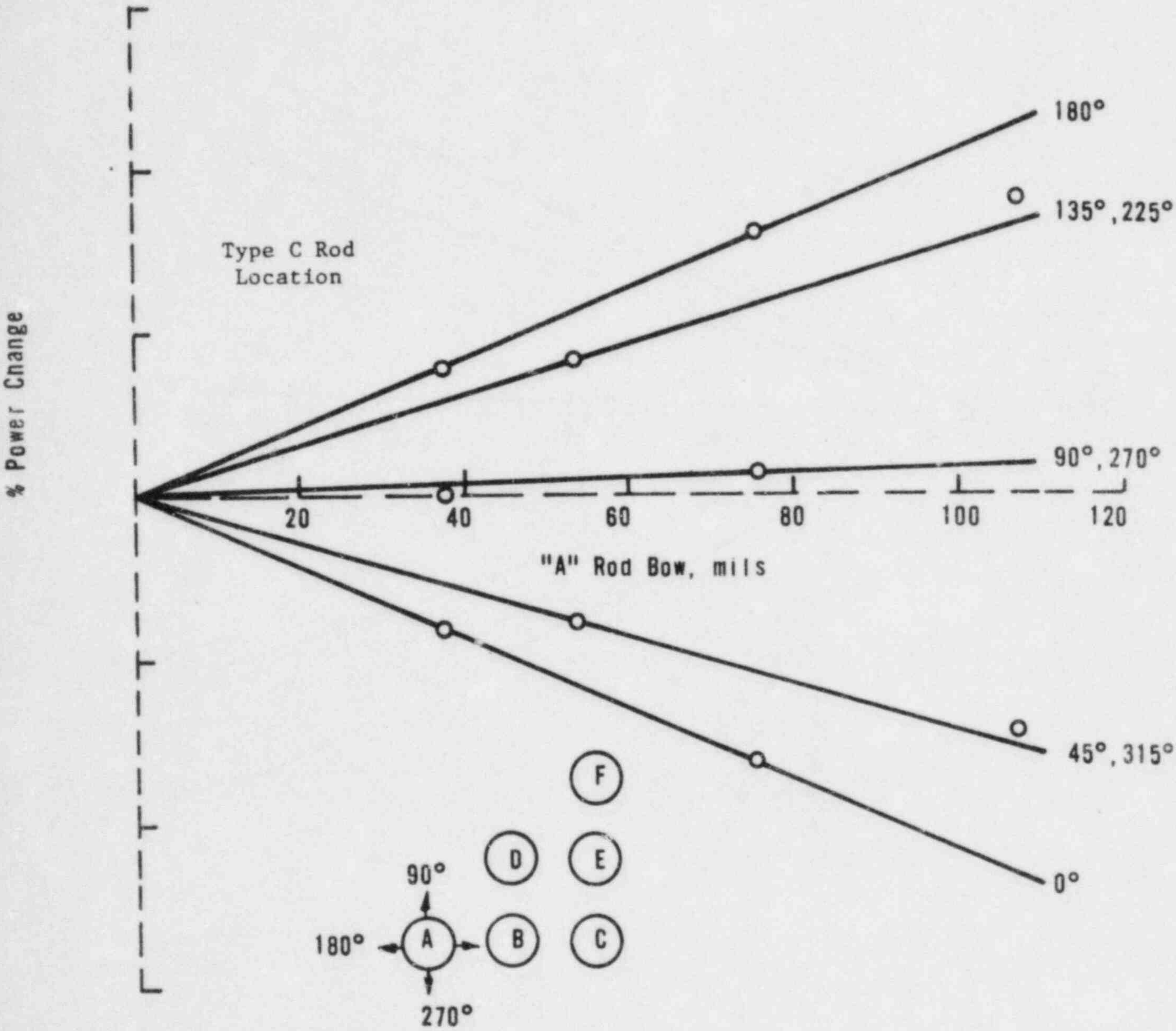

Figure G-6. Percent Power Change in Rod D Due to Rod A Bow, Mark B Geometry, E = 3.00 wt %

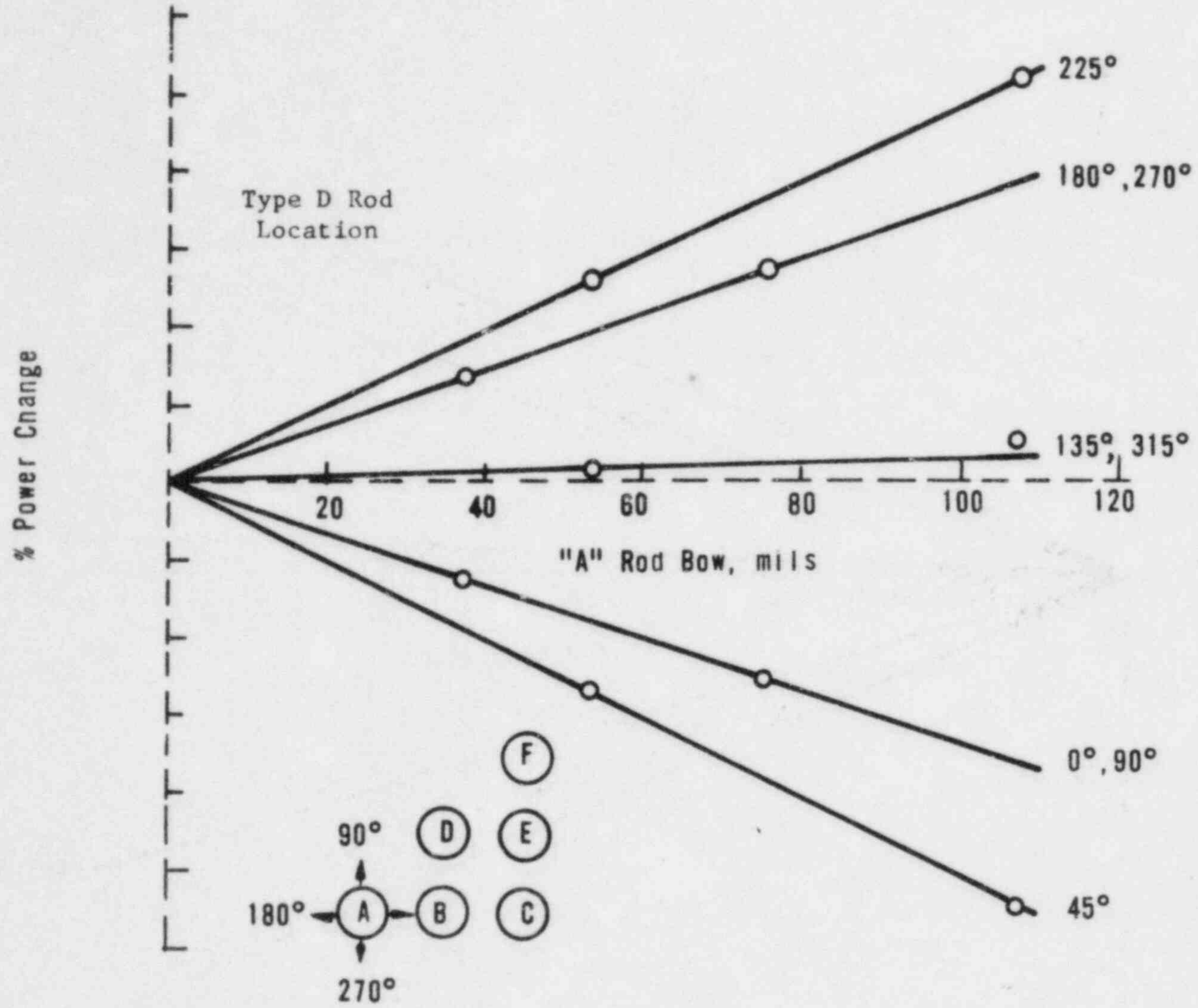

Figure G-7. Percent Power Change in Rod E Due to Rod A Bow, Mark B Geometry, E = 3.00 wt %

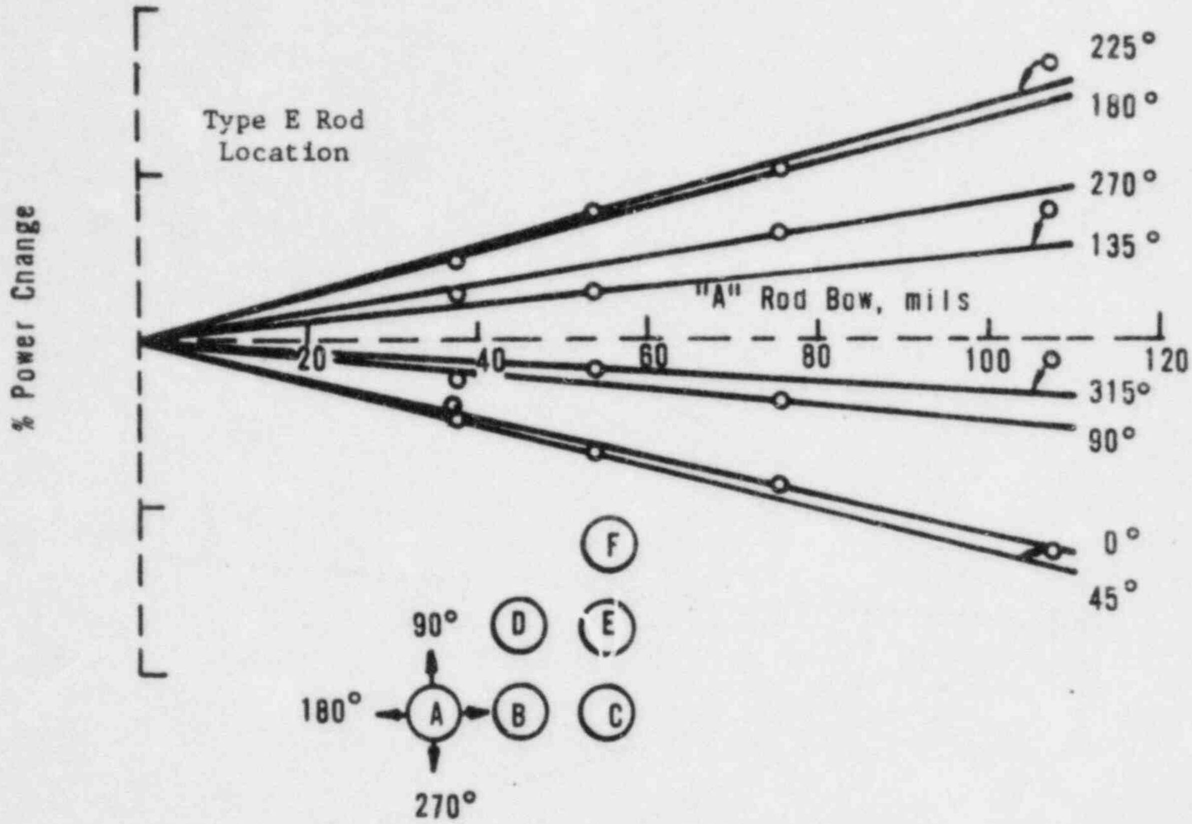

Figure G-8. Percent Power Change in Rod F Due to Rod A Bow, Mark B Geometry, E = 3.00 wt %

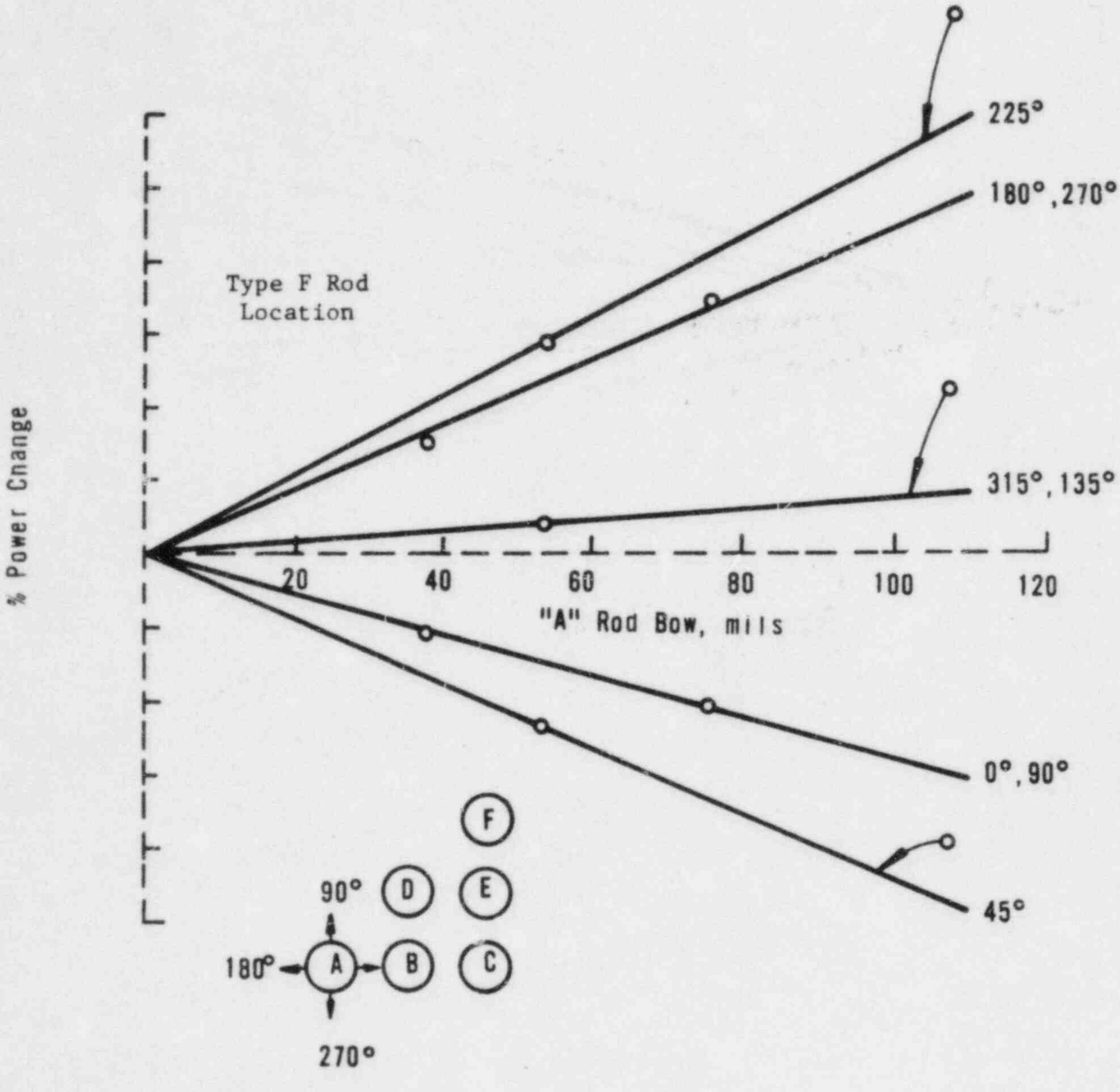

Figure G-9. Percent Power Change in Rod B Due to Rod A Bow, Mark C Geometry, E = 3.45 wt %

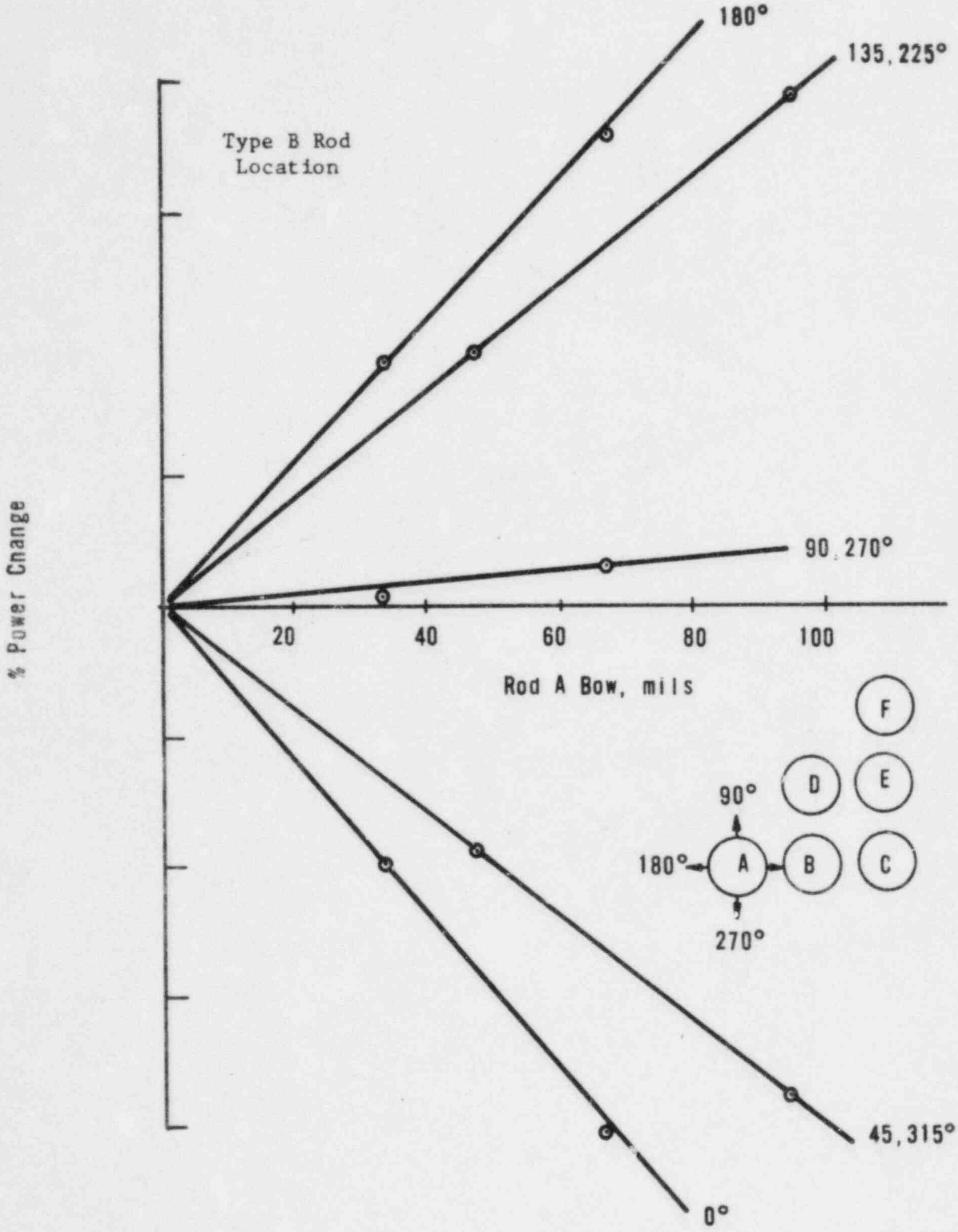

Figure G-10. Percent Power Change in Rod C Due to Rod A Bow, Mark C Geometry, E = 3.45 wt %

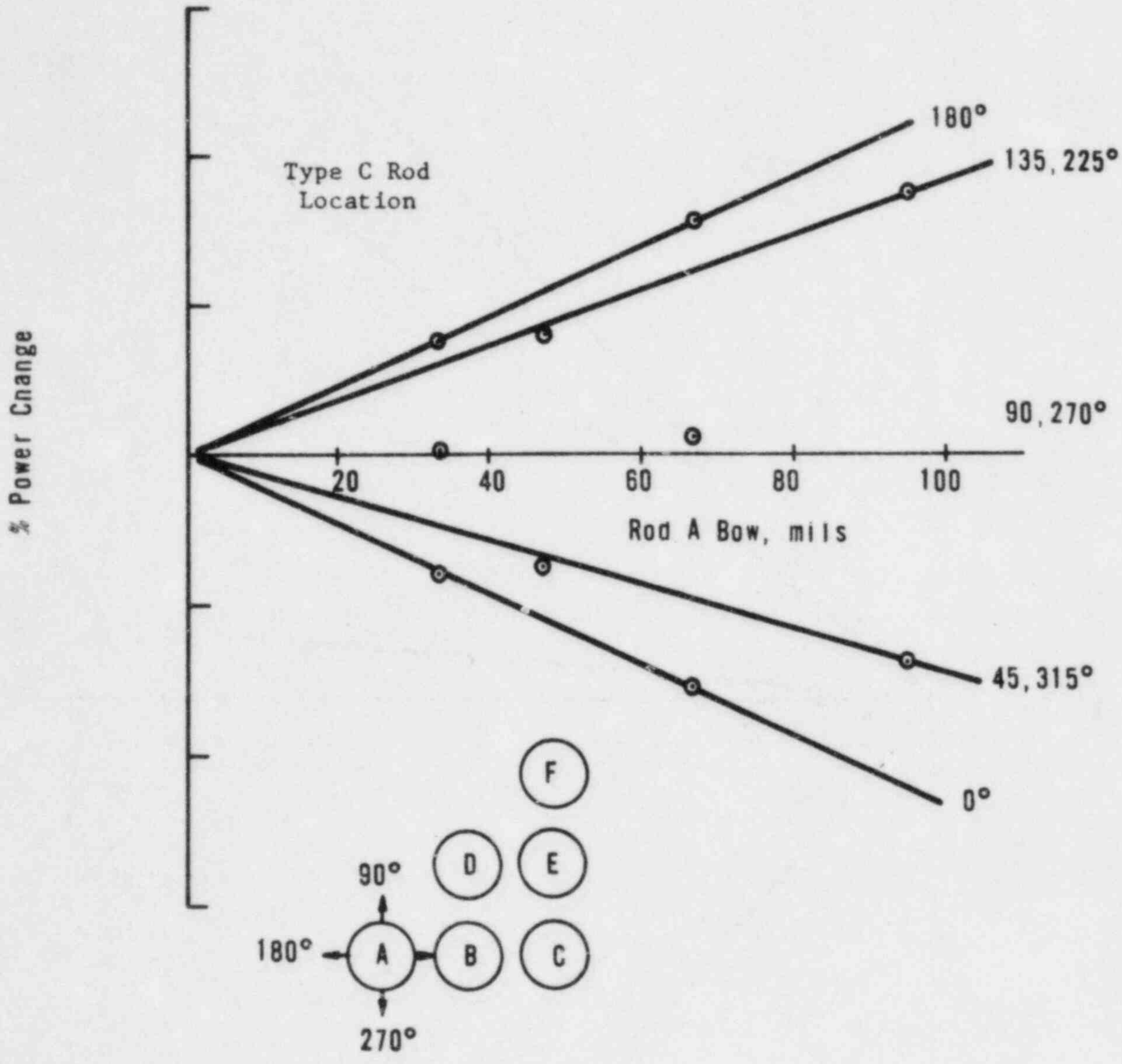

Figure G-11. Percent Power Change in Rod D Due to Rod A Bow, Mark C Geometry, E = 3.45 wt %

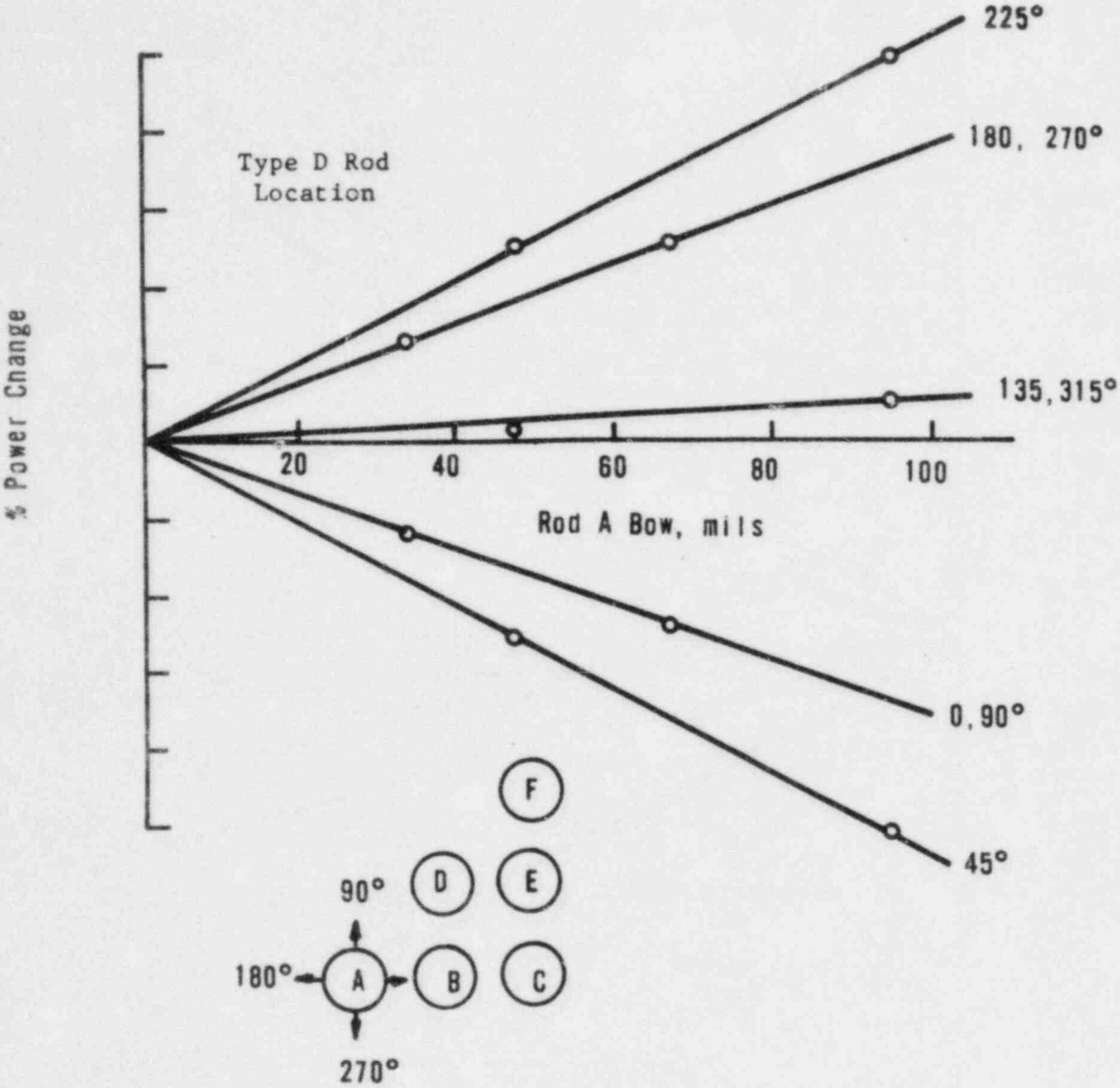

Figure G-12. Percent Power Change in Rod E Due to Rod A Bow, Mark C Geometry, E = 3.45 wt %

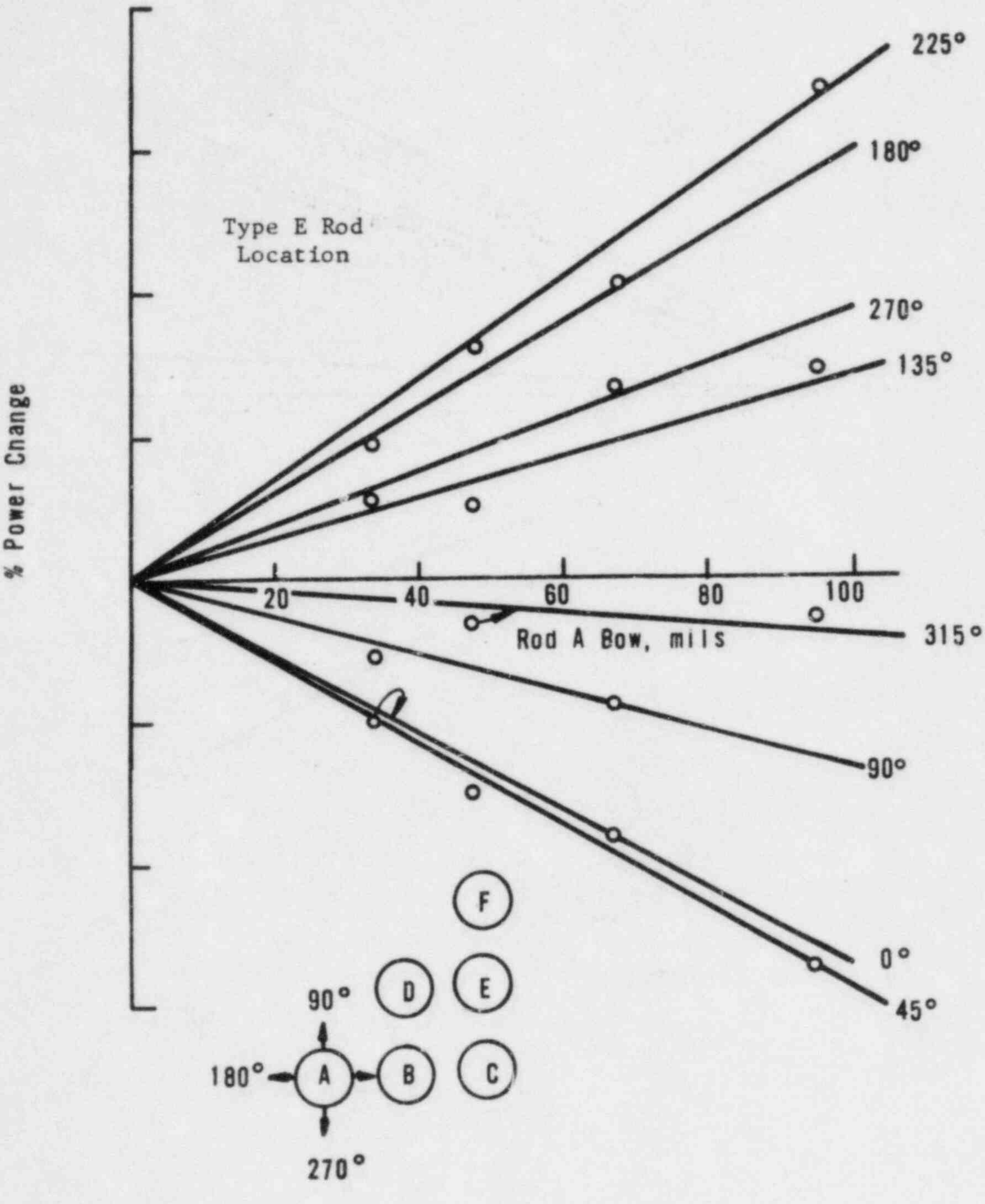

Figure G-13. Percent Power Change in Rod F Due to Rod A Bow, Mark C Geometry, E = 3.45 wt %

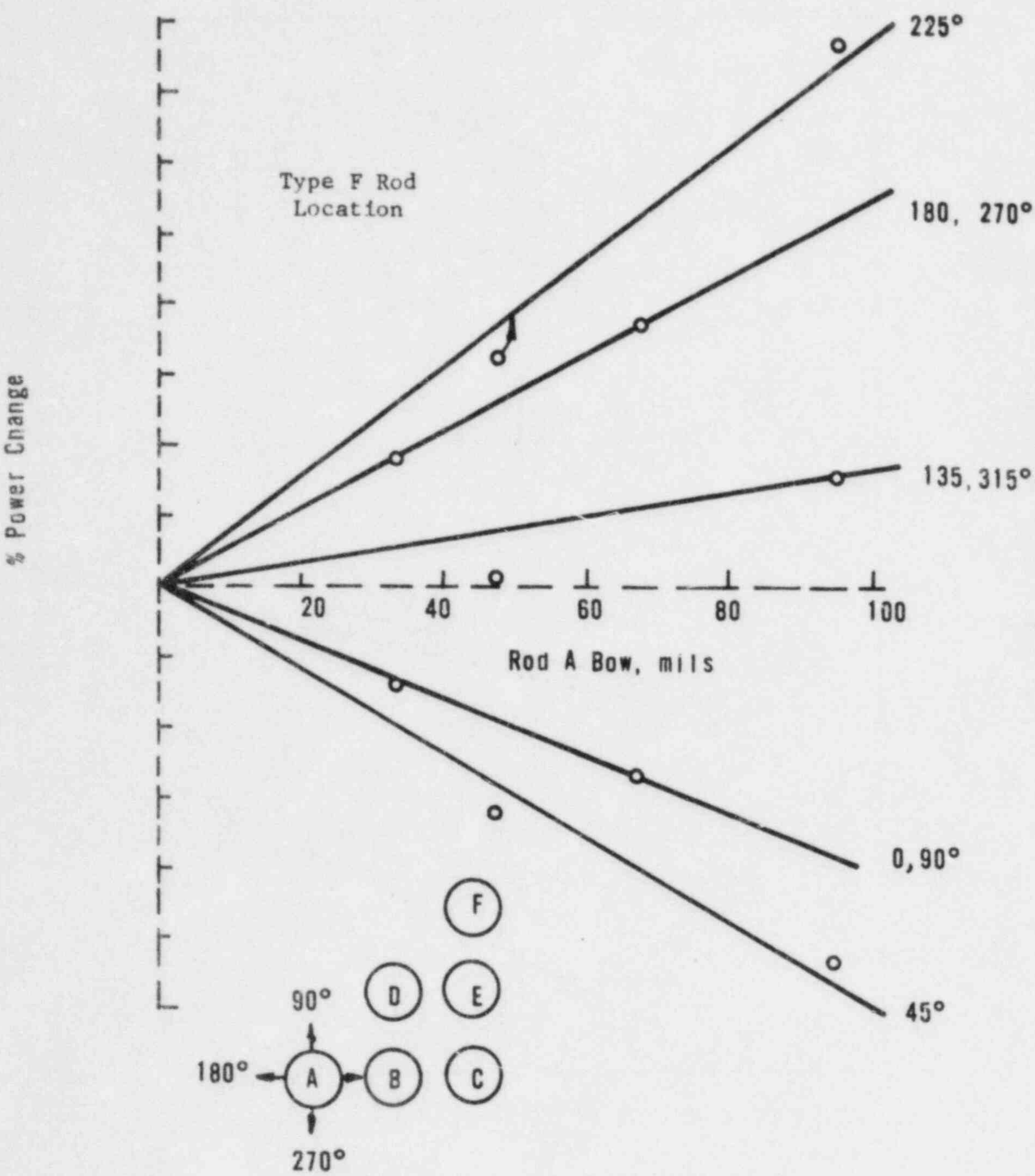

Figure G-14. Power Change in Rod B Due to Adjacent Rod Bow, Mark B Geometry

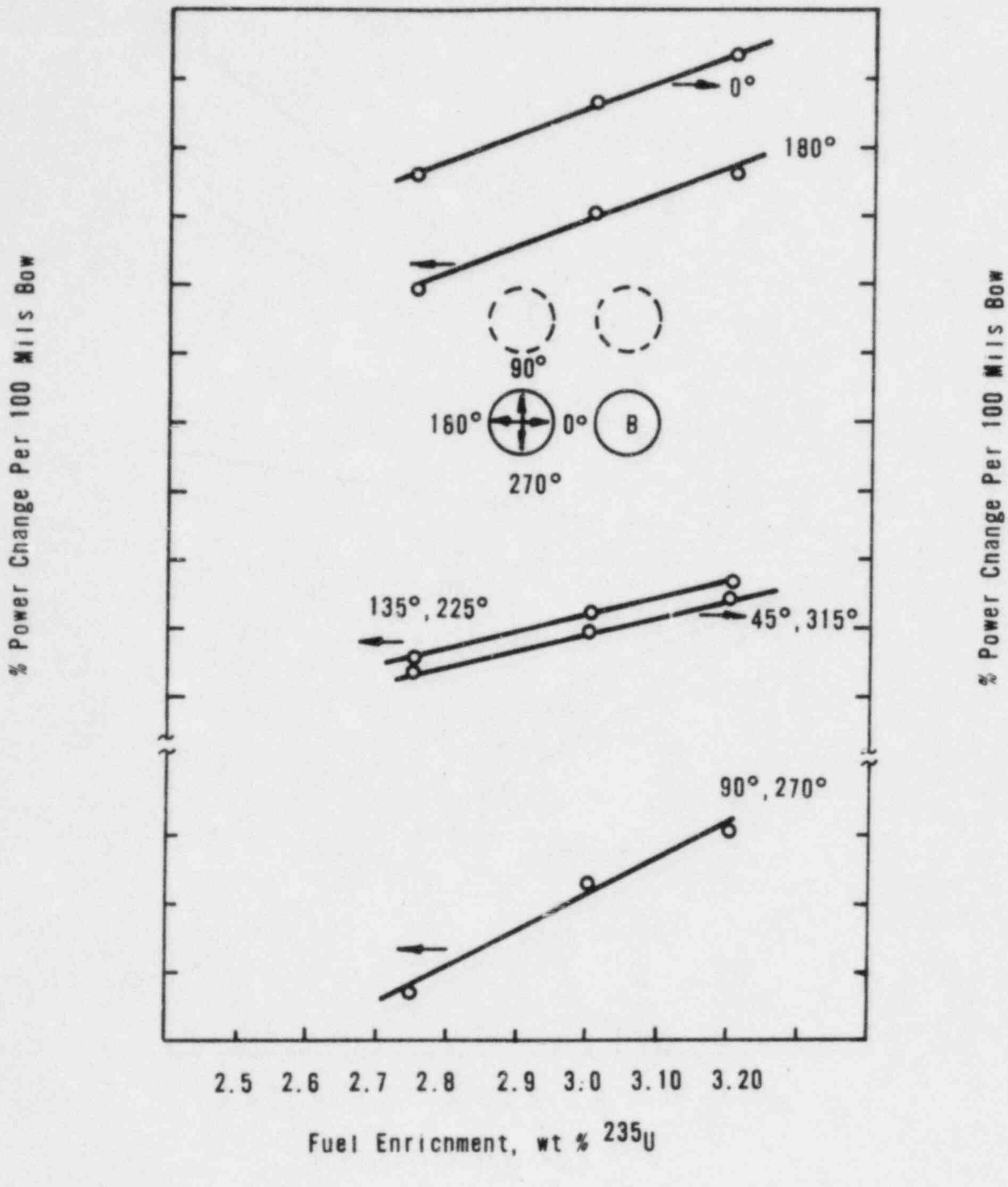

Figure G-15. Power Change in Rod D Due to Adjacent Diagonal Rod Bow, Mark B Geometry

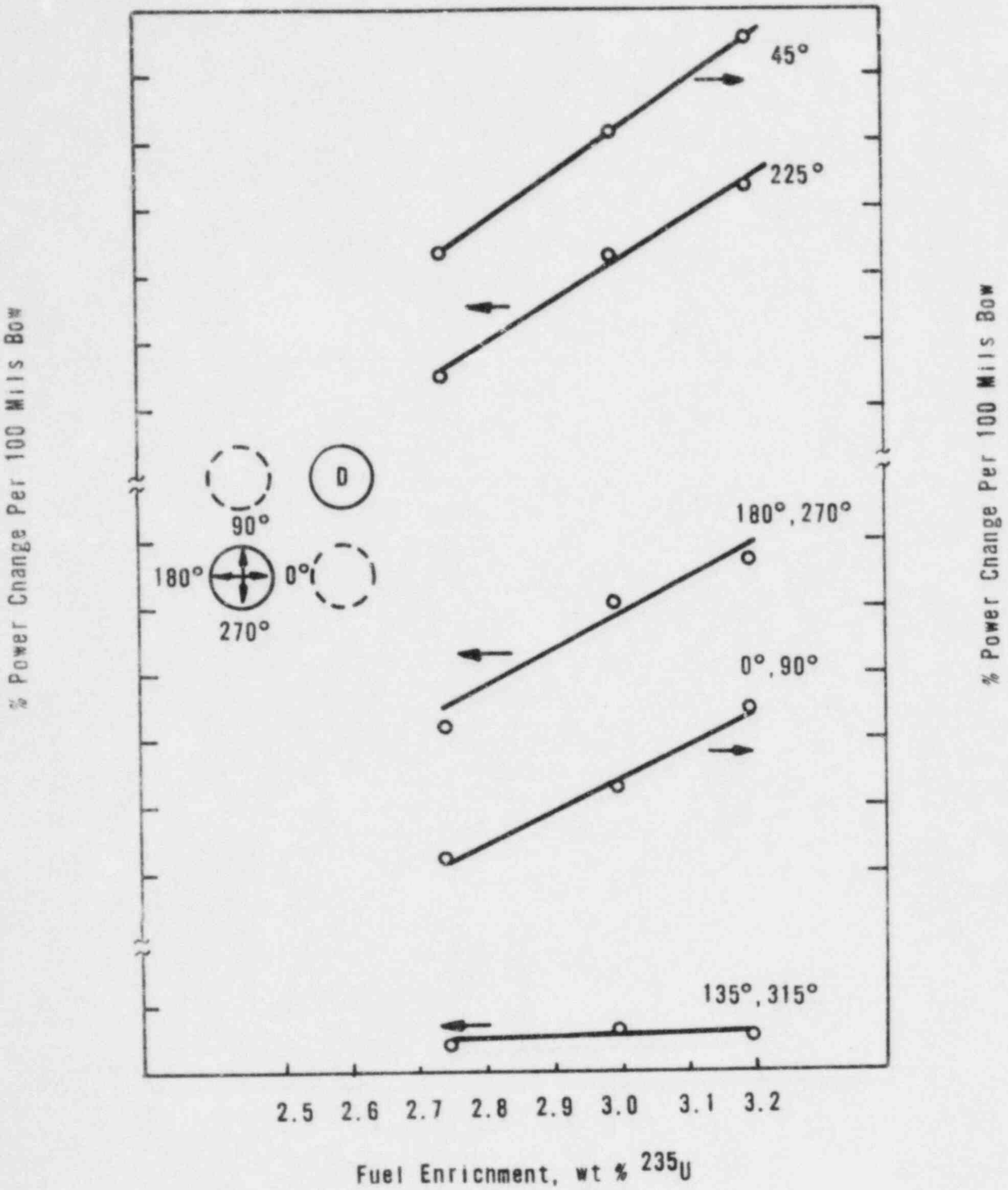

APPENDIX H

References

[1] D. B. Vassallo (USNRC) to J. H. Taylor (B&W), Letter, June 12, 1978, with enclosure, "Calculation of the Effect of Fuel Rod Bowing on the Critical Heat Flux for Pressurized Water Reactors," USNRC, April 1978. Revised by letter, D. B. Vassallo to J. H. Taylor, September 15, 1978.

[2] J. H. Taylor to D. B. Vassallo, Letter, "Determination of Fuel Rod Bow DNB Penalty," with enclosures, December 13, 1978.

[3] J. H. Taylor to S. A. Varga (USNRC), Letter — Enclosure 1, Appendix A, (Rev. March 26, 1979), "The Analysis of the Bowed and Unbowed CHF Test Data," March 27, 1979.

[4] J. H. Taylor to S. A. Varga, Letter, "B&W Rod Bow Penalty Calculations," June 22, 1979.

[5] L. S. Rubenstein (USNRC) to J. H. Taylor, Letter, "Evaluation of Interim Procedure for Calculating DNBR Reductions Due to Rod Bow," October 18, 1979.

[6] Nuclear Safety Criteria for the Design of Stationary Pressurized Water Reactors, ANSI N-18.2-1973, American National Standards Institute, New York.

[7] M. R. Stephens (B&W) to File, Memorandum, November 17, 1978, Record of Telecon with R. Lobel (USNRC) on October 30, 1978.

[8] D. F. Ross and D. G. Eisenhut (USNRC) to D. B. Vassallo and K. R. Goller (USNRC), Memorandum, "Revised Interim Safety Evaluation Report on the Effects of Fuel Rod Bowing on Thermal Margin Calculations for Light Water Reactors," February 16, 1977.

[9] J. H. Taylor to S. A. Varga, Letter, "Statistical Combination of B&W Peaking Factors," March 25, 1977.

[10] "American National Standard Assessment of the Assumption of Normality" (based on individual observations), ANSI N15.15, American National Standards Institute, New York (1974).

[11] G. E. P. Box, "Correcting Inhomogeneity of Variance with Power Transformation Weighting," Technometrics, Vol 16, No. 3, August 1974.

[12] R. G. Miller, "Simultaneous Statistical Inferences," McGraw-Hill Book Co. (1966).

[13] A. R. Barber, et al., "Ultrasonic Temperature Profiling System for Detecting Critical Heat Flux in Nonuniformly Heated Tube Bundles," Topics in Two-Phase Heat Transfer and Flow, Winter ASME Meeting, December 1978.

[14] LYNX2 — Subchannel Thermal-Hydraulic Analysis Program, BAW-10130, Babcock & Wilcox, October 1976.

[15] R. H. Wilson, D. A. Farnsworth, and R. H. Stoudt, BWC Correlation of Critical Heat Flux in 17 × 17 Geometry Rod Bundles, BAW-10143P, Babcock & Wilcox, January 1980.

[16] The DOTIV Two-Dimensional Discrete Ordinate Transport Code With Space-Dependent Mesh and Quadrature, ORNL/TM-6529, Oak Ridge National Laboratories, August 15, 1978.

[17] ANISNBW — A One-Dimensional Discrete Ordinate Transport Code, NPGD-TM-491, Rev. 2, Babcock & Wilcox, October 1980.

[18] NULIF — Neutron Spectrum Generator, Few-Group Constant Calculator, and Fuel Depletion Code, BAW-426, Rev. 2, Babcock and Wilcox, December 1980.

[19] PROLIB — Code to Create Production Library of Nuclear Data for Design Calculations, BAW-416, Babcock & Wilcox, June 1973.

[20] A. J. Duncan, Quality Control and Industrial Statistics, Irwin, Tennessee (1965), p. 510.

APPENDIX I

Letter, J. H. Taylor to J. R. Miller, April 15, 1982 and Responses to First and Second Round Questions 1

Babcock & Wilcox

a McDermott company

Nuclear Power Generɛ ..on Division

3315 Old Forest Road
P.O. Box 1260
Lynchburg, Virginia 24505-1260
(804) 385-2000

April 15, 1982

Mr. James R. Miller, Chief
Standardization and Special Products Branch
Division of Licensing
Office of Nuclear Reactor Regulation
U.S. Nuclear Regulatory Commission
Washington, D.C. 20555

Dear Mr. Miller:

Attached are ten (10) copies of the responses to first and second round questions on BAW-10147P, "FUEL ROD BOWING IN BABCOCK & WILCOX FUEL DESIGNS".

In accordance with 10 CFR Section 2.79, we are requesting that certain portions of the responses be treated as proprietary. An affidavit supporting this request as well as proprietary and non-proprietary versions of the responses are attached.

Should you require further information on this submittal, please call Frank McPhatter or me (Ext. 2401).

Very truly yours,

J. H. Taylor
Manager, Licensing

JHT:CFM:dr

Attachments

cc: R. B. Borsum - B&W Bethesda Office

bcc: C. F. McPhatter

Babcock & Wilcox

AFFIDAVIT OF JAMES H. TAYLOR

A. My name is James H. Taylor. I am Manager of Licensing in the Nuclear Power Generation Division of Babcock & Wilcox, and as such I am authorized to execute this Affidavit.

B. I am familiar with the criteria applied by Babcock & Wilcox to determine whether certain information of Babcock & Wilcox is proprietary and I am familiar with the procedures established within Babcock & Wilcox, particularly the Nuclear Power Generation Division (NPGD), to ensure the proper application of these criteria.

C. In determining whether a Babcock & Wilcox document is to be classified as proprietary information, an initial determination is made by the unit manager who is responsible for originating the document as to whether it falls within the criteria set forth in Paragraph D hereof. If the information falls within any one of these criteria, it is classified as proprietary by the originating unit manager. This initial determination is reviewed by the cognizant section manager. If the document is designated as proprietary, it is reviewed again by Licensing personnel and other management within NPGD as designated by the Manager of Licensing to assure that the regulatory requirements of 10 CFR Section 2.790 are met.

D. The following information is provided to demonstrate that the provisions of 10 CFR Section 2.790 of the Commission's regulations have been considered:

(i) The information has been held in confidence by the Babcock & Wilcox Company. Copies of the document are clearly identified as proprietary. In addition, whenever Babcock & Wilcox transmits the information to a customer, customer's agent, potential customer or regulatory agency, the transmittal requests the recipient to hold the information as proprietary. Also, in order to strictly limit any potential or actual customer's use of proprietary information, the following

Babcock & Wilcox

AFFIDAVIT OF JAMES H. TAYLOR (Cont'd)

provision is included in all proposals submitted by Babcock & Wilcox, and an applicable version of the proprietary provision is included in all of Babcock & Wilcox's contracts:

"Purchaser may retain Company's Proposal for use in connection with any contract resulting therefrom, and, for that purpose, make such copies thereof as may be necessary. Any proprietary information concerning Company's or its Suppliers' products or manufacturing processes which is so designated by Company or its Suppliers and disclosed to Purchaser incident to the performance of such contract shall remain the property of Company or its Suppliers and is disclosed in confidence, and Purchaser shall not publish or otherwise disclose it to others without the written approval of Company, and no rights, implied or otherwise, are granted to produce or have produced any products or to practice or cause to be practiced any manufacturing processes covered thereby.

Notwithstanding the above, Purchaser may provide the NRC or any other regulatory agency with any such proprietary information as the NRC or such other agency may require; provided, however, that Purchaser shall first give Company written notice of such proposed disclosure and Company shall have the right to amend such proprietary information so as to make it non-proprietary. In the event that Company cannot amend such proprietary information, Purchaser shall, prior to disclosing such information, use its best efforts to obtain a commitment from NRC or such other agency to have such information withheld from public inspection.

Babcock & Wilcox

AFFIDAVIT OF JAMES H. TAYLOR (Cont'd)

Company shall be given the right to participate in pursuit of such confidential treatment."

(ii) The following criteria are customarily applied by Babcock & Wilcox in a rational decision process to determine whether the information should be classified as proprietary. Information may be classified as proprietary if one or more of the following criteria are met.

a. Information reveals cost or price information, commercial strategies, production capabilities, or budget levels of Babcock & Wilcox, its customers or suppliers.

b. The information reveals data or material concerning Babcock & Wilcox research or development plans or programs of present or potential competitive advantage to Babcock & Wilcox.

c. The use of the information by a competitor would decrease his expenditures, in time or resources, in designing, producing or marketing a similar product.

d. The information consists of test data or other similar data concerning a process, method or component, the application or which results in a competitive advantage to Babcock & Wilcox.

e. The information reveals special aspects of a process, method, component or the like, the exclusive use of which results in a competitive advantage to Babcock & Wilcox.

f. The information contains ideas for which patent protection may be sought.

Babcock & Wilcox

AFFIDAVIT OF JAMES H. TAYLOR (Cont'd)

The document(s) listed on Exhibit "A", which is attached hereto and made a part hereof, has been evaluated in accordance with normal Babcock & Wilcox procedures with respect to classification and has been found to contain information which falls within one or more of the criteria enumerated above. Exhibit "B", which is attached hereto and made a part hereof, specifically identifies the criteria applicable to the document(s) listed in Exhibit "A".

(iii) The document(s) listed in Exhibit "A", which has been made available to the United States Nuclear Regulatory Commission was made available in confidence with a request that the document(s) and the information contained therein be withheld from public disclosure.

(iv) The information is not available in the open literature and to the best of our knowledge is not known by Combustion Engineering, EXXON, General Electric, Westinghouse or other current or potential domestic or foreign competitors of B&W.

(v) Specific information with regard to whether public disclosure of the information is likely to cause harm to the competitive position of Babcock & Wilcox, taking into account the value of the information to Babcock & Wilcox; the amount of effort or money expended by Babcock & Wilcox developing the information; and the ease or difficulty with which the information could be properly duplicated by others is given in Exhibit "B".

E. I have personally reviewed the document(s) listed on Exhibit "A" and have found that it is considered proprietary by Babcock & Wilcox because it contains information which falls within one or more of the criteria enumerated in Paragraph D, and it is information which is customarily held in confidence and protected as proprietary information by Babcock & Wilcox. This report comprises information utilized by Babcock & Wilcox in its business which afford Babcock & Wilcox an opportunity to obtain a competitive advantage over

Babcock & Wilcox

those who may wish to know or use the information contained in the document(s).

James H. Taylor
JAMES H. TAYLOR

State of Virginia)
)   SS.   Lynchburg
City of Lynchburg)

James H. Taylor, being duly sworn, on his oath deposes an says that he is the person who subscribed his name to the foregoing statement, and that the matters and facts set forth in the statement are true.

James H. Taylor
JAMES H. TAYLOR

Subscribed and sworn before me
this 16th day of April 1982.

Natalie M Lampman

Notary Public in and for the City
of Lynchburg, State of Virginia

My Commission Expires Aug 18, 1985

Exhibit "B"

Criteria for Proprietary Classification of Responses to First and Second Round Questions on BAW-1[illegible]47P, "FUEL ROD BOWING IN BABCOCK & WILCOX FUEL DESIGNS", April 1981.

Round No.	Question No.	Item	Applicable Criteria
1	3	Power Change Predictions	c
1	4	Differences between Model and Physical Parameters	c
1	6	Penalty Values	b, c, d
1	12a, b, c, e	Model Information	b, c
1	15	Peaking Uncertainty	b, c
1	18	Peaking Value Predictions	b, c
1	19	Design Dimensions	c
1	28, 29	Contact Penalty Parameters	*
1	31	Penalty Predictions	b, c, d
1	32	Peaking Uncertainty	b, c
1	50	Measurement Uncertainties	d
1	54	Gap Measurements	d
1	56	Correlation Parameter	b, c, d
1	65	Power Predictions	b, c
2	16	Design Information	b, c
2	23	Correlations	b, c, d
2	27	Correlations	b, c, d
2	29	Correlations	b, c, d
2	31	Peaking Margin	b, c, d
2	31 - Figure 1	Peaking Margin vs. Burnup	b, c, d

* This is proprietary data from a competitor which was made available to B&W by the NRC.

Non-Proprietary Responses to First and Second Round Questions on BAW-10147B, "FUEL ROD BOWING IN BABCOCK & WILCOX FUEL DESIGNS", April 1981.

Question 1

Does the available data indicate that rod bow is greater in regions of limiting DNBR and power and if so, how is this accounted for in the statistical analysis?

Response

The available data indicates that rod bow is less in regions where limiting DNBR and power usually occur (upper half of the core). Table 4-3 provides a distribution of the location of worst spans and shows that the worst span is located near the bottom of the assembly (measurement plane 12 in Figure 3-2) in 33% of the spans measured. In addition, in 90% of the spans measured the worst span was located on the bottom half of the fuel assembly. 1

No credit was taken for this however, as the worst span data only was used as the basis for developing a rod bow correlation.

Question 2

Is there correlation between the direction and magnitude of bow in adjacent grid spans and if so, how is this incorporated in the statistical analysis?

Response

The rod bow correlation was developed based on the bow within the grid span with the largest standard deviation in the rod-to-rod gap measurements. 1
This conservatively brackets the bow in the other spans of the assembly. The DNB analysis considers only the worst span case. Therefore, the axial variation in the water channel gap is not significant and was not incorporated into the rod bow correlation development.

Question 3

In the determination of the effects of rod bowing on local rod power only configurations with a single bowed rod were considered. What error is introduced by assuming that superposition is valid and determining the change in rod power for configurations in which several rods are simultaneously bowed by combining the effects from single rod bowed configurations? It should be noted that this approximation is expected to deteriorate at larger rod displacements.

Response

The reported data does address only configurations with a single bowed rod; however, prior to the selection of superposition theory as a valid analytical approach, the theory was tested with an extensive selection of bowed rod combinations to establish that this approach was satisfactory and conservative. Two extreme tests were calculated. Referring to Figure G-4 of BAW-10147P, one case addressed the situation of 2 B-type rods (rod B and its 180° counterpart relative to Rod A) bowed away from Rod A to contact with Rod C and its 180° counterpart. The power change in rod A 1
was less than two times the equivalent power change in rod A when a single type B rod was bowed to contact with rod C. The second superposition extreme tests was the simultaneous movement of all 24 rods in the 5 x 5 pin array away from rod A and towards rod A by mils; i.e., each rod was moved one mesh interval along a 45° angle relative to the 90° X-Y geometry orientation. The simultaneous rod bow effect upon rod A was approximately less than the power calculated by superposition theory.

Therefore, it is concluded that superposition theory overestimates the absolute value of combined rod bow.

Regarding the deterioration of the superposition approximation with larger rod displacements, the explanation given above, in addition to the results which show power changing linearly for a single bowed rod, supports the B&W position that this analytical approach is valid also for large displacement combination rod bowing.

Question 4

What effect does the rectangular rod representation in the neutronic calculations have on the calculated rod power perturbation.

Response

The accuracy of the incremental power change with rod bow is primarily dependent on modeling lattice parameter changes. Rectangular to cylinderical geometry changes have a negligible, secondary effect.

A measure of the modeling adequacy is provided by the following differences between modeled and physical parameters: 1

pellet area
pellet diameter
rod to rod surface

A 5 x 5 fuel cell array was considered adequate with a 15 x 15 mesh and discrete representation of the fuel pellets. Equal mesh spacing was required to avoid region area changes when a fuel rod was moved within a fuel cell. The overall results agreed well with a standard, unbowed calculation model used in core design analyses.

Question 5

In the determination of a DNBR penalty, only single-rod displacement configurations are employed. What is the effect of multiple rod placements and gap closures on the DNBR penalty function and how is this effect accounted for?

Response

In the bowed rod test (Appendix E), the effect of gap closure was examined by displacement of a single rod. Since the CHF occurs in the gap between heated rods (see the response to question 60), the primary variable is the amount of closure in the rod-to-rod gap. Thus, for the determination of the DNBR penalty due to rod bow (gap closure), the effect of multiple rod displacements would be the same as the effect of a single rod displacement as long as either of these displacements resulted in the same amount of closure in the rod-to-rod gap. 1

Question 6

Several conservatisms have been identified in the bowing analysis including (1) selection of the maximum span bowing and (2) neglect of rod power reduction on DNBR, etc. List known conservatisms in the bowing analysis of power peaking and DNBR and give estimates of their magnitudes.

Response

Major conservatisms included in the bowing analysis will first be identified and a discussion of each will follow. These conservatisms include:

1.) Selection of worst span bowing

2.) The global tolerance level used in the gap closure prediction model

3.) Analytical modelling for power peaking calculations 1

4.) Upper tolerance level of DNBR penalty at contact

5.) Gap closure threshold value of 0% DNBR penalty determined from bowed rod CHF test

6.) Linear correlation between δ DNBR and gap closure.

1.) Selection of Worst Span Bowing
As described in BAW-10147P Section 5, the rod bow prediction correlation was based on the worst span gap closure data rather than on the data from all spans. This approach is considered to be conservative since the worst span data is bounding and because the worst span location was usually in the lower half of the assembly, where CHF does not usually occur. Further discussion is provided in the response to question 1.

If all the rod-to-rod data were used as the basis for the prediction data instead of the worst span only, the estimated magnitude of this conservatism is equivalent to a reduction in the DNBR penalty

(Figure 7-1) of approximately DNBR (on the average) and or greater reduction in penalty at a burnup of 40,000 MWd/mtU.

2.) The global tolerance level used in the gap closure prediction model.

A detailed description of the global tolerance factor is provided in Appendix D and additional comments are provided in the response to questions 28 and 29. When compared to the suggested value of 1.5 (reference 1) to be applied to estimated bow to account for bow variations between batches, the global tolerance factor is increasingly conservative with burnup as shown in Figure D-1. The estimated magnitude of this conservatism is equivalent to a reduction in DNBR penalty (Figure 7-1) of approximately DNBR at a burnup of 40,000 MWd/mtU.

3.) Analytical modelling for power peaking calculations. 1

Calculations of local power changes due to rod bow were based on configurations of single bowed rods by using superposition theory. The response to question 3 supports this method and identifies the magnitude of the conservatism determined for two extreme cases. Beyond this no additional estimates of the magnitude of the conservatism have been determined.

4.) Upper tolerance level of DNBR penalty at contact.

The method used to determine the DNBR contact penalty was provided by the NRC (ref. 7) with no requirements for justifying a confidence limit on the penalty. B&W chose to treat this contact penalty (based on 10 data points) in a conservative fashion as described in section 6 and in the response to question 58 by determining a 95% confidence limit on the penalty. The estimated magnitude of the conservatism, in terms of DNBR penalty vs. burnup, is less than a 1% reduction in DNBR penalty.

5.) Gap closure threshold value of 0% DNBR penalty determined from a bowed rod CHF test.

A bowed rod CHF test was performed at 55% closure, a value that was expected to show no degradation in DNB performance as well as to bound the expected magnitude of gap closure in B&W fuel. The test data presented in Appendix E for the bowed rod test and for an otherwise identical unbowed rod test bundle does not indicate conclusively that a penalty exists at a 55% closure. Additional discussion is provided in the response to question 52. Although the threshold value of gap closure below which no DNBR penalty exists may be higher than 55%, no estimate can be made for the magnitude of this conservatism since test data for gap closures greater than 55% is not available.

6.) Linear correlation between δ DNBR and gap closure.

As pointed out in the response to question 63 the expected DNBR penalty over the applicable range of gap closure is less than predicted DNBR penalty based on a linear correlation over the same range of gap closure. The degree of conservatism resulting from using the linear correlation has not been quantified for BAW-10147P since B&W has not performed rod bow CHF tests at gap closures greater than 55%, the closure value used as the threshold closure below which there is no penalty.

Question 7

In the determination of the effects of rod bowing on local rod powers, the effect of poison rod bowing has been neglected. Describe in detail the effects of poison rod bowing and incorporate this effect into the F_Q^B and DNBR penalties.

Response

The design of B&W fuel assemblies does not incorporate poison rods as an integral part of the fuel assembly lattice. Rather, poison rods are separate components which are contained in guide tubes. This design precludes any significant poison rod bowing and therefore F_Q^B and DNBR penalties are not applicable. The response to Question 21 provides a discussion of control rod and guide tube bowing which indicates no evidence of poison rod (control rod) bowing. 1

Question 8

During certain transients and accidents, large local flux and thermal gradients and stresses are expected. Can these or other mechanisms give rise to greater bowing and a larger decrease in gap closures than would be determined using the proposed gap closure correlations? If so, how are these bowing increases accounted for?

Response

The rod bow correlation was developed from a very extensive data base that included over 125,000 individual measurements from 26 fuel assemblies. 1
These assemblies were from 2 reactors and were irradiated to fuel assembly average burnups up to 40,000 MWd/MTu which encompasses a wide range of actual operating conditions. Infrequent transient and accidents are not expected to significantly effect the rod bow because the grids are not fixed but are allowed to move axially to limit the build up of axial stesses in the rods. Also, it is unlikely that the flux and thermal gradients which would be in the same direction would be sufficiently different between adjacent rods to cause a significant increase in gap closure.

Question 9 Revision 1 (5/13/83)

For what fuel designs will the rod bow span length scaling be used to determine the bowing closure reduction?

Response

No span length scaling is required for B&W fuel assembly designs. Both the 15 x 15 and the 17 x 17 Mark-C designs incorporate 6 spacer grids approximately equally spaced along its length resulting in almost identical span lengths. Also, the data base includes measurements from both assembly designs. 1

Question 10

Have statistical tests been performed to determine if the closure data that has been combined (e.g., for different rod types, spans, plants, exposures, etc.) is poolable and if not, give the basis for pooling this data.

Question 52

Describe in detail how the data was reduced to a "common burn-up". 1

Response

The water channel measurements from several assemblies was not pooled into a single data point at a common burnup-up. Instead, the statistical analysis treated the span wise distributions for each assembly as individual data points at the assembly average burnup.

Question 11

The rod peaking on certain rods in the neighborhood of guide tubes, water gaps, water holes and instrument tubes, is larger than for an infinite lattice of rods. Describe in detail how this is accounted for in the determination of the power peaking penalty.

Response

The bowing of a fuel rod in the vicinity of a control rod guide tube or instrument guide tube can result in a slightly higher change in magnitude of the power of surrounding rods than if the bowed rod is surrounded by a uniform lattice of fuel rods. Conversely, the change in power of a single rod due to self bow is more negative for rods near guide tubes. The presence of a guide tube reduces by one the number of available rods which can bow and thus have a detrimental peaking effect on the hot rod. Thus, there are two power reduction contributors and one power increase contributor. The bow induced power changes on rods near guide tubes is expected to be bounded by the results of peaking studies based on uniform lattices and requires no additional penalty. 1

Question 12

Please discuss in detail the effect of the following, on the neutronic calculations of the effects of rod displacement on local power peaking:

(a) spatial mesh size

(b) order of scattering and angular quadrature if a transport calculation was performed

(c) number of choice of energy groups 1

(d) ability of diffusion theory to track the effects of small geometry changes

(e) effects of spectral changes on the few-group cross sections used

(g) reduced rod array size (e.g., 5 x 5 vs. 15 x 15) and the effect of perturbed image rods introduced by the boundary conditions.

Question 12

(a) Spatial mesh size?

Response

The mesh spacing was selected to facilitate modeling the fuel cell in X-Y geometry.

1

These constraints resulted in a mesh spacing of
This dimension is small compared to the neutron mean free path in the fuel rod pellet, clad and moderator. This mesh spacing is comparable to that used in conventional lattice studies to calculate neutron flux and reaction rates in fuel and absorber rods.

Question 12

(b) Order of scattering and angular quadrature if a transport calculation was performed.

Response

P_0 scattering order and S_4 quadrature options were used in the DOT code analyses.

The importance of scattering order (P_0, P_1) was evaluated in terms of the change in fast to thermal flux ratio in the pellet region and in the average thermal flux ratio of the pellet to moderator region of the fuel cell. The difference in the fast to the thermal flux ratio in the pellet was for the two scattering options. The difference in the average thermal flux ratio of the fuel to moderator region was percent. An assessment was 1
made of the computer memory requirements for the P_0 and P_1 options in the DOT code.

Question 12

(c) Number and choice of energy groups?

Response

The energy group structure for the DOT code's spatial analysis consists of one fast group and five thermal groups with energy boundaries as follows:

Group	Energy Range
1	
2	
3	
4	
5	

Emphasis was placed on describing the thermal energy spectrum because rod bow neutronic analysis is primarily a study of local moderation changes arising from local redistribution of water between adjacent fuel rods. Multithermal groups are a means to account for neutron energy variations in the thermal energy range. Energy break points were chosen to accommodate resonances in the fuel isotopes. Cross sections for group 1 (>1.855 ev) were 1
calculated with the NULIF code. This is a B&W code that generates a microgroup neutron spectrum and calculates spectrum weighted few group parameters for use in a spatial diffusion code. A B&W data processing code, ANTY, merges the single fast group data with cross section data from an 80 thermal group B&W cross section library (PROLIB) for isotopes of interest. These cross section sets were then input to a second B&W data processing code, TAPMAKE, which created on magnetic tape an 81 group macroscopic cross section set for each material zone of the fuel rod cell for use with the ANISN code. ANISN solves the multigroup transport equation for the space- and energy-dependent flux for an inifinte array of fuel cells with appropriate boundary conditions. The ANISN results are used to obtain flux and volume weight six group cell averaged cross sections for the two dimensional DOT analysis.

(d) Ability of diffusion theory to track the effects of small geometry changes?

Response

The principal neutronic problem in rod bow analysis is the treating of
moderator asymmetry in the perturbed (bowed rod) fuel cell and the
propogation of this perturbation into adjacent and nearby fuel cells as a 1
power change.

The neutronic model used in the analysis was Discrete Ordinate Transport Theory with a P_0 scattering order and S_4 angular quadrature. Test cases were calculated to assess the effect of a few group energy structure, scattering order, and quadrature level upon the relative change in fuel rod power. The differences in perturbed power were sufficiently small to have a negligible effect on the analytical results.

Question 12

(e) Effects of spectral changes on the few-group cross sections used.

Response

The selection of cross section energy grouping and the methodology of collapsing the microgroup cross sections to the few group structure for the fuel cell was based on previous experience, and are described in the answer to question 12 (c). The change in local moderation due to redistribution of water between fuel rods with rod bow was the primary cause of spectral 1
change. The effect of interest is mainly a thermal energy effect. Therefore, the thermal energy range was described by five groups with the energy break points chosen to satisfy key isotopic resonance parameters.

Other studies performed at B&W have indicated that when the thermal energy range is represented by groups, the DOT calculation will account correctly for the interactions due to spectral changes. Above 1.855 ev the mean free path of neutrons is large compared to the lattice pitch, and hence the effects of spectral changes in the epithermal range are insignificant.

Question 12

(g) Reduced rod array size (e.g., 5 x 5 vs. 15 x 15) and the effect of perturbed image rods introduced by the boundary conditions.

Response

Studies were performed to assess the geometric propagation of rod bow
induced power perturbations. There is approximately a factor of 4 reduction
in the magnitude of the power perturbation two rod pitches from the nominal
position of the perturbed rod. See Figures G-4 and G-5 of BAW-10147P. It 1
was concluded that fuel cells more than two rod pitches from the perturbed
rod could be modeled as a homogenized fuel zone. The thickness of the
homogenized fuel zone was selected to isolate the effect of imaged perturbed
rods from the quadrant of interest. The test for isolation was equal mirror
image power distribution in the quadrant when the central fuel rod (rod A
of Figure G-1 BAW 10147P) was moved in opposite directions. This was achieved.

Discuss the effect of rod bowing on clad corrosion.

Response

It has been B&W operating experience that corrosion of the fuel rod cladding is insignificant. Theoretically, a high percent gap closure of the water channel would increase cladding temperatures and associated corrosion. However, for the closures measured in B&W reactors and conservatively predicted by the rod bow correlation, these effects are very small and any resulting corrosion is insignificant. 1

Question 14

Are all operating plants and fuel designs covered by the submitted topical report analysis? If not, identify those plants and designs that are not covered and indicate why these results are not applicable.

Response 1

All operating plants and fuel designs are covered by the topical report. The rod bow correlations were developed from data base that included measurements from both the 15 x 15 and 17 x 17 design configurations.

Question 15

The nuclear uncertainty factor, which accounts for the inability of the standard nuclear design codes to calculate the exact rod power, will increase for off-nominal bowed configurations. How is this increase in uncertainty due to bowing accounted for?

Question 32

In the determination of the effect of rod bowing on local power peaking, bowing of only a single rod has been considered. Therefore, either determine the 95/95 tolerance limit on the local rod power when all surrounding rods bow randomly according to the assumed distribution or demonstrate that the selected penalty is conservative.

Response

The power peaking uncertainty of presented in Section 7.2 was determined as a result of calculations which considered the effect on a pin surrounded by eight rods bowed in a random manner. The calculations incorporated a 1
Monte Carlo technique which used a normal distribution for the amount of rod displacement and a uniform distribution for the angle of bow, and determined the change in power peaking on the center rod at a 95% confidence level. Values of Δ% power per rod were input to the calculations and which were determined for a 5 x 5 rod array over a range of rod displacements and directions. The calculated values of Δ% power for the bow of various rods plus the effects of self bow of a single rod in a 5 x 5 rod array were performed, and are shown in the figures of Appendix G. The maximum power peaking change quoted in Section 7.2 demonstrates the change due to the self bowed rod.

In the Monte Carlo technique, the total power change on the center rod was recomputed 100000 times for each selected axial increment to develop a statistical sample. The resulting calculations of power change on the center rod provided the basis that a peaking uncertainty would bound the calculated power peaking change over the range of burnup (corresponding to predicted gap closure) that would be expected to occur in B&W reactors.

Question 15 & 32 Continued

The peaking uncertainty due to rod bow was combined statistically (square root of the sum of squares) with the standard nuclear uncertainty factor of (total peak) and the manufacturing "hot channel" factor of , in the manner detailed in Reference 9. The combined total of is less than the total uncertainty currently used in analyses. When higher burnup cycles (which are anticipated in the future) are considered, along with the predicted gap closure determined as a function of burnup as described in Appendix D, the total peaking uncertainty of remains valid for fuel assembly burnup to MWd/mtU for MKB fuel and MWd/mtU for MK fuel. It is very unlikely that fuel assemblies with burnup values of these magnitudes will be found limiting when determining core operating limits because of the decreased power producing capability of the fuel (see response to Question 31). However, to ensure that all fuel assemblies and burnups are considered, a burnup dependent rod bow power peaking uncertainty can be determined and combined statistically as described in Reference 9 and will be applied to these fuel assemblies. 1

Question 16

A. Over what specific range of burn-up is the gap closure correlation and proposed bowing analysis applicable?

B. If there is any increase in uncertainty due to lack of data at high burn-ups, describe quantitatively how this is accounted for.

C. If the gap-closure data is being extrapolated outside the domain of actual measurement data, describe quantitatively how the increase uncertainty is estimated and how it is accounted for in the analysis.

1

Response

The rod bow equation was developed from a data base with a range of 0. to 40,000 MWd/MTu. The data may be extrapolated to higher burnups using equations 5-1 and 5-4 of BAW-10147P. It should be noted that the global tolerance as well as rod bow is a function of burnup. Increasing burnup increases the ratio of the global tolerance to the predicted value. Additional discussion of the global tolerance is contained in Appendix D of BAW-10147P.

Question 17 Revision 1 (5/13/83)

Are the calculated power peaking senstivities to rod-bow conservative with respect to all fuel designs? If not, identify the non-conservative designs and explain in detail how this non-conservatism is properly accounted for in the proposed analysis.

Response

The Mark-B and Mark C-fuel assembly designs identified in BAW-10147P have fuel rod peaking characteristics that are conservative when compared to modified ("wet-lattice") Mark-B and C assembly designs that are currently under consideration. In addition, it is anticipated that any future changes in Mark-B and C class assembly designs will be no greater in magnitude than the differences between the Mark-B and C designs. Therefore, results in this report should be applicable to those designs as well. 1

Question 18

Describe in detail the application of the proposed rod bow analysis to a typical plant, including the input parameters and their basis (either explicitly or by reference) and the equations and figures (appropriately referenced) used to determine both the DNBR and F_Q^B penalties. Indicate what parameters are plant and cycle dependent.

Response

The assessment of a rod bow DNBR penalty to B&W fuel designs is not applicable as concluded in Section 7 and further demonstrated in the response to Question 31. As discussed in the response to Question 31 the net penalty is zero for fuel assembly average burnup values less than 24000 MWd/mtU. Assemblies with burnup values greater than 24000 MWd/mtU do not produce enough power to achieve design limit peaking values and a DNBR penalty due to rod bow has no valid meaning. The philosophy and method of applying a rod bow penalty used previous to BAW-10147P (approved for use as an interim method by the NRC in Reference 5) is presented by example, however, to show how the limiting assembly in the core is determined and to demonstrate typical DNBR margins present relative to design limit values. The following example uses the DNBR penalty model described in Section 6 and Appendix F of BAW-10147P. Numbers shown correspond to Cycle 6 of Oconee Unit 3 and are based on the Reload Licensing Report for that cycle (BAW-1634). 1

1) for a specific plant and cycle design, the maximum predicted end-of-cycle (EOC) fuel assembly burnup value is determined for each fuel batch (column 2 of Table 18.1).
2) The net fuel rod bow DNBR penalty corresponding to each burnup value determined in 1) is determined from Figure 7-1 or 7-2 of BAW-10147P. These values are each adjusted by subtracting 1%, which corresponds to the DNBR value of the pitch reduction factor used in thermal-hydraulic analyses (column 4 of Table 18.8).
3) The maximum predicted steady-state radial x local peaking factor ($F\Delta h$) is determined for the limiting assembly in each fuel batch, by examination of the fuel cycle design (column 4 of Table 18.1). The maximum value is selected without regard to cycle burnup. This is generally a beginning-of-cycle value.

4) The minimum DNBR corresponding to each of the $F_{\Delta h}$ values determined in 3) is estimated for the design overpower (112% of full power) condition (column 5, of Table 18.1).
5) The rod bow DNBR penalty for each batch is subtracted from the minimum DNBR for that batch (Column 6 of Table 18.1). This provides an indication of which fuel is limiting (batch 8 for the example shown) as well as showing DNBR margin relative to the design case.
6) The rod bow DNBR penalty to be applied in the determination of Reactor Protection System limits is determined by examination of column 4 of Task 18.8. The penalty value selected for application is that corresponding to the fuel batch with the highest predicted $F_{\Delta h}$, or, if a batch with higher burnup (and penalty factor) has an $F_{\Delta h}$ within 5% of the maximum value, the penalty would be based on this batch. For the example shown in Table 18.1 this results in the penalty being based on batch 7, which has an $F_{\Delta h}$ of , rather than batch 8, which has an $F_{\Delta h}$ of . 1
7) The design DNBR limit value, DNBRL, is adjusted by adding the rod bow DNBR penalty determined in 6). For example, when the B&W-2 (BAW-10000A, May, 1976) CHF correlation is used, with its limit value of 1.30, a rod bow DNBR penalty of 1% would result in a DNBRL = 1.313.
8) DNBR - dependent Reactor Protection System limits are evaluated to insure that the minimum DNBR is greater than or equal to DNBRL.

The peaking uncertainty (F_Q^B penalty) used to verify plant and cycle specific operating limits and applied in this example would be a generic value used for previous cycles. A detailed discussion of the peaking uncertainties is provided in the response to Question 15 and 32.

Table 18.1

Oconee 3 Cycle 6 DNBR Penalty

Fuel Batch	Maximum Assembly Burnup MWd/mtU	Net Fuel Rod Bow Penalty * % DNBR	Maximum Predicted $F_{\Delta H}$	Minimum DNBR @112% Power	DNBR less Rod Bow Penalty
Design Case					
5B					
6					
7					
8					

*Penalty as determined from Figure 7-1 less 1%

1

Question 19

In the measurements of the DNBR penalty, what effect do the rod holders that maintain the rods in their bowed locations have on the measured DNBR penalty?

Response

Referring to Figures E-3 and E-2 of Appendix E, intermediate grid E is used to position rod 17 in its bowed position. This intermediate grid is identical to the other intermediate (or minimum turbulence) grids in both the C-9 (unbowed) and C-10 (bowed) tests except for the necessary structure for the positioning of rod 17. The minimum turbulence grids are used in all B&W CHF tests to maintain proper tube spacing in the span between the regular Mark C grids where electrically induced magnetic forces could cause bundle deformation. As opposed to the heavily formed -inch long regular grids, the minimum turbulence grids are specifically designed to produce negligible additional turbulence or flow upset. They are extremely thin, chemically etched wafers laminated to an approximately -inch length. A photograph comparing the intermediate and regular grids is shown in Figure 2-8 of Reference 15, and visibly illustrates the minimum turbulence nature of the intermediate grids. Furthermore, referring to Table E-9, the DNB length (axial position of CHF detection) in the vast majority of data points occurs downstream of the point of maximum bow (usually at the leading edge of the regular Mark C grid #6). This observation is consistent with that of the base comparison test (C-9, table E-8) and, indeed, the observed CHF locations for all of our Mark C tests (Reference 15). These results evidence the lack of effect of the minimum turbulence grids on CHF level. 1

Question 20

Describe the surveillance procedures and other measures that will be used to confirm and update when necessary the rod bowing data base and analysis.

Response

The rod bow correlation was developed from an extensive data base as described in Appendix B of BAW-10147P. Included in this data base are gap measurements from assemblies representative of the design evolution leading to the current configuration. It is expected that this correlation will be valid in the future for assemblies incorporating minor changes. This position will be reassessed on a case by case basis. If in the course of the design evolution it is desirable to make additional measurements, the data base will be updated and the effect on the rod bow correlation will be evaluated. 1

Question 21

Provide a discussion of the likelihood ano any measurements of control rod bowing.

Response

The control rods are suspended within the assembly's guide tubes where the diametral gap limits the amount of control rod bow relative to the guide tube. The thin walled control rod will conform to the shape of the guide tube. Any significant bow could result in wear of the guide tube. 1
B&W has not experienced any guide tube wear attributed to control rod bow.

The control rods are not subject to many of the postulated causes of fuel rod bow. The rods are free to grow axially which prevents a build-up of axial strains.

No direct measurements of control rod bow have been made but hot cell examinations of an axial power shaping rod showed no significant distortion.

Question 22

In the evaluation of the MDNBR penalty, are the pressure and Q_{AVG} values corresponding to the high pressure and over power trip setpoints used? If these values are not used, justify the values selected.

Response

The Q_{AVG} value used in the evaluation of the DNBR penalty corresponds to
the design overpower limit (112% of full power). This value is used to 1
establish a value of DNBR reduction at full contact as described in Section 6.
There is no pressure dependent function that is factored into the penalty
equation. The B&W bowed rod CHF test data (Appendix E) included the range
of allowable plant operating pressure which includes the high pressure
trip limit (2400 psia). The conclusion of the test was that no penalty
existed for the gap closure tested (55%).

Question 23

In the determination of the fuel rod DNBR penalty, the bowing of the eight surrounding rods and associated gap closures determined the reduction in DNBR margin. The penalty for each gap is determined by summing over the contributions from each possible closure. The closure contribution is given by the product of the probability of occurrence for that closure and the associated closure penalty. (In Reference 1 this method was used to determined the penalty arising from the bowing of two rods on opposite sides of the rod of interest). Therefore, update the bowing analysis to include the contribution to the DNBR penalty from all eight surrounding rods.

Response

Variations in gap closure (which would be expected to have corresponding variations in predicted DNBR penalty) were measured within fuel assemblies and this data forms the rod bow correlation data base as described in sections 4 and 5. The gap closures measured for a given fuel assembly were considered to have a burnup equal to the assembly average burnup. The probability distribution of gap closure is included in the burnup dependent gap closure correlation and the DNBR penalty correlation described in section 6 and Appendix F. The response to questions 28 and 29 provide additional information regarding the statistical treatment of the variability in gap closure. The variations in DNBR reduction due to variations in gap closure within a fuel assembly are therefore accounted for in the manner described in BAW-10147P.

Question 24

Discuss the extent to which the gap closure measurements span the actual operating spectrum of rod-to-rod spacings including enrichment, exposure, poison rods, instrument thimbles, guide tubes, fuel design, etc.

Question 40

In deriving the data base, in what way has a distinction been made between different types of assemblies (presence of water holes, burnable poison rods, control rods, etc.)?

Response

The data base used in the development of the rod bow correlations includes more than 125,000 individual gap measurements. It spans a range of design and manufacturing variations that have been incorporated during the evolution and improvement of the Mark-B and Mark-C designs. Also, the data base includes the effects of variations in the irradiation and operation environment during numerous reactor operating cycles.

The statistical analysis used to develop the rod bow correlation is based on the data from the 15 x 15 Mark-B assemblies. This correlation was shown to conservatively envelope the data from the 17 x 17 Mark-C assemblies and, thereby, can be used to predict the rod bow for both designs. No distinction was made between the assemblies within each configuration.

The data base included measurements on 26 assemblies of the Mark-B and Mark-C designs from 8 manufacturing batches with enrichments from 2.15 % U^{235} to 3.2 % U^{235}. These assemblies were used in two reactors during 8 operating plant cycles. They were inserted into core locations that contained orifice rods, burnable poison rods, control or safety rods or were open assemblies. The assemblies were exposed for 1 to 4 plant cycles with burnup to 40,000 MWd/MTu.

Question 25

Provide the most recent gap closure correlation and coefficients for all fuel designs. 1

Response

The most recent correlation and coefficients for all B&W fuel designs is found in BAW-10147P, Section 5.

Question 26

Large assembly bow of the order of hundreds of mils has recently been measured at several plants.[2,3,4] This bow is of concern because (1) the bow magnitude is at least an order of magnitude larger than the reported rod bow measurements, (2) the resulting rod bow is apparently extremely correlated with all rods in an assembly face bowing together and (3) the bow involves inter-assembly gap closure. All of these aspects are outside the scope of the proposed bowing analysis. Therefore, discuss in detail the effects of assembly bow on fuel rod gap closure and the assumptions and methods used to evaluate rod bowing.

Response

The rod bow correlation documented in the topical roport BAW-10147P addresses the random variation of the water channel gap at midplane between spacer grid elevations. Assembly bow is a measure of the relative lateral movement of the spacer grids (i.e., the mode shape) and is a function of the overall structural characteristics of the assembly. 1

The geometric configuration of the spacer grid design maintains minimum intra-assembly gaps as well as the inter-assembly gaps. As discussed in Section 4.1 of the topical, there is nc significant difference between the bow of the periphery or interior rods. In the case of spacer grid contact between adjacent assemblies, the grid's outer strip which extends beyond the peripheral rod maintains an inter-assembly rod-to-rod gap as large as the rod pitch within an assembly in the grid region. Fuel assembly bow is addressed in thermal hydraulic analysis as an issue separate from rod bow. For purposes of conservative thermal hydraulic design analysis, grids of adjacent fuel assemblies are assumed to bow to touch at an imaginary fuel assembly midplane and the limiting assembly flow area is calculated on this basis. DNBR calculations performed on this basis yield conservative results.

Question 27

Describe in detail the derivation and basis for Equation (D-4) in BAW-10147P.

Response

Equation (D-4) is used to calculate a 95% upper tolerance level on values of bow predicted by equation (D-2) which in turn is based on rod-to-rod gap measurements as described in section 5 of BAW-10147P. The derivation of equation (D-4) is found in reference 12 of BAW-10147P, "Simultaneous Statistical Inferences", R. G. Miller, McGraw-Hill Book Co. (1966). 1

Question 28

Please provide the details of the determination of the DNBR penalty at full closure, δ_c = ( ), the associated uncertainty, ( ), and also Reference 7 in BAW-10147P.

Question 29

In the determination of the DNBR penalty, the effect of the uncertainty in the penalty due to variability in gap closure (denoted σ_u in Reference 1) has been neglected. Incorporate this variability using a 95/95 upper tolerance limit as outlined in Reference 1, Equation (4.10), or indicate how this effect has been accounted for in the DNBR penalty.

Response

As seen from Figure 6-3, the size of the penalty region is affected by the variability of two factors: 1) the shape of the probability density function and 2) the slope of the boundary line, i.e., the line that forms a boundary for the penalty region. 1

B&W chose to treat the uncertainty in the penalty due to each effect in a conservative manner.

1) The shape of the density function is due to the variability in gap closure. Variability in the shape of the density function is related in $\sigma(\frac{\Delta C}{C_o})$ as illustrated in Figure 6-3. Thus in estimating $\sigma(\frac{\Delta C}{C_o})$ a very conservative approach was taken by B&W and a global tolerance value established (Eqn. D-4) at a 95% significance level. In all calculations involving penalty, where σ^* was indicated in equation F-10, the value of σ^* was replaced by the global tolerance value of σ 95/95 $(\frac{\Delta C}{C_o})$. This treatment results in a very broad penalty region as Figure 6-3 illustrates. All penalty curves, Figures F-2 and F-3, as well as their simplified versions, Figures 7-1 and 7-2, were derived with the above procedure.

2) The line forming a boundary to the penalty region of Figure 6-3 was also treated conservatively.

B&W had estimates for "K" as described in appendix E but not for δ_c. The NRC provided estimates for $\overline{\delta}_c$, σ_{δ_c} based on 10 experimental points (Ref. 7, see note below). From the available information K and and δ_c were both applied in a conservative manner, as illustrated in Figure 6-2.

However, the solid line should be labelled correctly as the "B&W final penalty region boundary."

In summary, the response to Questions 28 and 29 examined both components that contribute to the uncertainty in the penalty and treat them both conservatively and subsequently arrive at a conservative penalty factor, that is also physically meaningful. 1

The variability in gap closure however was not denoted by B&W as σ_u (of Reference 1). The method of that reference is not physically meaningful nor statistically precise (See response to Question 57).

Note: In the Reference 7 telephone conversation of October 30, 1978, R. Lobel (NRC) provided M. R. Stephens (B&W) with data associated with CHF testing of rods bowed to contact, testing which B&W has not conducted. The NRC agreed to provide the data in a previous call on October 26, 1978. The values provided are:

Question 30

Discuss in detail the basis (using either calculations or observations) for concluding that the fretting wear due to rod-to-rod contact is insignificant.

Question 33

How many complete gap closures have actually been observed? Provide details including fuel design, burn-up level, axial position, etc.

Question 41

Has any fretting wear due to rod bowing ever been observed on fuel rods?

Question 42

Has any fretting corrosion due to bowing to contact of two rods and the high clad temperature in the area of rod contact ever been observed? 1

Question 43

Have any calculations of fretting wear and corrosion been performed.

Response

It has been B&W's operating experience that fuel rod bow greater than 50% gap closure is very unlikely and that complete closure has not been observed at any plant. Only one case of near contact (gap $\approx$ .020 inch) has been observed on a high burnup (40,000 MWd/MTu) Mark-B assembly in the mid core region. This pattern is also evident in the empirical rod bow equation. The predicted 95% tolerance level of rod bow is well below 50% closure at burnup level experienced by the Mark-B and Mark-C fuel assemblies.

To date, no analytical studies have been performed to assess the consequences of rod-to-rod contact, such as fretting wear of the clad. As described above, only one case of near contact of the rods has been observed and no fretting was evident.

Complete gap closure has not been observed and based on the rod bow correlation it is very unlikely it will occur. Therefore, the mechanical consequences of bow, such as clad fretting are not critical design concerns for B&W fuel assemblies. 1

Question 31

In order to relieve the DNBR rod bowing penalty, it must be demonstrated conclusively that assemblies with sufficient exposure to receive a penalty are never limiting. Therefore, demonstrate that assemblies with exposure greater than 14,000 MWd/mtU are never DNBR or F_Q limiting.

Response

A limiting assembly in a given cycle is the assembly which has the highest predicted peaking during the cycle. This limiting assembly may have a predicted burnup at the end of cycle as high as 24000 MWd/mtU (not 14000 MWd/mtU) or greater. For design purposes the limiting assembly is assumed to have a design radial x local ($F\Delta h$) peaking value which has been established as a maximum peaking criteria. This design peak is used in thermal hydraulic design analyses to establish core operating limits based on DNBR criteria. In Section 7.1 of BAW-10147P, the DNBR penalty associated with both Mark-B and Mark-C fuel designs for burnups below 24,000 MWd/mtU is less than 1% (see Figures 7-1 and 7-2) and this penalty is offset by a 1% DNBR credit in the form of a flow area (pitch) reduction factor. Fuel assemblies with burnups $\geq$ 24000 MWd/mtU have penalties greater than 1% but the penalty is unnecessary since the power production capability relative to other fuel assemblies in the core is diminished by fissile inventory depletion to the point where the design limit peaking values cannot be reached. With respect to the 36 reload cycles that have been designed for the Mark-B 177 fuel assembly plants, all fuel assemblies with a burnup of $\geq$ 24,000 MWd/MTu have had greater than   margin to the design limit peaking values. These cycles include both rodded and feed/bleed operational modes plus the out-in-in and in-out-in fuel shuffle schemes and are therefore representative of what can be expected for future cycles. This decrease in real peaking more than offsets the peaking which corresponds to DNBR reduction associated with the burnup dependent rod bow.

For example, consider a limiting assembly in a MK-B core which has a rod bow penalty applied at a burnup of 40,000 MWd/mtU. Referring to Figure 7-1 (MKB fuel) a rod bow penalty of   is determined. Subtracting the 1% DNBR credit the resulting net penalty is . This DNBR reduction can be offset by a corresponding reduction in peaking of . Since an assembly with a burnup ≥ 24000 MWd/mtU was shown in the previous paragraph to have at least a peaking margin (an even greater margin is expected at 40,000 MWd/mtU) the DNBR reduction due to rod bow is easily offset, by a large margin. A similar example for MK-C fuel can be easily constructed and shown to have more than enough peaking margin to offset the rod bow penalty.

Clearly then the application of a DNBR penalty due to rod bow is inappropriate and has no significance for B&W fuel designs.

Question 32

The question and response are found in conjunction with Question 15. 1

Question 33

The question and response are found in conjunction with Question 30. 1

Question 34

Why does the worst gap closure occur in the lower spans?

Question 51

It has been observed that the peak bowing is most likely to occur below the core midplane, but it has been observed in all but the top grid span. What significance does B&W attribute to observation?

Response

The largest magnitude of the standard deviation of the water channel 1
gap measurements in most likely to occur below mid-core as shown in table 4.3. It is theorized that bowing of a fuel rod is influenced by the thermal and irradiation histories of the rod as well as its mechanical loading and resulting creepdown. All of these parameters vary axially during the assembly's life depending on a number of factors such as the axial power distribution. The relative importance of the individual parameter has not been determined since the worst span closure can be conservatively used to bracket all of the gaps within the assembly. The fact that the largest rod bow is below mid-core is not considered significant for the B&W analysis technique.

Question 35

Is there a preferred direction for pre-bow in fresh assemblies? If yes, what is the reason for this behavior and how is it accounted for in the analysis?

Question 39

Is there any evidence that bowing is not isotropic?

Response

It has been B&W's experience that as built and operational rod bow is a random isotropic behavior. There is no evidence that a preferred direction for as built rod bow exists. 1

The analytical techniques used to develop the rod bow correlation are based on water channel gap widths, not on direct measurements of the lateral shift (bow) of the individual rods. Also, the DNBR reduction is a direct function of the water channel or cell dimensions and not the axial mode shape of the rods.

Question 36

Early pictures of rod bowing presented in the Westinghouse report WCAP-8346 showed very severe bowing for the outermost fuel rods. More recently, spacer grids were damaged during refueling at Rancho Seco (March 1980) and Indian Point-2 (January 1981). In the latter case, 272 assemblies were examined and 108 assemblies showed anomalies of some degree. Of these 108 assemblies, 33 assemblies were judged to require some repair and 10 assemblies were judged to have sustained more damage than would be acceptable for reinsertion. Fuel rod bowing seems to be a contributing factor to this grid damage. Has rod bowing typical of these plants been included in the reported data base? 1

Response

The rod bow correlation was developed from a data base that includes measurements from assemblies which are typical of the type used in the Rancho Seco reactor and which were irradiated at plants very similar to Rancho Seco. There is no evidence that fuel rod bowing was a cause of, or contributed to, the spacer grid damage that was observed at Rancho Seco.

Question 37

How do the correlations depend on the data base selected? For example, how would correlations for the burn-up ranges 0.10 GWd/mtU, 10-20 GWd/mtU, and 20-30 GWd/mtU compare?

Response

The rod bow correlation represents the best estimate of the standard deviation of the water channel measurements as a function of burnup. The correlation was reviewed to assess its sensitivity to the range of the data base used in the derivation. 1

The data base was subdivided into 4 sequential groups based on burnup. For each grouping, the average of the measured gaps compared favorably with the preidicted gap based on the average burnup. The deviation between the average measured and predicted gaps was not significant compared to the tolerance band of the data.

Question 38

In deriving the gap closure correlation, how has the fact that the number of measurements differs from assembly to assembly been accounted for?

Response 1

The gap closure correlation was developed from the statistical characteristics of the data distribution of the gap measurement in the worst span of the assembly. In all cases, the large number of data points measured were sufficient to determine the distribution for that span. No adjustment was considered necessary to account for the differences in the number of measurements from assembly to assembly.

Question 39

The question and response are found in conjunction with Question 35. 1

Question 40

The question and response are found in conjunction with Question 24. 1

Questions 41, 42, 43

The questions and responses are found in conjunction with Question 30. 1

Question 44

In carrying out the CHF experiments, the heated rod was bent toward the other rods. In a reactor, this bowing will cause a change in power in the rod. Has this effect been taken into account in these experiments or analysis?

Response 1

In CHF experiments, the objective is to measure the effects of the controlled (independent) variables on the dependent variable (CHF). In a bowed rod test, one of the controlled variables is the amount of closure. The dependent variable of CHF (ie: rod power to DNB) is then correlated to the independent variables including the closure. Since the allowable rod power is the result, it is implicitly included in the correlation and the associated bow penalty which results from experiment.

Is there any justification to support a flow dependence in the DNBR penalty?

Response

In the discussion and analysis of the bowed rod test (Appendix E), the data was examined for both flow and pressure dependence with respect to DNBR penalty. The examination was conducted on both a subchannel (Tables E-3 and E-4) and a bundle average basis (Table E-5). All the paired difference comparisons fell within results of the uncertainty analysis as developed in Section 4.2 of Appendix E except for the extreme high mass velocity comparison of Table E-4. Examination of this comparison indicates that the major part of the deviation is due to the C-9 (unbowed) value as opposed to the C-10 (bowed) value. Based on the paired difference comparisons, the deviations between C-9 and C-10 results were judged to be independent of both pressure and mass velocity. 1

Furthermore, the entire analysis in Appendix E indicated that any differences in results between C-9 and C-10 were within CHF testing repeatability, and thus there was no DNBR penalty at 55 percent closure. The use of the upper tolerance level bow penalty at 55 percent closure is viewed as a conservative treatment of the data designed to remove any uncertainty on the threshold value of penalty versus closure.

Question 46

What data points were used in BAW-10147P in Figures 4.1-4.3? How was this data selected?

Response

The rod bow correlation was developed from an extensive data base (Appendix B of BAW-10147P) that includes over 125,000 individual measurements of the water channel gaps from 26 fuel assemblies for burnups to 40,000 MWd/mtU. The comparisons presented in Figures 4.1-4.3 were derived from this data base.

Figure 4.1 presents a comparison of the data from the span(s) with the largest magnitude of the rod-to-rod and/or rod-to-guide tube gaps for each Mark-B assembly. The source of data points in the figure are given in Tables 3-1 and 4-1. 1

Figure 4.2 presents the standard deviations of the rod-to-rod gaps involving only peripheral rods and those involving interior rods for the assembly span with the largest standard deviation for all the rod-to-rod gaps for the Mark B assemblies. The sources of the data points used in the figure is Table 4-2.

Figure 4.3 presents the standard deviation of rod-to-rod gap measurements for all of the Mark-B assemblies within the range of interest of assembly burnup. Different notation is used to distinguish the rods lifted assemblies (NJ008M and NJ008N) and the spiral eccentricity assemblies (NJ00P7 and NJ00PG) compared to the standard configuration assemblies. The source of the data base is Table 3-1.

Question 47

Is there a reason for the trend in BAW-10147P in Figure 4.1 which suggests that the rod-guide tube gaps are larger at low burn-ups but smaller at high burn-ups than the rod-rod gaps?

Response

The design and fabrication of the fuel assembly results in different "as built" bow in the guide tubes than the fuel rods. The magnitude of the irradiation induced bow can be expected to be much lower in the guide tubes compared to the fuel rods. This results in a lower standard deviation for the rod-to-guide tube gaps than the rod-to-rod gaps. The trend is more apparent at the higher burnup levels due to the larger magnitude of the values involved. At low burnups, the data scatter represents a larger percentage of gap magnitudes so that any correlation between the groups is less pronounced. 1

Question 48

If only 12% of the MK-C spacing distributions passed the normality test, why is it justified to treat all distributions as if they were normal?

1

Response

On page C-2 it is shown that 38% of the Mark C test data passed the D´ test for Normality. In addition, Figure C-1 shows that when the distribution is very concentrated about the mean, as this data is, it is more conservative to assume the 84th percentile estimate from the normal distribution, than from the actual data points. Thus B&W took the conservative approach of assuming Normality.

Question 49

Is the bow correlation based on interior rod-rod gaps only?

Response

The rod bow correlation was developed from a data base that included all the rod-to-rod measurements (interior and periphery) for that particular assembly configuration. 1

Question 50

What is the uncertainty in the gap measurement in mils?

Response

The uncertainty in the gap measurements is estimated to be inch for the mean with a maximum increase of inch in the standard deviation of the poolside data. This uncertainty includes the effects of the accuracy tolerance of the probe itself and its electronic signal, fuel rod ovality, probe positioning and the accuracy of recording and reading the data from the strip chart. Also included is the uncertainty in the data correction techniques used to account for fuel rod spreading during probe insertion. 1

Question 51

The question and response are found in conjunction with Question 34. 1

Question 52

The question and response are found in conjunction with Question 10. 1

Question 53

How many batches have been considered in the determination of the 95/95 upper one-sided tolerance limit?

Response

The rod bow correlation was developed from a data base of eight manufacturing batches which included over 125,000 individual measurements.

Question 54

It is stated in BAW-10147P that a review of the data base shows a trend for the rod bow behavior to saturate at high levels of burn-up (>35,000 MWd/mtU) with the magnitude of the standard deviation of gap measurements remaining constant or decreasing. Describe in more detail the results of this review.

Response

The magnitude of the standard deviation of the gap measurements, σ_{gap},
for the assemblies (1D13, 1D42, 1D45, 1D55) that obtained burnups 1
greater than 35,000 MWd/mtU exhibit a tendency to remain constant or
decrease. The results of a span-by-span comparison of the third and
fourth burnup cycle data from the intermediate spans for these assemblies
is shown below:

Direction of Relative Change	Percent of Spans Exhibiting Change
Decrease	
No Change*	
Increase	

* Only changes greater than .0005 inch were considered significant.

Question 55

Does B&W have a basis for the 1.2 cold-to-hot correction factor other than the NRC recommendation? 1

Response

The 1.2 cold-to-hot correction factor was used based on the NRC recommendations.

Question 56

Why has the B&W gap correlation been changed from a square root to a linear burn-up dependence? Is the high burn-up data increasing faster than E?

Response

The relationship between the B&W low and high burn-up data does not support a square root dependence. As noted in Appendix D, the best fit model was found to be linear (burnup exponent of   ). The data does indicate that the rod bow behavior tends to saturate at high burnup levels (Ref. Question 54) with the magnitude of bow remaining the same or decreasing in the majority of cases. The correlation equation with its linear burnup dependence will conservatively predict rod bow in the high burnup regions. 1

Question 57

In the letter, Taylor to Vassallo, dated December 13, 1978, B&W used the NRC (Reference 1) procedure for determining the DNBR penalty. In the latest report, BAW-10147P, a new method is presented. Why was it decided not to use the model which was used two years earlier?

Response

The NRC procedure (Reference 1) was written as a proposed procedure, one to be used as an interim document in lieu of a Topical Report (and not a NUREG or procedures ruling).

Since 1978, B&W has produced a data base as well as performed a thorough review of the reference 1 techniques. It has become apparent that in the techniques of reference 1, sufficient thought was not given to the physical consideration of the problem.

The values of gap closure go from 0% to 100% or $0 \leq \frac{\Delta c}{c_0} \leq 1.0$, due to the fact that closure is complete at contact. Thus, also the penalty function goes only to contact and is a step function essentially, as defined in eqn. 6-4. 1

On the other hand, the gap closures assumed to be normally or rather 1/2 normally distributed have arguments between zero and infinity which produce inconsistencies with the above. These two physical and statistical considerations should be reconciled (and were indeed done so in BAW-10147P) by truncating the normal (1/2 normal) distribution and renormalizing the area so that it integrates to unity.

This method results in having more weight assigned to physically feasible gap closures and no weight to physically impossible ones.

By neglecting to truncate the gap closure distribution functions at 100% closure, the NRC procedure becomes physically unrealistic and statistically meaningless because it assigns weight (probability) to physically impossible gap closures between full closure and infinity! B&W does not accept the NRC proposal that $\delta = \frac{\delta_c}{1-K}(X-K)$ is a product of two random variables.

The fact that $X = \frac{\Delta C}{C_O}$ is random is not disputed. However, if "δ_C" is random, then so is "K"! Since they are two points on the same straight line, it seemed more realistic to estimate them and to do so conservatively. Otherwise, the problem statement is unrealistic as well as inconsistent. Finally δ_C, for instance, was considered by the NRC to have a normal distribution, one that has arguments to infinity, yet the penalty at closure is clearly limited by a value of one hundred percent. B&W has carefully considered the above points and concluded that the method presented in BAW-10147P is more realistic. 1

Question 58

What is the basis for assuming that the distribution of the contact penalty δ_c is normal?

Response

In appendix E, the B&W data was used to estimate a value of K as well as the penalty at 55% closure. These two best estimates would yield best estimate values for the slope of the penalty boundary line (Figures 6-2, 6-3). The B&W data indicated that the normal assumption for the scatter was reasonable. 1

The contact penalty best estimate value, $\bar{\delta}_c$, as well as σ_{δ_c}, were values at closure supplied by the NRC (ref 7). Due to the proprietary nature of the data, the actual data points were not released. Thus non-parametric bounds were unavailable.

B&W wished to be conservative in estimating the slope in Figures 6-2 and 6-3 and followed this conservative development in Section 6.1.2. It seems reasonable to assume normality of experimental errors for <u>both</u> points on the <u>same</u> curve, when evidence supports the assumption for one point and lack of evidence prevents one from refuting it on the other.

Question 59

In BAW-10147P, is the difference between Figure 7.1 and Figure 7.2 solely attributable to the 12% difference in MK-B and MK-C water channel widths?

Response

As pointed out in Section 5 and Appendix D, the same prediction equation relating gap closure to burnup is used for MK-B and MK-C fuel designs. Although the equation was developed using the MK-B data base it conservatively bounds the MK-C data. The development of the DNBR reduction (penalty) equation includes the probability distribution of gap closure which utilize the mean μ, the value of which is dependent on the fuel design-138 mils for MK-B and 122 mils for MK-C. In this respect then the difference between Figure 7.1 and 7.2 is attributable to the difference in MK-B and MK-C water channel widths.

Question 60

What is the basis for measuring the bowing effect on CHF for rod-guide tube bowing rather than rod-rod or rod-instrument tube bowing? Justify that this is bounding.

Response

In the bowed rod test (C-10) described and analyzed in Appendix F, the
bundle is typical of the guide tube geometry. The bowing effect on CHF,
however, is investigated in a rod-to-rod configuration (dimension b,
figure E-2). The basis for this configuration is that CHF has been found
to occur in the gap between heated rods and not in the gap between one
heated and one unheated rod. This observation is based on both heat
marks found during post-test inspection, and on the relative frequency of 1
corner versus adjacent hot rod CHF occurrence on unbowed tests of the
guide tube geometry (reference 15). Furthermore, the difference in CHF
level has been found to be a function of only the resultant local
conditions of quality and mass velocity for guide tube versus unit type
geometry, and not a specific geometry term such as the hydraulic diameter
(also reference 15). Therefore, any observed CHF penalty due to rod bow
would be expected to be the same for unit, guide tube, or instrument
tube geometry as long as the closure is relative to heated rod gaps. The
degree of CHF degradation for closure in a heated to non-heated rod gap
would be expected to be somewhat less than for the tested heated rod
to heated rod gap.

Question 61

In calculating the effects of rod bowing on power peaking in BAW-10147P what is the effect of bowing rod-A diagonally towards rod-D? How is this effect accounted for? 1

Response

The effect of bowing rod-A diagonally towards rod-D is shown in Figure G-6 and Figure G-11 of BAW-10147P by curves labeled 45^{0} for Mark B and Mark C geometry, respectively.

Question 62

Is there an explanation why there is no CHF penalty up to 55% closure?

Response

CHF is dependent on and correlated as a function of the local thermal-hydraulic conditions of pressure, quality, and mass velocity, and the radial and axial heat input distributions. The mass velocity is a characteristic local value, while the local quality is basically an integrated average value based on the mass velocity, geometry, and heat input up to that position. The sensitivity of CHF to changes in quality 1 is roughly an order of magnitude greater than that to changes in mass velocity. Since the presence of a bowed rod would tend to degrade the local mass velocity with no increase in quality, it is reasonable to expect a threshold value of gap closure below which no degradation in CHF would be observed. As discussed in response to Question 45, the bowed rod CHF data for 55% closure was actually within the range of uncertainty of the other (unbowed) CHF data. This would indicate that the threshold value is at least 55% closure and is most likely somewhat higher.

Question 63

What is the conservatism introduced by using a linear correlation between δ DNBR and gap closure?

Response

A linear correlation relating δ DNBR and gap closure was used between the value of gap closure below which there is no DNBR reduction, and 100% closure (contact), the point at which maximum DNBR reduction occurs.

The actual expected behavior of δ DNBR over the range of zero DNBR reduction to the maximum reduction is that δ DNBR will initially increase gradually from the gap closure of 0 DNBR reduction and increase more rapidly as gap closure approaches contact, as illustrated in Figure 6-1 (and in Reference 1, Figure 4.2). The degree of conservatism resulting from using the linear correlation has not been quantified for BAW-10147P since B&W has not performed rod bow CHF tests at gap closures greater than 55%, the threshold closure below which there is no penalty. 1

Question 64

What is the basis for the heat flux allocation in Figures E-1 and E-2 in BAW-10147P? Why is there a flatter heat flux distribution in the case of rod bow? Does this bias the rod bow results?

Response

In our 5x5 array CHF tests, the inner 8 rod heat fluxes are peaked higher (usually 10%) than those of the outer 16 rods. This is to insure that primary CHF occurrence is associated with the inner subchannels which are typical of in-reactor geometry. 1

The design relative heat flux distribution for both the unbowed and bowed rod tests were identical. The as-built rod electrical resistances (which determine the heat flux distribution) varied slightly between the two sets of rods, and resulted in the values shown in figures E-1 and E-2. In the CHF analysis, the actual heat fluxes based on the measured distributions are used. Thus, no bias is included in the results.

Question 65

As a bowed rod burns with a perturbed power, the resultant late-in-life power distribution will be further perturbed due to changes in isotopics. What effect does this perturbation have on the local F_Q^B penalty?

Response

This additional effect on the power is negligible, being less than 0.02%. The change in isotopic composition resulting from a fuel rod being depleted in a bowed position was assessed with calculational checks of the analytical procedure.

The analysis was performed with a fuel pellet composition that simulated end of cycle conditions. End of cycle conditions were chosen because the rod bow increases with in-reactor operating history. The maximum difference in the perturbed power in any fuel rod due to a mil bow of rod A along the 90° axis (Figure G-4), with fuel having MWD/T exposure, was less than power. The same difference was calculated for fuel having MWD/T. 1

Since the actual isotopic composition was quite different between these several pellet material models, it was concluded that the non-uniform fuel cell burnup is accurately accounted for in the design analysis and no perturbation is required for the non-uniform burnup of a bowed rod.

Question 5

2nd Round:

One cannot conclude from the fact that the CHF occurs in the gap between heated rods that the effect of the location of the remaining rods is not important. Therefore, determine quantitively the effects of multiple rod displacements on the bowing penalty δ_B. If necessary, incorporate these effects in the F_Q^B and DNBR operating limits.

2nd Round Answer:

The following discussion provides an assessment of the effect of multiple rod displacements on the bowing penalty, δ_B, of a particular gap of interest.

Two effects are predominant in the determination of CHF level. The first, the integral effect, is basically the thermodynamic quality of the coolant at the axial location of interest. This in turn is just the integrated 1
effect of mass velocity and heat input up to that point. The integral effect represents the progressive deterioration of the capacity of the coolant to accept heat input. Secondly there is the localized effect. This can be viewed as the contribution (or detraction) of the mass velocity at any given axial location to the capacity of the coolant to accept localized heat input. CHF testing has established that of these two effects, the integral effect is much greater than the local effect.

Extensive testing has established that CHF occurs in the gap between heated rods. In testing a bowed rod configuration, the bundle is constructed such that a specified minimum clearance occurs between heated rods where coolant heat capacity becomes critical. CHF is then detected at (or downstream) of this minimum clearance axial location in the heated rod gap. Thus, rod bow clearly has a localized mass velocity effect on CHF level. Up to and including this axial region, the effects on the integral (quality) effect due to rod bow is negligible.

While it is true that the heated rod gaps close to the heated gap of interest could affect the localized mass velocity in that gap, the change (if any) would be a secondary (probably order of magnitude lower) effect on this localized mass velocity. Coupled with the fact that localized mass velocity exhibits only a secondary effect in itself, the compounding additional secondary effect of rod gap variability in the region of the heated gap of interest would be negligible.

Moreover, when considering variable rod gaps close to the gap of interest, any reasonable distribution would result in some gaps larger and some smaller than nominal. This would imply, then, less or more (respectively) flow in the critical gap. Thus the effect would be further reduced. 1

On the basis of the above reasoning, it is concluded that the penalty due to gap closure can be determined by exclusive consideration of the reduction of the heated rod gap of interest.

Question 7

2nd Round:

What magnitude of poison rod bowing will the guide thimbles permit and what is the effect of this bowing? Consider both the bowing of poison rods and the bowing of fuel rods in the presence of poison rods.

2nd Round Answer:

The poison rods are separate components which are inserted into the guide tubes (thimbles) of the fuel assembly matrix. The guide tubes limit the poison rod bow.

The maximum poison rod bow within the guide tube (thimble) annulus is 34 mils for MK-B and 30 mils for MK-C. This is one half of the diameteral clearance between the poison rod and guide thimble.

An assessment of effect of poison rod bowing on local power peaking considers the types of poison rods used in B&W core designs. There are three types of poison rods used in the B&W core design: full length control rods, part length control rods and burnable poison rods. 1

The effect of control rod (full length or part length) bow and adjacent fuel rod bow upon power in nearby fuel pins is not a concern, because a fuel assembly containing a control rod assembly of either type does not simultaneously have the maximum power producing fuel pin in a B&W core design.

The third type of poison rod, burnable poison rod, is accounted for in the standard nuclear reliability factor (NRF) that is applied to the B&W nominal design core peak pin power. This is because burnable poison rod bow is equivalent to the nominal design radial position uncertainty of the poison rod in the guide thimble. The radial position uncertainty along the axial length of the guide thimble is due to causes such as rod straightness. The standard nuclear reliability factor was established by comparison of calculated to measured peak pin power from a large data base that includes both operating plant and critical experiment data for core designs using burnable poison rods.

Fuel rod bow adjacent to a burnable poison rod is expected to induce a smaller fuel rod power change for the peak rod power than occurs for a uniform lattice configuration for several reasons. The water fraction is slightly less in the immediate area of the bowed rod due to the presence of the guide thimble and poison rod. The peak power producing fuel rod is generally located in a fuel assembly lattice region having higher than average water fraction. Secondly the burnable poison rod is a neutron absorber throughout the fuel cycle with some residual poison remaining at the end of the cycle. This effect adds assurance that the peak power producing fuel rod will not be adjacent to a poison rod. Finally there are less fuel rod contributors in the lattice position statistical population in the vicinity of guide thimbles than was used in the uniform fuel lattice analyses that established the total fuel rod bow induced power change of BAW-10147P. 1

Question 15

2nd Round:

In the Monte Carlo simulation of rod bowing only the 8 nearest neighbor rods were allowed to bow. What is the effect of bowing of second nearest neighbor rods on the central rod power?

2nd Round Answer:

The calculations which considered the variation in local power peaking with
random bowing of surrounding assemblies included the effect of bowing 1
the eight nearest rods plus the next nearest group of sixteen rods. As
described in the response to Question 15 (first round) and in Appendix G
of BAW-10147P, the Monte Carlo technique used to determine the sensitivity
of local power peaking with random rod bow considered a 5 x 5 rod array.
With this model the change in power peaking in the center rod was determined
as result of bowing each of the surrounding rods in the 5 x 5 array.

Question 16

2nd Round:

What specific burnup is this analysis and gap closure applicable to?

2nd Round Answer:

The rod bow analysis presented in BAW-10147P is expected to be valid for
any range of fuel assembly burnup expected to occur in current or future core
operation. The maximum burnup for current fuel assembly designs for which this
analysis applies is MWd/mtU, and is based on mechanical design considerations.
Modifications to existing fuel assembly designs and to fuel cycle designs may 1
allow fuel assembly burnup of MWd/mtU or greater and the current rod
bow analysis presented in BAW-10147P is expected to remain applicable.

The rod bowing data presented in BAW-10147P, which included fuel assembly burnups to 40000 MWd/mtU, indicates that the rod bow behavior tends to saturate out at burnup levels greater than 35000 MWd/mtU. The response to Q-54 of the first round questions provides a data summary showing this trend. The prediction of gap closure for burnups greater than 35000 MWd/mtU is conservative because of the linear burnup dependence of the correlation, eq. 5-1 of BAW-10147P. In addition, the global tolerance applied to the correlation, as determined by eq. 5-4 and described in detail in Appendix D of BAW-10147P, increases with burnup, thus providing additional conservatism to the analysis for burnup levels greater than 35000 MWd/mtU.

Question 17

2nd Round:

Provide a typical range of fuel design parameters (including variations in enrichment, poison rods, rod pitch, burnup, water holes, guide thimbles etc. covering all NSSS's supplied) to which this analysis is applicable.

2nd Round Answer:

The data base used in the development of the rod bow correlation encompasses a wide spectrum of fuel design parameters. It includes more than 125,000 individual gap measurements on a range of fuel assembly designs, manufacturing variations, operational and irradiation histories.

The data base includes measurements on 26 assemblies of the 15 x 15 Mark-B (.568" pitch) and 17 x 17 Mark-C (.502" pitch) configurations. The assemblies represent 8 manufacturing batches with enrichments from 2.15% U^{235} to 3.2% U^{235}. 1
They were used in two reactors during 8 operating plant cycles for individual exposures of 1 to 4 cycles whith burn-up to 40,000 MWd/mtU. The assemblies were inserted into core locations that contained orifice rods, burnable posion rods, safety or control rods or were open guide tube assemblies.

The rod bow analysis presented in BAW-10147P is considered valid for the current fuel assembly designs from which the data base for the analysis was obtained plus future designs which may have design parameters (such as pin pitch, enrichment, etc.) which differ from those described in the previous paragraph. As discussed in the response to the first round Question 20 the need to acquire additional gap closure measurements and to update the analysis for minor fuel assembly design changes will be reassessed on a case by case basis.

Question 18

2nd Round:

Update the description of the application of this analysis to include any changes resulting from this review.

2nd Round Answer:

B&W has concluded that no changes to the methods of rod bow evaluation presented in BAW-10147P are justified from this review. Additional information provided in the responses to the second round review support our conclusion. In particular the data presented in the 2nd round response to Question 31 illustrates the level of pin peaking margin which exists as burnup increases, relative to the design limit peaking value. 1

Because of the magnitude of peaking margin available, which is much more than necessary to offset the DNBR penalty determined in Figure 7-1 or 7-2, it would seem conclusive that the application of a DNBR penalty due to rod bow is inappropriate and has no significance for B&W fuel designs.

Question 23

1st Round:

In the determination of the fuel rod DNBR penalty, the bowing of the eight surrounding rods and associated gap closures determined the reduction in DNBR margin. "The penalty for each gap is determined by summing over the contributions from each possible closure. The closure contribution is given by the product of the probability of occurrence for that closure and the associated closure penalty. (In Reference 1 this method was used to determine the penalty arising from the bowing of two rods on opposite sides of the rod of interest)." Therefore, update the bowing anlaysis to include the contribution to the DNBR penalty from all eight surrounding rods.

2nd Round:

The determination of the DNBR penalty using equation (F-3) does not properly account for the gap closures of all eight surrounding rods. Therefore, update the analysis to include the contribution to the DNBR penalty from all eight surrounding gap closures.

2nd Round Answer:

The methods of analysis presented in BAW-10147P have resulted in a treatment of the subject of rod bow in a manner which can be used to conservatively assess the impact of rod bow on core design and operating limits based on DNBR criteria. The treatment of rod bow in BAW-10147P is, we feel, consistent with the objectives suggested in Reference 1 of BAW-10147P. 1

In consideration of the probability distribution of gap closure, and the associated DNBR penalty, referring to the underlined portion of the 1st round question please note the following equation F-3.

Is the associated closure penalty

Probability of occurrence for closure

The above integral (instead of sum) is analogous to the underlined statement in the 1st round question. Also the equation F-1 utilizes the same principle presented in Reference 1 Appendix 2.

The ultimate consideration of the analysis is the effect of rod bow on core design and operating limits based on DNBR. The first round responses to questions 18 and 31 and the second round response to question 31 discuss the philosophy and methods of applying a rod bow penalty and quantifies the degree of pin power peaking margin that is present with increasing fuel assembly burnup. This peaking margin is more than sufficient to offset DNBR penalty values predicted in BAW-10147P, or by predictions made prior to the current analyses such as by the interim method of Reference 5. In view of the above considerations an update to the analysis to include a contribution to the DNBR penalty from the eight surrounding gap closures is not considered to be appropriate. 1

Question 26

2nd Round:

Determine the effects of assembly bow on local rod powers and incorporate these effects in the $F_Q{}^B$ penalty.

2nd Round Answer:

Thermal hydraulic design analyses incorporate a conservative bundle (pin by pin) peaking distribution which was established from nuclear analysis that considered the influence of water gap variation between fuel assemblies when determining rod powers. This peaking distribution represents the worst case associated with the range of assembly bow considered feasible, which included maximum, minimum, and nominal spacing between adjacent fuel assemblies. This conservative peaking distribution is used in limiting assembly DNBR analyses along with the conservative method of modeling subchannels between adjacent assemblies to account for assembly bow as described in the response to Q-26, (first round). Thermal hydraulic DNBR analyses performed with the conservative peaking and modeling assumptions therefore properly account for the effects of fuel assembly bow. 1

Question 27

1st Round:

Describe in detail the derivation and basis for Equation (D-4) in BAW-10147P.

1st Round Answer:

Equation (D-4) is to calculate a 95% upper tolerance level on values of bow predicted by equation (D-2) which in turn is based on rod-to-rod gap measurements as described in Section 5 of BAW-10147P. The derivation of equation (D-4) is found in Reference 12 of BAW-10147P, "Simultaneous Statistical Inferences," R. G. Miller, McGraw-Hill Book Co. (1966).

2nd Round:

Define the symbols and discuss the basis and applicability of equation (D-4) to the calculation of the bow tolerance. 1

2nd Round Answer:

Equation D.4 is defined as:

Bow Tolerance (at 95/95) =

This term is obtained from the least squares regression program that was used to evaluate coefficients of the prediction equation. The standard error is a measure of the deviation between predicted and measured values (of bow in this case).

(A)

$C_{Bu} = \sqrt{X_0'(X'X)^{-1}X_0}$, the model correction factor is also obtained directly from the regression program. This factor is statistically necessary in order to account for the greater uncertainty in the model predictions, the further one goes from the mean of the independent variable (BU in this case). It may be seen in Figure 5-1 what a "fanning out" effect this term has on the tolerance curve. (X_0 = vector of input for evaluation of regression function and $(X'X)$ is the matrix from which regression coefficients are estimated.)

ρ = degrees of freedom used for estimating the regression coefficients

$n-\rho$ = degrees of freedom available for error

$F_{\rho, n-\rho}^{.95}$ = the 95% value of the F- Statistic with ρ and $n-\rho$ degrees of freedom.

Up to this set of terms the form of D-4 is very much like any other regression function confidence interval on the mean prediction. By using the "F" rather than the "t" statistic the entire regression surface is covered, hence the adjective "global".

(B)

$Z_{.95}$ = the 95% value of the Normal Statistic

$\chi^2_{.05,\ n-\rho}$ = the lower 5% value of the CHI-square statistic with $n-\rho$ degrees of freedom

The unknown scale factor of σ(bow) is bounded with 95% confidence, by:

To quote the author of Reference 12 on Page 124: "A quick and easy family of simultaneous tolerance intervals can be patched together with the aide of the Bonferroni inequality."

The result is equation D-4.

Miller refers to the above technique as being most useful in cases where the total number of predictions one may make in the future are unknown or may be subject to change.

Question 29

1st Round:

In the determination of the DNBR penalty, the effect of the uncertainty in the penalty due to variability in gap closure (denoted σ_u in Reference 1) has been neglected. Incorporate this variability using a 95/95 upper tolerance limit as outlined in Reference 1, Equation (4.19), or indicate how this effect has been accounted for in the DNBR penalty.

2nd Round:

The NRC guidance requires that the variability in gap closure (denoted σ_u in Reference 1) be accounted for explicitly in the calculation of the DNBR penalty. It also requires that a 95/95 upper tolerance limit be used to describe the expected distribution of gap closures. Therefore, incorporate this variability as outlined in Reference 1 (of BAW-10147P), Equation (4.19), or indicate how this effect has been accounted for in the DNBR penalty.

2nd Round Answer:

From Reference 1 of BAW-10147P, equation 4-19 is: 1

$$\left(\frac{M}{P}\right)_b^{95 \times 95} = \left(\frac{\overline{M}}{\overline{P}}\right) - \overline{\delta} - k_b^{95 \times 95}\sigma_b \quad (4.19) \qquad \text{or}$$

$$= \left(\frac{\overline{M}}{\overline{P}}\right)_{nb} - \left(\overline{\delta} + K_b^{95 \times 95}\sigma_b\right)$$

The method chosen by B&W to incorporate the variability of gap closure into the DNBR penalty is such that the term

$$\left(\overline{\delta} + K_b^{95 \times 95}\sigma_b\right)$$

cannot be expressed explicitly as in the Reference 1 method, equation 4.19 above. It is accounted for never-the-less, inherently, in the calculation of values from Equation F-3 of BAW-10147P.

An explanation follows. One way of rewriting equation D-4 of the report is:

However, it must be stressed, once more, that in D-4 the term calculates a global simultaneous tolerance and is therefore much more conservative than a simple "$(K^{95/95}\sigma)$" type value.

Next: Step 1

The expression of D-4 above is then used in F-3 by substituting, appropriately, into the term as follows:

1

Step 2

Instead of implementing a simple $\overline{\delta}$, the upper tolerance ($\overline{\delta}$ + K^{95} $\sigma(\delta)$) is used in F-3 above. The upper bound is represented by the equation F-1 and illustrated in Figure 6-2 of BAW-10147P.

Question 31

2nd Round:

What reload assumptions have been made in establishing the margin in power peaking of assemblies with burnups in excess of ( ) MWd/mtU? In support of this margin, provide the limiting assembly local peaking as a function of burnup.

2nd Round Answer:

An evaluation of nine typical B&W reload cycles has quantified the level of rod power peaking margin that exists as burnup increases. The cycles selected cover a wide range of reload parameters as indicated below:

# Cycles	Cycle Length	BPRAs Used	Mode of Operation
2	Annual	No	Feed/Bleed
1	Annual	No	Rodded
2	18 Month	Yes	Rodded
2	18 Month	Yes	Feed/Bleed
2	15 Month	Yes	Feed/Bleed

1

For each of the above cycles pin burnup and peaking data was compiled for the once and twice burned fuel assemblies. The conservative assumption was made that within a given assembly the highest burnup pin was also the pin with the highest power.

The resulting pin burnup and pin peaking data * are shown in Figure 1. These data show greater than a margin in peaking for burnups above 24000 MWd/mtU as identified in the 1st round response to Question 31.

* Fuel pin relative power densities (RPDs) are shown in terms of margin to the design limit.

Figure 1

PEAKING MARGIN TO DESIGN LIMIT vs FUEL ROD BURNUP

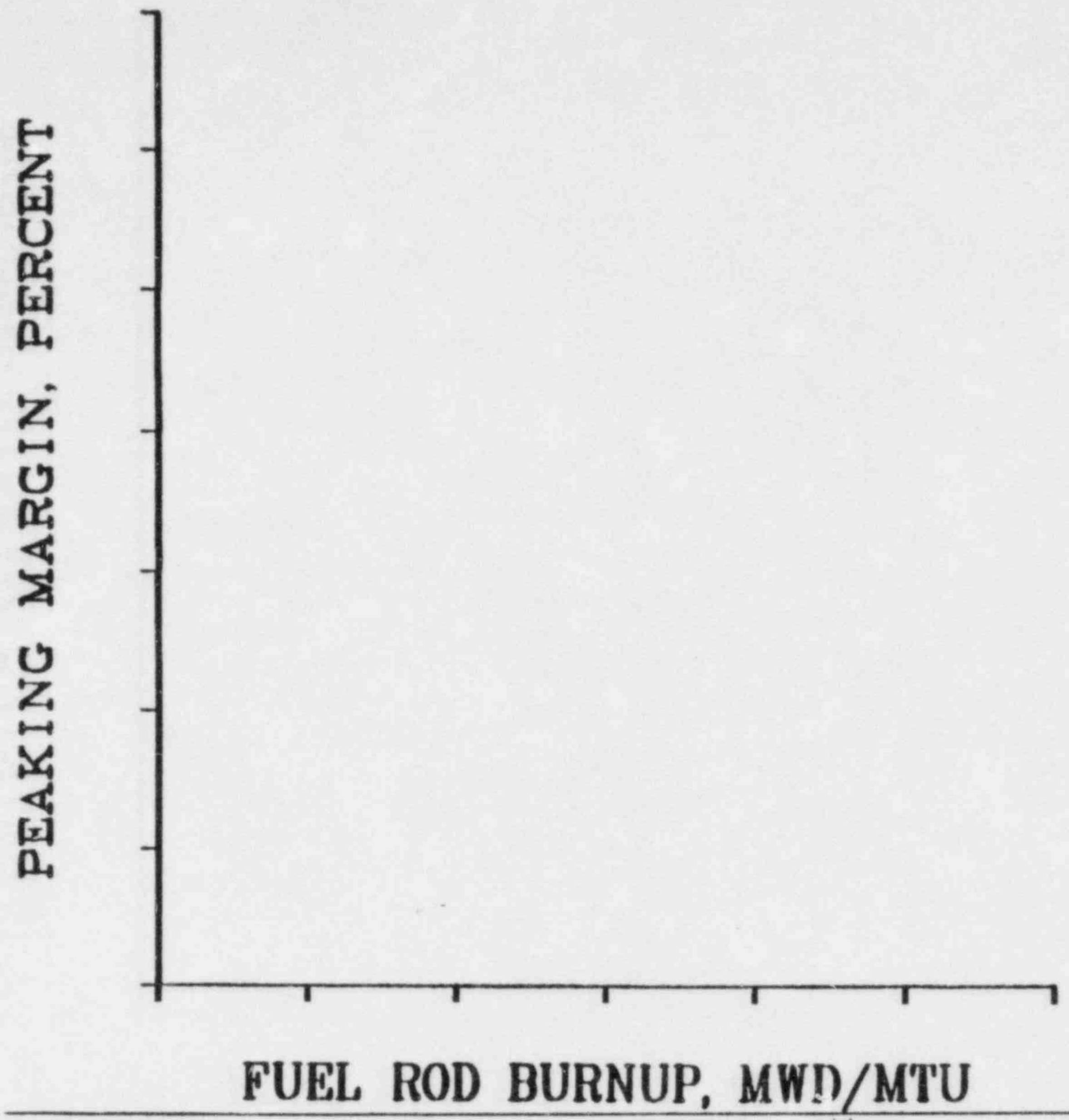

APPENDIX J

Letter, J. H. Taylor to Carl Berlinger,
July 23, 1982 and Supplementary Response to
Second Round Question Number 26 1

Babcock & Wilcox

Nuclear Power Generation Division

a McDermott company

3315 Old Forest Road
P.O. Box 1260
Lynchburg, Virginia 24505
(804) 384-5111

July 23, 1982

Mr. Carl Berlinger, Chief
Core Performance Branch
Division of Systems Integration
Office of Nuclear Reactor Regulation
U.S. Nuclear Regulatory Commission
Washington, D.C. 20555

Dear Mr. Berlinger,

In a phone call between B&W and members of NRC staff on June 25, 1982, B&W agreed to provide a supplementary response to second round question number 26 on BAW-10147P, "FUEL ROD BOWING IN BABCOCK & WILCOX FUEL DESIGNS". The requested information is attached.

Should you require further information on this submittal, please call Frank McPhatter (Ext. 2401) or me.

Very truly yours,

J. H. Taylor
Manager, Licensing

JHT:CFM:kb

Attachment

cc: R. B. Borsum - B&W Bethesda Office

bcc: T. A. Coleman
J. B. Andrews
J. C. Moxley
G. A. Meyer
K. O. Stein
R. V. Demars
G. E. Hanson
R. A. Kochendarfer
C. F. McPhatter
T. L. Baldwin

QUESTION 26

1st Round:

Large assembly bow of the order of hundreds of mils has recently been measured at several plants.[2, 3, 4] This bow is of concern because (1) the bow magnitude is at least an order of magnitude larger than the reported rod bow measurements, (2) the resulting rod bow is apparently extremely correlated with all rods in an assembly face bowing together and (3) the bow involves inter-assembly gap closure. All of these aspects are outside the scope of the proposed bowing analysis. Therefore, discuss in detail the effects of assembly bow on fuel rod gap closure and the assumptions and methods used to evaluate rod bowing.

2nd Round:

Determine the effects of assembly bow on local rod powers and incorporate these effects in the F_Q^B penalty.

The B&W response to a request for additional information concerning local power effects of assembly bow supplements the information provided in the response to the first and second round questions which focused on fuel assembly gap closure and the effects on DNBR.

The effects of fuel assembly bow on local rod power and on the F_Q^B penalty were evaluated in terms of a magnitude of fuel assembly bowing expected to occur in-reactor. The evaluation found that no additional penalty in F_Q^B should be included for assembly bow effects.

Fuel assembly bowing has been an inherent characteristic of all PWR fuel assembly designs. Fuel assembly bowing is believed to be a function of several parameters, including fuel assembly design and manufacture, fuel management practices (viz. cross-core shuffle versus quadrant shuffle), burnup, flux gradient across the core, and fuel assembly handling techniques.

Babcock & Wilcox Post-Irradiation Examination (PIE) programs have included fuel assembly bow measurements to provide data for evaluating fuel handling concerns. Because the measurements were made out of reactor, the data provides only an indication of trends in the behavior of in-reactor fuel assembly bow.

The actual amount of in-reactor bow is expected to be constrained by the limited in-reactor clearance (.051 inches) between fuel assemblies. The subsequent spacer grid interaction of all fuel assemblies in the core ensures that the magnitude of in-reactor fuel assembly bow is limited. Additional constraints to in-reactor fuel assembly bowing are provided by fuel management practices. Cross-core shuffling places bowed assemblies adjacent to new or oppositely bowed assemblies, providing additional, continuous, restraint to fuel assembly bowing.

A fuel assembly bowing configuration that could reasonably be expected to occur in core is illustrated in Figure 1. For a 2 x 2 fuel assembly array, a fuel assembly bowing diagonally away from its three adjacent assemblies increases the fuel assembly gap from .051" (nominal) to .102". (Nominal rod gap and fuel assembly grid gap dimensions are provided in Table 1.) This bowing configuration, shown in Figure 1, represents the assembly bowing away such that its outer adjacent gaps are closed and is used as the geometric basis for assessing bowing effects on local rod power.

The radial-local rod power change due to in-reactor fuel assembly bow has been evaluated with the B&W PDQ code employing a geometric model of four one-quarter fuel assemblies with a discrete representation of inter-fuel assembly water gaps and lattice cells as shown in Figure 2.

The four fuel assembly array consisted of two 3.02% and two 2.06% enriched UO_2 B&W Mark B fuel assemblies with common enrichments on diagonal arrays. The fuel enrichments were chosen to represent fresh fuel adjacent to partially depleted fuel in a typical reload fuel assembly shuffle plan. This modeling plan for off normal inter-assembly water gaps is applicable to both the B&W Mark B (15x15) and Mark C (17x17) fuel performance due to their similar water/fuel volume fractions (lattice plus gap).

A 51 mil inter-assembly water gap addition to the nominal gap yields a 2.8% maximum power increase in a peripheral rod. This increase is applicable to two types of fuel assembly bowing configurations, i.e. one fuel assembly bowing laterally or diagonally relative to three other fuel assemblies, as shown in Figures 3 and 4.

The effects on the F_Q^B penalty resulting from fuel assembly bow related local power changes were evaluated in terms of Technical Specification Limits based on Centerline Fuel Melt criteria and LOCA.

Assembly bow effects have not been included explicitly in the peaking uncertainty factors applied in the Centerline Fuel Melt analysis because the effects are covered by other conservatisms used in the derivation of the total peaking factor used to determine Technical Specification Limits. These conservatisms include the following credits:

1) The present calculation of the total peaking factor includes separate multipliers for the densification power spike penalty and the penalty representing the statistical combination of the nuclear reliability factor, the engineering hot channel factor and the rod bow peaking factor (Reference 1). If B&W were to include the spike factor in the statistical combination with the other three factors, the resulting factor would be less than the product of the the original two penalties, thereby yielding a peaking credit.

2) Since the nuclear reliability factor described in Topical Report BAW-10119A for the worst combination of peak power and assembly radial-local factors is less than the standard B&W analysis value of 1.075, there is a peaking credit available. This conservatism was recognized in the NRC Topical Report Evaluation of BAW-10119.

3) The limiting location in the fuel assembly occurs between the 2 and 3 foot elevations. The amount of bow at these heights is less than the bow at the core midplane, resulting in a reduction of the effect of assembly bow on any associated power peaking increase in the region of greatest importance.

4) The limiting peak rod location in the core in the LBP shuffle scheme (used in all but one operating B&W reactor) is normally on the periphery of a fresh LBP-containing assembly, and is sensitive to the effects of assembly bowing. However, since the assembly is in its first cycle of operation, the actual rod bow power peaking effects are zero or very small, compared to the conservative value used in Topical Report BAW-10147P. Thus the rod bow peaking allowance is available to offset peaking increases caused by assembly bow, since the maximum effects of fuel rod bowing on the limiting pin in the core do not occur simultaneously with the effects of assembly bowing.

For the above reasons the continued use of the product of the

Nuclear Reliability *
Engineering Hot Channel Factor *
Densification Power Spike Factor

conservatively accounts for any credible effects of both fuel rod and assembly bowing on the linear heat rates calculated in establishing the CFM related Technical Specification Limits.

Assembly bow effects have not been included explicitly in the analysis of the Technical Specification Limits based on LOCA linear heat rate criteria because assembly bow effects will not impact the results of the transient. During the LOCA the increased gap will result in improved cooling ability. The reflood portion of the transient is also improved by the enhanced convective cooling. In addition, the assembly bow effects are offset by conservatisms in the total peaking factor used to determine LOCA related Technical Specification Limits. These conservatisms include credits 2, 3, and 4 from the list of credits presented after the Centerline Fuel Melt analysis. These benefits will offset the small power peaking increases which may occur if assembly bowing is considered.

Reference 1: Letter, J. H. Taylor (B&W) to S. A. Varga (NRC), "Statistical Combination of B&W Peaking Factors," March 25, 1977.

Table 1

NOMINAL GAP DIMENSIONS

	Mark B (15x15)	Mark C (17x17)
Nominal Inter Assembly Grid-Grid Gap, Inches	.051	.051
Nominal Rod-Rod Gap, Fuel Assembly Interior, inches	.138	.123
Rod Pitch	.568	.502

Figure 1

FUEL ASSEMBLY BOW CONFIGURATION

Gap Sizes (Mils)

$$\left.\begin{array}{l} G_1 = 51 \\ G_2 = 51 \end{array}\right\} \text{Nominal}$$

$G_3 = 102$

$G_4 = 102$

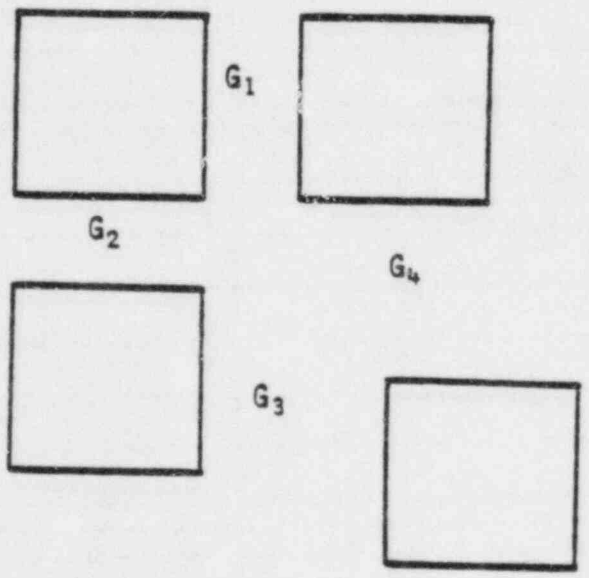

Figure 2

GEOMETRY MODEL
OF FOUR ONE-QUARTER FUEL ASSEMBLIES

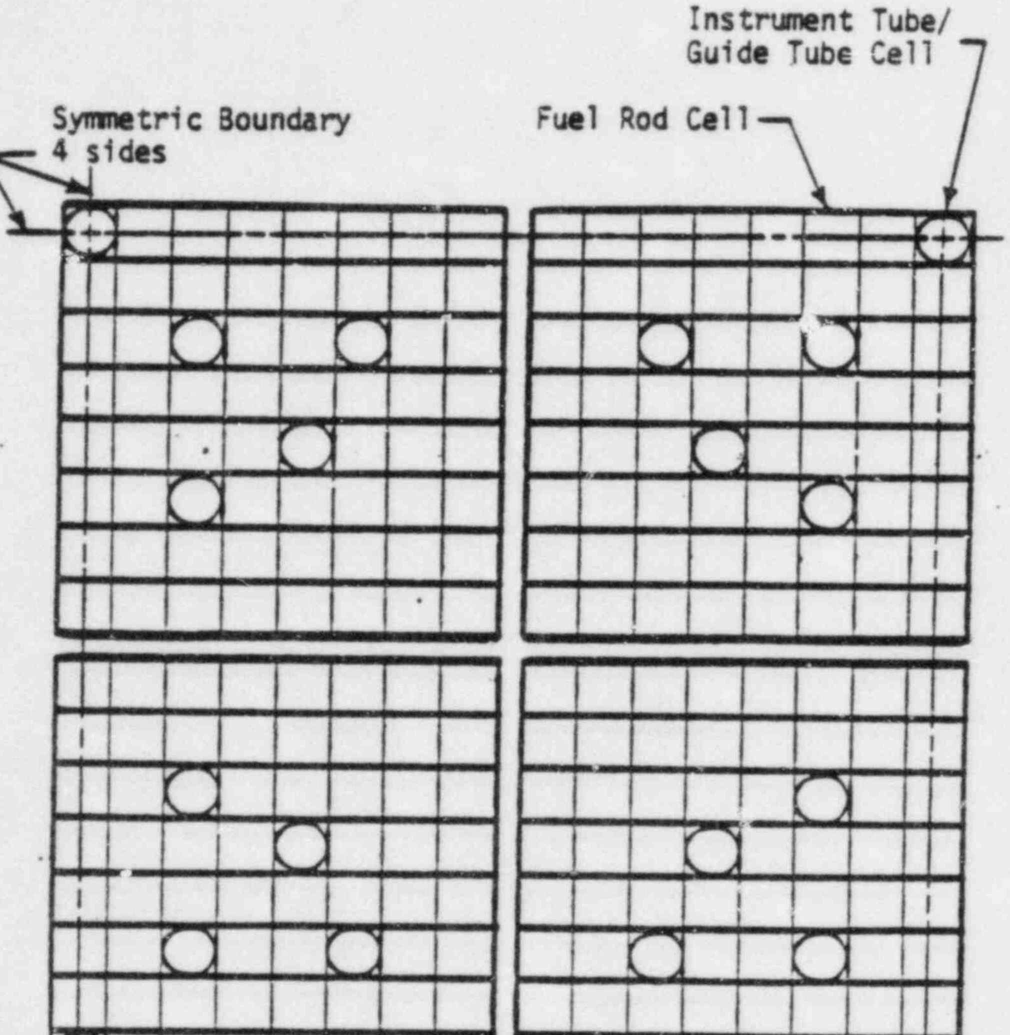

Figure 3

FUEL ASSEMBLY LATERAL MOVEMENT

(4-½ FA Model)

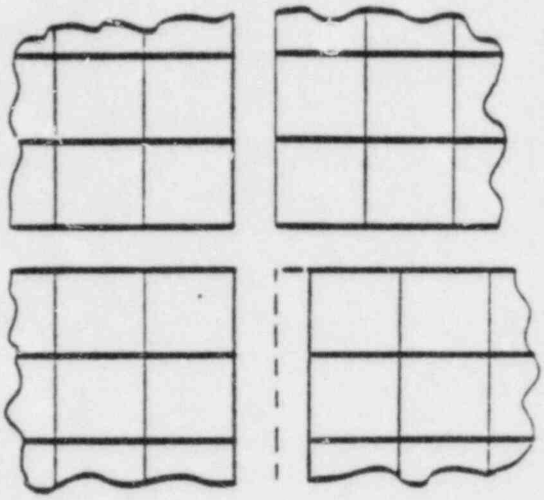

Figure 4

FUEL ASSEMBLY DIAGONAL MOVEMENT

(4-½ FA Model)